



A Bioreactor for chondrocyte differentiation: design, modelling and prototyping

Pedro Manuel Mesquita Pereira

Thesis to obtain the Master of Science degree in

Biological Engineering

Supervisor: Prof. Frederico Castelo Alves Ferreira PhD

Examination Committee:

Chairperson: Prof. Tiago Paulo Gonçalves Fernandes PhD

Supervisor: Prof. Frederico Castelo Alves Ferreira PhD

Member of the committee: Marta Monteiro Silva Carvalho PhD

December 2019

Declaration:

I declare that this document is an original work of my own authorship and that it fulfills all the requirements of the Code of Conduct and Good Practices of the Universidade de Lisboa.

“Our world is built on biology and once we begin to understand it, it then becomes a technology.”

Ryan Bethencourt

Preface

This document was written and made publically available as an institutional academic requirement and as a part of the evaluation of the MSc thesis in Biological Engineering of the author at Instituto Superior Técnico. The work described herein was performed at the Stem Cell Engineering Research Group (SCERG) of iBB - Institute for Biosciences and Bioengineering a research group of Instituto Superior Técnico of Universidade de Lisboa (Lisbon, Portugal), during the period of February to September of 2019, under the supervision of Prof. Frederico Ferreira.

Acknowledgements

I would like to start thanking all that contributed to this present work directly. The most important being Kaue, Dr. João Silva and Prof. Frederico Ferreira that in long discussions contributed with their experience and expertise in the development of the work that is here presented.

I would like to thank all the people that have been part in the last five years of my academic life, that culminates with this work. All the professors that have gave me so much knowledge and so many tools to face my future life and inspired me to look further than I previously would I am very happy to thank.

To all the colleagues that faced adversity and the effort needed to be now finishing this long walk I would like to thank all, for such a cohesive group and all the solidarity shown by all.

I would especially like to thank all the good friends I have found in this arduous walk that the last five years represent. Especially Sofia Amorim, Margarida Rodrigues, Isabel Doutor and Renata Quintino. Without you all I would not be here today. I would like to thank you for being beside me in the most trying moments as well as the best moments of fun and camaraderie.

Finally, I would like to thank my best friends Tiago Taborda and Carolina Richheimer that have been there all along these years, that have been there for me in all moments when I was at my best and my worst in both work and life and only thanks to you, I could keep going in the worst times. With you I celebrated all the victories I found in these years and found solace in the moments of defeat.

To the most important people in my life goes the most important thanks, my family, my mother Adelina, my father Paulo and my sister Mariana. Without you forming the bedrock on which my life is built upon I could never have gotten here.

To all thank you very much.

Abstract

Articular cartilage is a tissue located in diarthrodial joints and responsible for transmission of loads and lubrication of these structures.

Current therapeutic methods for this tissue are limited by the quality of the neocartilage and its ability to long-term withstand the physiological loads. The need for Articular cartilage tissue engineering arises from these limitations.

Mechanical stimulation is considered important for the correct differentiation of Mesenchymal stromal cells (MSC) and for maintenance of phenotype of cultured chondrocytes. The most common forms of stimulation are hydrostatic pressure (HP), direct compression (DP) and shear stress.

In this work ideation and development of a bioreactor, design is done considering the mechanical stimulation of articular cartilage tissue engineering constructs. The final bioreactor here proposed is chamber perfused and includes two independent chambers, associated with each side of the construct, for osteochondral differentiation.

The novel mechanical stimulation apparatus proposed administers a combination of direct compression with contact shear, it was designated cam for the resemblance mechanical part with the same name.

The various evolutions of the design were modeled in 3D with the Computer-aided design program Solidworks. This program's tools were also used for computational fluid dynamic simulation of the perfusion chamber and scaffold. It was concluded that for a typical porous scaffold the interstitial velocity felt by the cells is in the relevant range for MSC differentiation.

The bioreactor was partially prototyped, with most parts being constructed by 3D printing. Additionally, a proof-of-concept circuit for driving and controlling the mechanical stimulation was also constructed.

Key words: Bioreactor, joint, cartilage, MSC, chondrocyte, compression, shear

Resumo

Cartilagem articular é um tecido localizado nas articulações diartrodiais, responsável pela transmissão de cargas e lubrificação destas estruturas.

Métodos terapêuticos atuais para reparar lesões neste tecido são limitados pela qualidade do tecido e sua subsequente durabilidade. A necessidade de engenharia de tecidos surge destas limitações.

Estimulação mecânica é considerada importante para a direção de diferenciação de células estromais do mesênquima (MSC) e para manutenção do fenótipo de condrócitos em cultura. As formas de estimulação mais comuns são pressão hidrostática, compressão direta e tensão de corte.

Neste trabalho a ideação e o desenvolvimento do desenho de um bioreator, são feitos considerando a estimulação de *constructs* para engenharia de tecidos de cartilagem articular. O reator final contém duas câmaras independentes para perfusão associadas a cada um dos lados do *construct*, esta capacidade será útil para diferenciação osteocondral.

O equipamento de estimulação inovador apresentado combina estimulação por compressão direta e tensão de corte por contacto. Este desenho foi designado de excêntrico devido às semelhanças com as peças mecânicas com esse nome.

As evoluções do bioreactor foram modeladas em 3D pelo software de CAD Solidworks. As capacidades de simulação deste programa foram utilizadas também para simulação CFD do escoamento da perfusão e os resultados obtidos indicam que as velocidades intersticiais de um scaffold típico serão compatíveis com condrogénese de MSC.

O bioreactor foi parcialmente prototipado e a maioria das partes foi produzida por impressão 3D. Finalmente, foi também contruído um circuito para controlar e acionar o mecanismo de estimulação, a um nível de *proof-of-concept*.

Palavras Chave: Bioreactor, articulações, cartilagem, MSC, condrócito, compressão, fricção

Table of contents

1.	Aim of Studies	1
2.	Introduction	2
2.1.	Overview of Articular Cartilage	2
2.1.1.	The Location and function of articular cartilage	2
2.1.2.	Articular cartilage composition and morphology	3
2.1.3.	Articular cartilage physiology	5
2.1.4.	Articular cartilage disease and dysfunction	12
2.1.5.	Current treatment methods.....	16
2.2.	Articular Cartilage tissue engineering	18
2.2.1.	The need for tissue engineering.....	18
2.2.2.	Cell Source for cartilage tissue engineering.....	18
2.2.3.	Scaffolds for chondrocyte differentiation	20
2.2.4.	Biochemical and environmental cues	20
2.2.5.	Mechanical Stimulation.....	21
2.2.6.	Bioreactors for articular cartilage tissue engineering.....	30
3.	Materials and methods	37
3.1.	CAD design.....	37
3.2.	Computational fluid dynamics	37
3.3.	Prototyping.....	39
3.3.1.	3D Printing/ Additive manufacturing	39
3.3.2.	Actuation Control/ Drive	40
4.	Results and discussion	41
4.1.	Design Objectives	41
4.1.1.	Mechanical stimulation	42
4.1.2.	Culture conditions	44
4.1.3.	Scaffold and tissue construct and Cell type	45
4.1.4.	Maintenance of sterility	46
4.1.5.	Scalability.....	46
4.1.6.	Construction methods.....	47
4.2.	Ideation for the Bioreactor design: Integration of different mechanical stimulus with perfusion	48
4.2.1.	The choice of Perfusion.....	48
4.2.2.	Integration of perfusion with hydrostatic pressure.....	49
4.2.3.	Integration of perfusion and Direct compression.....	51

4.2.4.	Integration of perfusion with direct compression and contact shear	52
4.3.	3D modeling for ideation and concept of novel bioreactor designs	53
4.3.1.	The two-scaffold contact bioreactor.....	53
4.3.2.	Rotor Bioreactor design	57
4.4.	The Cam design: ideation and modelling.....	58
4.5.	Computer fluid dynamics modeling	69
4.6.	Prototyping.....	72
5.	Conclusions and future work	77

List of Figures

Figure 1 - Simplified representation of a diarthrodial joint ³	2
Figure 2 - Various locations and classes of synovial joints with regards to movement type ⁵ ..	3
Figure 3 - a) Microscopy image of chondrocyte after toluidine blue staining; b1) Cross section representation the cellular organization of healthy articular cartilage; b2) cross section representation of the collagen fibre architecture in healthy articular cartilage; adapted from Fox, et al (2009) ⁶	4
Figure 4 - Representation of the various important components of the articular cartilage extra cellular matrix; the two main components responsible for the mechanical properties of articular cartilage are represented, collagen (mostly type II) and proteoglycans (most importantly aggrecan). The interaction of these two opposite charged molecule types provides the tensile and compressive strength of the tissue. Other minority components are also represented mostly non collagenous proteins and smaller proteoglycans ⁶	5
Figure 5 - Graphical synthesis of SOX9 up and downstream regulation. In the context of MSC chondrogenic differentiation, paracrine factors like TGF- β , FGFs, or BMPs up regulate N-cadherin and SOX9 while Wnts down regulate these. The activation of the effectors SOX5 and SOX6 activates the characteristic chondrogenic genes, adapted from Quintana et al (2009) ³²	7
Figure 6 - Schematic representation of the differentiation pathway of chondrogenesis and endochondral bone; a) the proliferation and associated condensation of MSC is a major cue for the initiation of the differentiation process; b) the first step in chondrogenesis is the differentiation of MSC into chondroblasts; c) the differentiation into mature chondrocytes is associated with the secretion of ECM components; d) under non physiological mechanical or environmental cues the differentiation continues into hypertrophy; e) endochondral ossification is the terminal differentiation status associated with apoptosis of chondrocytes, degradation of ECM, vascularization and invasion of the tissue by osteoblasts ⁶⁸	9
Figure 7 - Illustration of the ploughing effect present in a moving joint, adapted from Mow et al (1993) ⁴	10
Figure 8 - Graphical representation of the morbidity of osteoarthritis worldwide. Data is of the age-standardised disability-adjusted life year rates by country per 100 000 inhabitants, from the WHO ³²	13

Figure 9 - Current surgical methods for articular cartilage regeneration; a) mosaicplasty; b) debridement; c) microfracture⁸² 17

Figure 10 – a) Schematic representation of ACI, autologous chondrocyte implantation first cell based therapy method for chondral defect repair; b) photography of a prior and post treatment lesion treated with ACI⁸². 17

Figure 11 – Chart of the published clinical and preclinical articles using either MSC or chondrocyte for scaffold/cell osteochondral defect repair, showing a trend for MSC to become the preferred cell. ²⁵⁸ 19

Figure 12 – Schematic representation of the three most common forms of mechanical stimulation used in articular cartilage tissue engineering, the red arrows represent the direction of the forces applied to the tissue engineering constructs; a) shear; b) hydrostatic pressure; c) direct compression; image adapted from¹⁵⁶..... 21

Figure 13 – Schematic representation of traditional bioreactors used for articular cartilage tissue engineering; a) spinner flask; b) rotating bead bioreactor; c) Uniaxial compression apparatus; d) rotating wall vessel; e) perfusion bioreactor. Adapted from Martin et al (2004)²⁰³ 31

Figure 14 – Schematic representation of various bioreactor architectures for hydrostatic pressure; a) direct pressurization by a piston to the culture media; b) Indirect pressurization by a compression fluid the cell cultures are placed within a sealed bag or other closed vessel; c) Pressurisation of the cultivation media through injection of gas to the culture chamber; d1) Bioreactor with perfusion and a pressure chamber with a membrane in the interface with the culture chamber; d2) Pressurization by injection of fluid to the pressure chamber; e) Perfusion system that induces moderate hydrostatic pressure by use of a actuated valve and a pump. Adapted from Zvicer et al (2017)²¹⁴ 33

Figure 15 – Representation of various configurations direct compression Bioreactors; a) traditional loading apparatus with a culture dish that can be operated within an incubator adapted from Waldman et al (2006)²¹⁹; b) multiple well stimulation apparatus adapted from Correia et al (2016)²²⁰; c) stimulation apparatus to be used submerged in culture media, includes a screw driven compression actuator and rollers as actuators capable of rotating and as such inducing contact shear Shahin et al (2012)²²¹; d) Bioreactor combining perfusion with direct compression, the beads or sheet constructs are placed in the well and the media perfuses in the greater chamber, the actuator is shaped as is the well like a semi-sphere adapted from

Gharravi et al (2012)²²²; f) Comercial bioreactor BOSE ElectroForce® with perfusion and compression, adapted from Brunelli et al (2019)²⁰⁶. 34

Figure 16 – Schematic representations and photographs of a selection of bioreactor designed to recapitulate the mechanical environment of the joint; a) dual axis actuating apparatus composed of a arm on rail that induces movement parallel to the plane of the construct inducing contact shear, this arm supports a compression actuator Bilgen et al (2013)²²³; b1) image of a typical pin and ball bioreactor design;b2) the bioreactor is composed of a pin capable of moving the ball actuator in the perpendicular plane to the plane of the construct, inducing compression, and the actuator the ball is capable to rotate producing contact shear, Vainieri et al (2018)¹⁸²; c1) cell culture part layout of the bioreactor ;c2) model of the culture chamber and 3D printed joint, these two halves of the chamber join to form an articulating perfused chamber, allowing the movements to mimic the moving knee-joint; c3) Driving mechanism that allows for movement of the 3D printed joint within the chamber to move in the two anatomical axis for the knee-joint, Jeong et al (2019)²²⁴. 35

Figure 17 – Image of the 3D printer used in the prototyping phase of this work, the MakerBot Replicator 2x; image obtained from pinshape.com..... 39

Figure 18- Mechanical regulatory model of Pendergast et al (1997)²³⁸ modified by Stops et al (2010)²³⁷ to include necrosis. Octahedral shear strain is the shear strain (described in the biomechanics section) as simulated the FE mesh cells in octahedral shape. Fluid velocity in this case refers to the velocity felt by the cells, in the case of porous scaffolds this is the interstitial fluid velocity. 44

Figure 19 - Schematic representation of the main possibilities for perfusion; a) direct perfusion on the big surface of the scaffold; b) direct perfusion on the smaller surface of the scaffold; c) chamber perfusion; d) orthogonal chamber perfusion; the → (blue arrow) represents the direction of flux, the yellow box represents the scaffold. 49

Figure 20 – Schematic cut representation of concepts for integration of perfusion with hydrostatic pressure actuated by a piston; a1) bioreactor with parallel perfusion including actuated valves and a piston for pressurization, in the unpressurized state; a2) same bioreactor in pressurized state with the piston pushed down and the valves closed; b1) bioreactor with orthogonal chamber perfusion, in this concept the entering fluid flow is incorporated within the piston shaft; b2) same bioreactor in the pressurized state; the → (blue arrow) represents the direction of flux, the yellow box represents the scaffold, grey represents

the piston, ; the → (orange arrow) represents the direction of movement of a component, the valve symbol when filled in black is in the closed state otherwise is open. 49

Figure 21 – Modification of the piston actuated hydrostatic pressure perfusion bioreactor instead using a membrane and a compressed fluid that can be air, pumped water or another fluid; a) system in the unpressurized state; b) system in the pressurized state with the membrane being stretched by the pressure fluid transmitting pressurization to the culture chamber; the → (blue arrow) represents the direction of flux, the yellow box represents the scaffold, green represents the membrane, ; the → (green arrow) represents the direction of flow of the pressurization fluid, the valve symbol when filled in black is in the closed state otherwise is open. 50

Figure 22 - schematic cut representation of a bioreactor concept including direct perfusion and hydrostatic pressure induced by a compressed fluid; a) bioreactor in the unpressurized state, it contains a biconical shaped chamber within a cubical shaped pressure vessel, the chamber is made of a flexible membrane material, the inner chamber is the culture chamber that contains the fixed scaffold; b) bioreactor in a pressurized state, when pressurized fluid is injected in the outer pressure chamber the flexible culture chamber shrinks increasing the hydrostatic pressure felt by cells in the construct. the → (blue arrow) represents the direction of flux, the yellow box represents the scaffold, green represents the membrane, ; the → (green arrow) represents the direction of flow of the pressurization fluid, the valve symbol when filled in black is in the closed state otherwise is open. 50

Figure 23 – Bioreactor design incorporating direct perfusion and direct compression, with a flexible culture chamber and an outside box structure that in the compression state presses against the culture chamber walls and trough this compresses the cell construct; a) bioreactor in the non-compressed state with direct perfusion culture; b) bioreactor in the compressed state in which the linear actuators push the outside box walls to compress the scaffold; the → (blue arrow) represents the direction of flux, the yellow box represents the scaffold, grey represents the mechanically actuating parts, ; the → (orange arrow) represents the direction of movement of a component, , green represents the membrane that forms the biconical shaped culture chamber, black represents the linear actuator. 51

Figure 24 – Schematic cut representation of a chamber perfusion, direct compression and contact shear bioreactor concept, the concept is composed of a culture chamber constituted by a flexible cylinder in which perfusion is made, this chamber contains a scaffold and a soft

material actuator fixed opposite each other; a) Indirect perfusion operation of the bioreactor with no mechanical stimulation other than perfusion; b) Direct compression operation, the z axis linear actuators push the actuator against the scaffold producing the deformation of the scaffold; c) the contact shear is produced by activating the x axis linear actuator moving the scaffold in relation to the actuator, producing drag between both surfaces; the → (blue arrow) represents the direction of flux, the yellow box represents the scaffold, grey represents the mechanically actuating parts, ; the → (orange arrow) represents the direction of movement of a component, , green represents the membrane that forms the biconical shaped culture chamber, black represents the linear actuator and orange box represents the soft material actuator..... 52

Figure 25 – reactor design concept including direct perfusion and mutual compression of two articular cartilage constructs, this design includes a culture chamber that contains two constructs, this chamber is flexible allowing the stretching and contraction that elicits the compression of the constructs against each other; a) direct perfusion operation of the bioreactor before compression action; b) compressed state of the bioreactor the linear actuator pushes the structure of the outside box that because of this pushes the construct against the other construct that remains static; the → (blue arrow) represents the direction of flux, the yellow box represents the scaffold, grey represents the mechanically actuating parts, ; the → (orange arrow) represents the direction of movement of a component, , green represents the membrane that forms the biconical shaped culture chamber, black represents the linear actuator..... 54

Figure 26 – Cut schematic representation of the joint mimicking bioreactor concept; a) direct perfusion operation similar to the one presented for the previous design concept, in the state without compression and contact shear; b) bioreactor state where the linear actuator is causing compression of both cell-scaffold constructs; c) stimulation state where an electric step motor is activated to trough a belt rotate a gear that is associated with the lower scaffold older, this gear travels through a gear rack that produces a linear motion that is transmitted to the scaffold holder that moves in a pendulum like motion producing surface drag between the two constructs; the → (blue arrow) represents the direction of flux, the yellow box represents the scaffold, grey represents the mechanically actuating parts, ; the → (orange arrow) represents the direction of movement of a component, 54

Figure 27- Two different profile views of the 3D model of the joint mimicking bioreactor concept design, produced in Solidworks 55

Figure 28 – The rotor bioreactor concept, a perfusion system; a) schematic cut representation of the rotor bioreactor concept , it is composed of a donut shaped culture chamber, a rotor with two “arms” in the centre of the donut, this arms are magnetically clamped to magnetic scaffold holder, this rotor rotating makes the scaffold travel in the culture chamber in a circular pattern; b) top-down vision of the 3D model of the bioreactor; c) profile of the bioreactor. → (blue arrow) represents the direction of flux, the yellow box represents the scaffold, grey represents the mechanically actuating parts, ; the → (orange arrow) represents the direction of movement of a component 57

Figure 29 – Representation of the motion profile of a mechanical stimulation device with the pendulum type motion profile; a – scaffold face length; b – maximum deformation of the construct; d – diameter of the motion profile. 58

Figure 30 – Charts for the dimensioning of the pendulum style actuating system; a) chart of $\Delta\bar{x}/b$ with dependence on the profile diameter in cm, with $b= 0.04$ cm and $a= 2$ cm it is valuable at indicating the trend in increasing the size of the apparatus versus the benefit of increasing the homogeneity of the stimulus; b) chart of Profile diameter (d) in cm needed to achieve a certain ratio $\Delta\bar{x}/b$ depending on scaffold size (a) also in cm, the ratios studied were $\Delta\bar{x}/b - 0.75, - 0.80, - 0.85, - 0.90, - 0.95$ 59

Figure 31- First iteration of design of the Cam Bioreactor; a) schematic top-down view of the bioreactor design with the cam in the middle of the culture chamber, the rotation of the cam produces a combination of contact shear and direct compression, perfusion is still designed to be direct; b) top-down view of the model for the design; c) profile view of the model..... 60

Figure 32 – Early designs for the Cam Bioreactor; a) Early design that proposed the use of two separate agitated chambers, the two agitators are represented in both the upper and lower end of the bioreactor, the cam remains in the centre of the bigger chamber; b) Second design in which the chambers are moved to one end, the bigger chamber contains a smaller media volume and the bigger agitated chamber should act as a pump producing perfusion in the bigger chamber; c) top-down view of the bioreactor model for the two mixing chambers initial design; d) detail of the bigger culture chamber containing the cam actuator; the → (orange arrow) represents the direction of movement of a component. 61

Figure 33 – Second evolution of the design of the cam bioreactor, including the screw design position adjustment system and revised perfusion/ agitation system. a) cut view of the model showing the internal channels that provide fluid flow into the main chamber, and the internal part of the two pumping chambers on the lower part, on each side of the secondary chamber; b) wire frame view of the bioreactor showing the agitators/ turbines in the pumping chambers as well as the channels to move the culture media within the bioreactor and the thread in the secondary chambers that would allow precise positioning of the scaffold; c) profile view of the design. 62

Figure 34 – Third evolution of the cam bioreactor design; a) top-down cut view of the bioreactor, the internal fluid flow chambers are visible as well as the complexity of the redesigned secondary chamber separated in two sub-chambers one for incoming and another for outgoing media; b) profile view of the modified bioreactor body design and where the modified main chamber is visible with further reduced space for fluid volume; c) top down view of the bioreactor with the exposed pumping chambers. 63

Figure 35 – Illustrative images of the fluid containing areas of the third evolution bioreactor design; a) 3D model of the rotating component of the secondary chamber, on the top right the conical culture chamber is visible with the diffuser like entrances, the entrance chamber is visible just below that as a donut like shaped cut of the component and lower is the exit chamber; b) cut of the 3D model of the secondary chamber including the rotating component in the middle with the represented scaffold in the top of the conical culture chamber, the static component of the secondary chamber that is fixed to the bioreactor body is represented in the outside, and the two smaller entrance and exit chambers that are limited by the conjunction of the rotating and stationary component, the sealing designs are not present since the design evolved before this were designed; c) channels of flow of media to the perfusion of the main chamber; b) channels of perfusion of media for the secondary chamber. The green painted areas represent the fluid filled areas. 64

Figure 36 – Detail of the final model for positioning system of the tissue engineering construct, to adjust the strain produced by the action of the mechanical stimulation apparatus. (screw is only a illustrative model) 66

Figure 37 – a) centrifugal pump design; b) centrifugal pump vertical axis cut; c) centrifugal pump horizontal axis with the detail of the turbine cut; d) peristaltic pump with the tubing in

yellow translucent; e) cut of the centrifugal pump with the detail of the pumps actuating gears. 67

Figure 38 – Model of a potential form of parallel integration of the bioreactor. 68

Figure 39- 3D models of the final bioreactor design; a) back view of the bioreactor showing the spot for entrance and exit tube fitting fixing on each of the chambers; b) lateral view of the bioreactor; c) cut of the lateral view of the bioreactor, on the top it shows the detail on the fixing of the actuator to the axel, lower the cut of the culture chambers is visible; d) front view of the bioreactor; e) top view of the bioreactor; f) top view cut of the bioreactor exposing the view of the culture chamber; g) frontal view cut of the bioreactor showing the internal channels for fluid flow into and out of the two chambers; h) profile view of the bioreactor. 68

Figure 40 – Graphical representation of the results of CFD for 2mL/s; a) Boundary conditions graphical synthesis; b) central cut of the chamber fluid velocity contours..... 69

Figure 41 – Graphical representation of the results of CFD produced in the Solidwoks flow simulation plugin; results obtained for 0.5 mL, 1 mL and 2 mL as signalled, on the right the results of total pressure exerted over the construct are represented on the right is the intensity of Shear stress exerted on the surface; the two contours chart bellow represent the velocity of the fluid in a cut at the middle plane of the culture chamber. 70

Figure 42- Mechanical regulatory model of Pendergast et al (1997)²³⁸ modified by Stops et al (2010)²³⁷ to include necrosis, the markings show the expected compression in operation conditions for the bioreactor and the associated interval of fluid velocities that are associated with chondrogenic differentiation of MSC..... 71

Figure 43 - 3D printed components of the bioreactor; a) main Bioreactor chamber; b) Cam actuator; c) Ball-bearing for the actuator axle; d) Actuator axle parts; e) Secondary chamber; f) bigger flat gear; g) smaller flat gear h) Nuts; i) Positioning system base; j) bigger bevel gear ; k) smaller bevel gear; l) bevel gear support; m) tubing fitting. 72

Figure 44 – Close comparison of the main components’ models and 3D printed parts; a) main Bioreactor chamber; b) Cam actuator; c) Actuator axle parts; d) Secondary chamber; e) bigger flat gear; f) smaller flat gear; g) bigger bevel gear; h) smaller bevel gear; i) positioning system base. 73

Figure 45 - 3D printed peristaltic pump initial prototype..... 73

Figure 46 - Final Bioreactor prototype 74

Figure 47 – Photography of the proof of concept circuit for controlling the actuating movement; a) step motor; b) Arduino board; c) Breadboard; d) Power source; e) step motor driver integrated circuit board; schematic representation obtained from makerguides.com and shows the wiring diagram for the circuit used..... 75

Figure 48 - Arduino sketch code in the Arduino IDE application, this code is designed to drive the step motor in a rotation that is exact to the travel needed in the bioreactor and then turn back and do the same movement in the inverse direction. 76

List of Tables

Table 1 - Load of the knee joint, forces presented in % of bodyweight (BW)	10
Table 2 - Cartilage Strains in Response to Dynamic Activity	11
Table 3 - Representative examples of studies targeting the effects of hydrostatic pressure stimuli for cartilage tissue engineering applications	22
Table 4 - - Representative examples of studies targeting the effects of contact shear stress stimuli for cartilage tissue engineering applications.	25
Table 5 - Representative examples of studies targeting the effects of contact shear stress stimuli for cartilage tissue engineering applications.	26
Table 6 - Representative examples of studies targeting the effects of direct compression stimuli for cartilage tissue engineering applications.	28
Table 7 – Synthesis of the frontier conditions and number of iterations by CFD assay	38
Table 8 - 3D printing parameters	40
Table 9 – Synthesis of the design Objectives for the Bioreactor	41
Table 10- Synthesis of the design objectives comparison with the capabilities of the final design	77

List of Abbreviations

ABS – Acrylonitrile Butadiene

AC – Articular cartilage

ACI – Autologous chondrocyte implantation

bCHD – Bovine chondrocyte

BMP – Bone morphogenic protein

BMP-2 – Bone morphogenic protein 2

CAD – Computer-aided design

canCHD – Bovine chondrocyte

CFD – Computational fluid dynamics

COL – Collagen

COL2A1 – Gene that codifies for the pro-alpha1(II) unit of collagen type II

COLII – Collagen type II

DC – Direct compression

ECM – Extra-cellular-matrix

eqCHD – Equine chondrocyte

eqMSC – Equine mesenchymal stem cells

ERK – Extracellular signal-regulated kinases

FGF-2 – Basic fibroblast growth factor

GAG – Glycosaminoglycan

GMP – Good manufacturing practices

hASC – Human adipose stem cell

HB – Hydrostatic pressure

hCHD – Human chondrocyte

hMSC – Human mesenchymal stem cells

IGF1 – Insulin-like growth factor 1

IL 1 – Interleukin-1

IL 4 – Interleukin-4

JAK – Janus kinases

JNK – c-Jun N-terminal kinases

MAPK – mitogen-activated protein kinase

MMP-13 - Gene that codifies for collagenase II

MSC – Mesenchymal stromal cell

NF- κ B – nuclear factor kappa-light-chain-enhancer of activated B cells

OA – Osteoarthritis

PCL – Polycaprolactone

PLGA - Poly(lactic-co-glycolic acid)

porCHD – Porcine chondrocyte

PTOA – Post traumatic osteoarthritis

Rho – Family of GTPases

Rho-A – Ras homolog family member A

Rock - Rho-associated protein kinase

RunX2 – Runt-related transcription factor 2

SOX9 – Protein encoded by the same named gene that acts as a transcription factor

STAT – Signal transducer and activator of transcription proteins

TGF- β – Transforming growth factor beta

TNF- α – Tumor necrosis factor alfa

1. Aim of Studies

Articular cartilage is a tissue that presents relatively high morbidity rates for the elder population with low physical activity, and consequently low demand on the tissue, as well as younger patients with high physical activity, elite athletes are a particularly affected population.

The physiology and anatomy of Articular cartilage (AC) creates a tissue with limited self-repair ability. Due to the limitations of the current therapeutic options a need for better solutions exists, one option to improve the current therapeutic techniques is the use of tissue engineering.

Tissue engineering is a multicomponent field of study, the most important components are, the cell, the scaffold and the culture methods, the culture is mediated by the bioreactor.

This master's thesis project focuses precisely in the development, design, modeling and prototyping of a novel bioreactor for AC tissue engineering. In particular the focus is in the development of a mechanical stimulation apparatus integrated into a bioreactor system.

Mechanical stimulation including hydrostatic pressure, direct compression and shear stress is well established in the current literature as an important cue for the definition of mesenchymal stem cell fate into osteochondral differentiation and specifically to chondrogenic differentiation. These mechanical stimulation cues are also associated with maintaining chondrocytes in culture with a hyaline cartilage like phenotype and avoiding expression of hypertrophic markers.

This project will be started with ideation of possible bioreactor designs, these designs should be developed into a final concept for the bioreactor. This final concept bioreactor will be modelled using a computer-aided design (CAD) program and its fluid flow characteristics will be verified by computational fluid dynamics (CFD) to verify if the mechanical stimulus of fluid induced shear stress can be of relevant magnitude for AC tissue engineering. Finally, a prototype of the bioreactor will be produced.

The expected outcome of this work is the prototype of a Bioreactor that can be used in a research setting but with clinical translation capacity, for this reason the clinical needs for AC constructs will be taken into account.

2. Introduction

2.1. Overview of Articular Cartilage

2.1.1. The Location and function of articular cartilage

Articular cartilage (AC) is a connective tissue that is mainly found in diarthrodial joints, also classified as synovial joints¹. These joints have a common anatomy composed by the articular cartilage and the synovial membrane enclosing the synovial cavity, which contains the synovial fluid. The synovial membrane encloses all of the articular surfaces other than the weight bearing surfaces that are covered by articular cartilage.

The previously mentioned synovial fluid is very important in joint physiology because, in addition to its role in tissue biomechanics, the articular joint cartilage is avascular and as such obtains most of its nutritional needs from the synovial fluid². Other than avascular, articular cartilage also lacks lymphatic vessels and nerves².

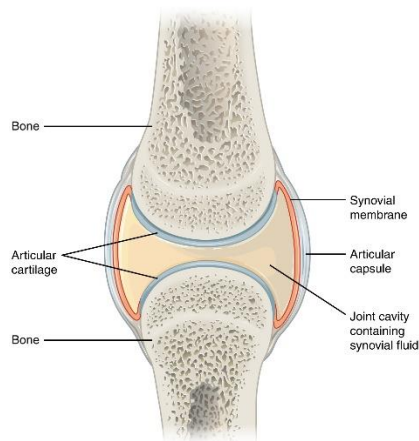


Figure 1 - Simplified representation of a diarthrodial joint³.

Diarthrodial joints are a common structure in animals, which are located between skeletal segments and allow the relative motion between such segments. These complex structures can be compared to man-made engineering bearings, having similar biomechanical requirements such as lubrication but also able of weight support. When healthy, these joints are capable to keep a virtually frictionless operation, diminishing wear between bone segments to a minimum⁴.

Various functions are associated with joint movement, the most obvious being locomotion, in humans associated with lower limbs as well as other functions like the use of the hands and digits. Different specific types of joints are associated with different types of movement¹. Various types of joints are represented in figure 2, according to the movement and anatomical characteristics as well as their places of occurrence in the human osteo-skeletal system.

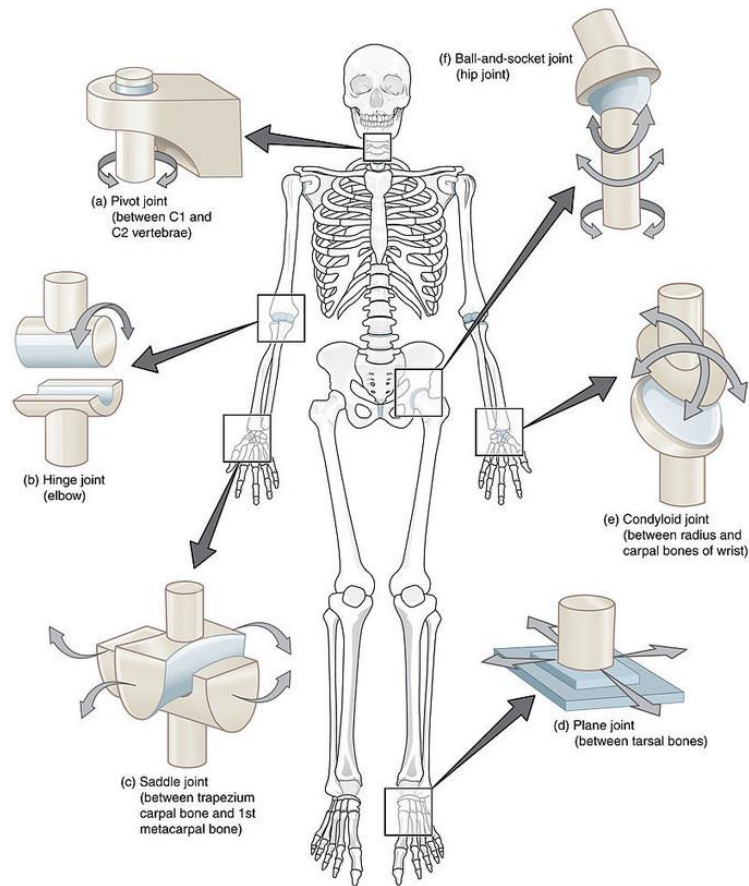


Figure 2 - Various locations and classes of synovial joints with regards to movement type⁵

Articular cartilage is also involved in the development and growth of bones, mostly cartilaginous joints of long bones such as the epiphyseal plate, composed of hyaline cartilage which is replaced by bone tissue as maturity is achieved¹. One other cartilage type, fibrocartilage, is also present in symphysis types of joints (for example, in the intervertebral symphysis), providing stronger connection between bones but with limited movement¹.

In this thesis, hyaline cartilage in synovial joints is focused on exclusively. This tissue's main function is to offer a coating surface with low friction for bones and a medium for mechanical load transfer in the joints⁶.

2.1.2. Articular cartilage composition and morphology

The articular cartilage, which is the specific name given to hyaline cartilage when located in joints, is composed of a dense extracellular matrix (ECM) and a relatively sparse population of cells, the chondrocytes⁷.

Chondrocytes represent about 2%⁸ of the total volume of tissue, which indicates the relatively low cellularization of articular cartilage. Nevertheless, these cells are essential for the formation and maintenance of the tissue, possessing high metabolic activity and synthesizing the ECM components⁶.

Chondrocytes are known to differentiate from mesenchymal stem/stromal cell origin⁸, an adult stem cell multipotent population that is known to give origin to cells of the skeletal system as well as others. The origin of the cell progenitors is important for tissue regeneration, as it will be discussed ahead. Depending on the cartilage region, chondrocytes are present in different densities and different morphological phenotypes. In the superficial regions, cells appear in higher density and with a smaller size and flatter phenotype⁶. A microscopy image of the chondrocyte is available in figure 3 a).

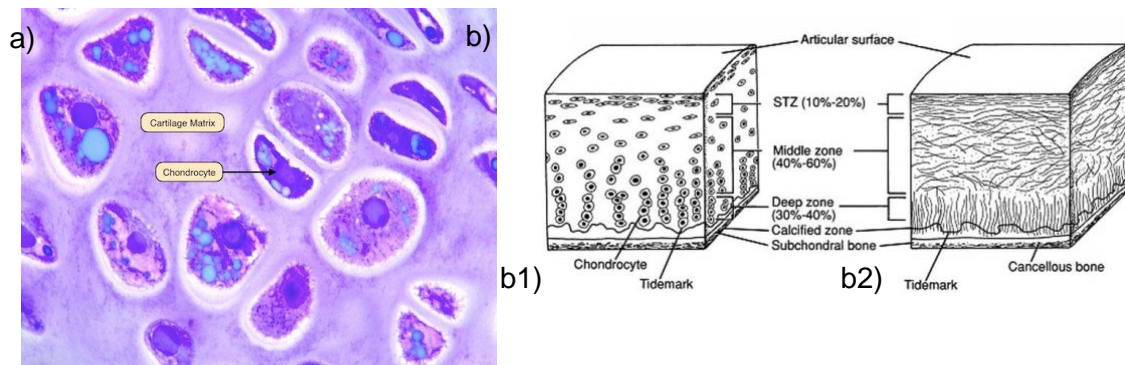


Figure 3 - a) Microscopy image of chondrocyte after toluidine blue staining; b1) Cross section representation the cellular organization of healthy articular cartilage; b2) cross section representation of the collagen fibre architecture in healthy articular cartilage; adapted from Fox, et al (2009) ⁶

Articular cartilage structure can be divided in four different zones, distributed along an axis from the surface to the underlying bone: superficial zone, the middle zone, the deep zone, and the calcified zone. These zones/regions are defined by different ECM compositions, ultrastructure and, as mentioned, chondrocyte density⁷. The zones of Articular cartilage are schematically represented in figure 3 b).

The ECM of articular cartilage is mostly composed of water, collagen, and proteoglycans. Collagen, the most abundant biomolecule of the ECM being two thirds of the dry mass of tissue ⁹, is mostly of type II ($\geq 90\%$ total of collagen), but collagens type III, VI, IX, X, XI, XII and XIV⁹ are also present in smaller quantities. The abovementioned zones of the tissue are in a great deal dependent on the organization and disposition of collagen fibrils. Accordingly, there is also some variation of collagen composition in the different zones. For example, collagen type X is generally only present in the calcified zone, the interface region between the cartilage and the underlying bone ⁹.

Proteoglycans are heavily glycosylated protein monomers and the second most abundant biomolecules in the ECM of this tissue. The most important and predominant proteoglycan in cartilage is aggrecan. In contrast to collagen, aggrecan's effect on the mechanical properties of articular cartilage is indirect. The most important function of aggrecan is to convey the tissue its osmotic properties that allow for the entrapment of water in such a way as to confer resistance to compression forces¹⁰. Moreover, aggrecan is also known to interact with hyaluronic acid forming large proteoglycan aggregates¹⁰. The remaining proteoglycans are smaller and mostly interact with collagen¹⁰. Proteoglycans as well as the other major ECM components are represented in figure 4.

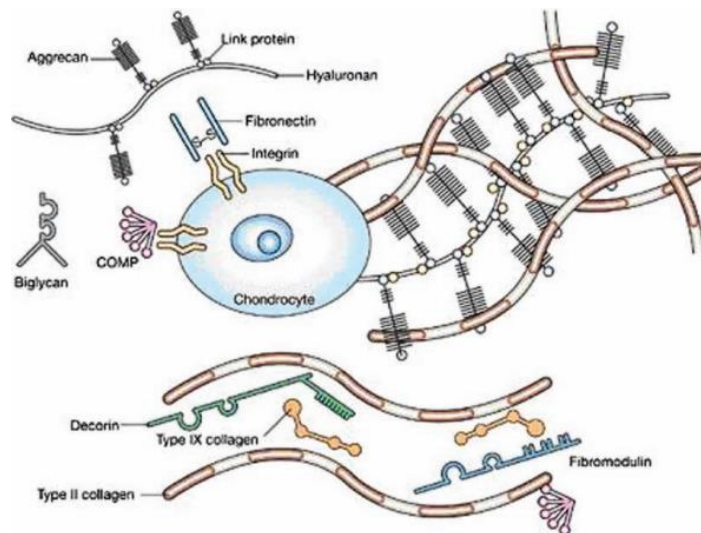


Figure 4 - Representation of the various important components of the articular cartilage extra cellular matrix; the two main components responsible for the mechanical properties of articular cartilage are represented, collagen (mostly type II) and proteoglycans (most importantly aggrecan). The interaction of these two opposite charged molecule types provides the tensile and compressive strength of the tissue. Other minority components are also represented mostly non collagenous proteins and smaller proteoglycans⁶.

2.1.3. Articular cartilage physiology

2.1.3.1. Mass transfer in Articular Cartilage

As discussed in the previous section, articular cartilage is an avascular tissue, which means that there is inherently limited mass transfer from and to this tissue. Therefore, mass transfer of solutes is driven only to or from the contacting tissues.

Synovial fluid is the main source of nutrients, oxygen, and factors, as well as the main place where waste products¹¹ of the metabolism are transferred². The exchange process between the fluid and the cartilage tissue is mostly limited by the diffusion within the tissue, giving rise to a nutrient and oxygen gradient, with the most superficial regions of the tissue being under greater abundance. Accordingly cell density is higher in such superficial areas⁶.

Although articular cartilage is a characteristically porous tissue, convection within it is practically in-existent due to the small pore diameter of the ECM in static liquid conditions, has been estimated at around 6 nm¹². The interstitial liquid present in the tissue is regarded to have a great influence in the biomechanical lubrication¹³ and elastic properties¹⁴ of articular cartilage in the joint.

The tissue that serves as support for articular cartilage is the subchondral plate, which is a thin cortical lamella¹⁵. The subchondral plate is sometimes thought as impregnable but it is actually porous and includes channels that allow interaction between the calcified cartilage region and the underlying subchondral trabecular bone¹⁶. This is the main way the tissue communicates with the underlying bone, but it is not regarded as a main way for nutrient and oxygen diffusion. Thus, the population of chondrocytes lacking direct access to blood vessels is dependent on diffusion within the ECM causing an oxygen limitation, and for this reason, chondrocytes have to rely on anaerobic metabolism⁶.

2.1.3.2. Chondrocyte metabolism

The chondrocytes metabolic activity mostly responds to the necessity of maintaining the ECM homeostasis⁶. For this, two types of activity are needed: a synthetic activity and a hydrolytic activity to generate and remodel the components of the ECM previously discussed.

Notoriously, the chondrocyte metabolism, and consequently, the composition of the ECM, are very responsive to the chemical and physical environment¹⁷. This is observed both *in vivo* and for tissue engineering approaches, which will be discussed in section 2.2.

The synthetic (or anabolic) activity of chondrocytes is dominated by the production of the most abundant molecules of the cartilage ECM, namely collagen (in particular type II) and proteoglycan (in particular aggrecan⁶). The catabolic activity needed for the maintenance of the tissue, and turnover of the ECM, is mostly associated to metalloproteinases¹⁸ and cathepsins⁶. The turnover of the main ECM components is such that the entire content of proteoglycan will be replaced in up to 25 years while the half life of collagen is estimated to take from some decades up to 400 years⁶.

Imbalance of the anabolic and catabolic activity in the tissue is associated with both physiological healthy processes as well as with pathology or loss of function. For example in fracture repair, the metalloproteinase and cathepsin activity is specially high in the fracture callus but, it is also generally associated with hypertrophic tissue¹⁹. Articular cartilage hypertrophy is associated with loss of function, particularly in osteoarthritis¹⁸.

The regulatory processes associated with the metabolism of articular chondrocytes involve a combination of chemical factors and physical cues, which are often interconnected.

The regulation of the chondrocyte metabolism by chemical factors as been studied to some extent, mostly in settings of developmental and differentiation studies or in the context of cartilage diseases such as osteoarthritis²⁰.

As previously discussed, the ECM of articular cartilage is a complex mixture of various macromolecules, mainly various types of collagen, aggrecan and others in smaller quantity. However, the majority component of the ECM in physiological condition is collagen type II⁹, and for that reason, it is the major marker for disease and chondrogenesis, and consequently, the most studied one in the chondrocyte metabolism²⁰. In light of this, the two main genes associated with the anabolic / catabolic control of the composition of the ECM in terms of collagen type II are COL2A1²¹ and MMP-13²², respectively. The gene COL2A1 codifies the pro-alpha1(II) chain, which trimerizes forming a procollagen molecule³, and after enzymatic processing²³, forms collagen type II. MMP-13 is the gene encoding for collagenase 3, the metalloproteinase with high catalytic activity for collagen type II²².

The transcription factor SOX9 is known to be a major regulator of chondrogenesis²⁴ and of various genes associated with the chondrocyte phenotype^{25, 26, 27}. SOX9 is a transcription factor from the SOX family and contains a highly conserved High mobility group²⁸, which binds a variety of regulatory sequences.

This transcription factor SOX9 is known to activate transcription of COL2A1 by binding to an enhancer region located in the first intron of the gene²⁹, acting cooperatively with the L-SOX5 and L-SOX6 factors³⁰. SOX9 is also known to mediate at least in part the anabolic action of extracellular signals³¹. The regulatory pathway of SOX9 is represented in figure 5³². The extracellular signals can be localized, paracrine and autocrine, or of endocrine origin. One of the factors with anabolic action on chondrocyte metabolism is insulin growth factor I (IGF-1), a endocrine signaling molecule with origin in the thyroid and associated with cell proliferation and differentiation in the skeletal growth plate³³. Another important signaling molecule is the bone morphogenic protein 2 (BMP-2). This cytokine in conjunction with IGF-1 is known to stimulate the production of major ECM proteins such as proteoglycans and collagen type II³⁴. Various BMP proteins have been determined to be involved in the chondrogenic differentiation³⁵. Such proteins belong to the greater family of transforming growth factor - beta (TGF- β)

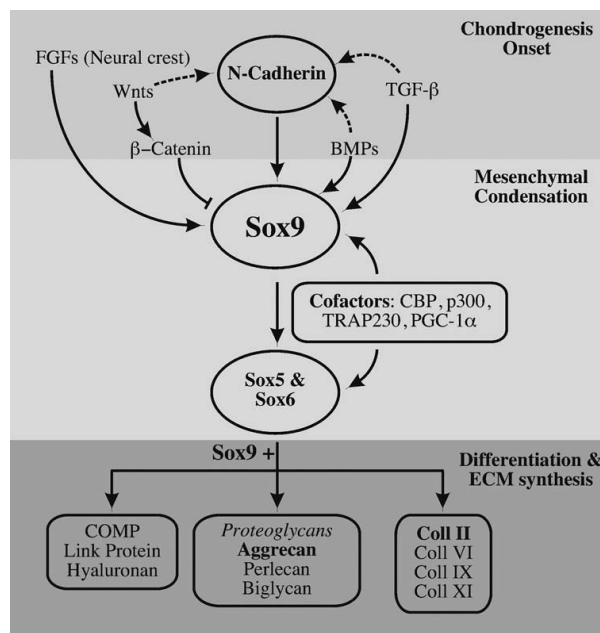


Figure 5 - Graphical synthesis of SOX9 up and downstream regulation. In the context of MSC chondrogenic differentiation, paracrine factors like TGF- β , FGFs, or BMPs up regulate N-cadherin and SOX9 while Wnts down regulate these. The activation of the effectors SOX5 and SOX6 activates the characteristic chondrogenic genes, adapted from Quintana et al (2009)³²

which itself belongs to the TGF superfamily.

One other signaling pathway associated to chondrocyte metabolic regulation and life cycle/differentiation control is the Indian hedgehog, which regulates its effect by a feedback control of parathyroid hormone-related protein³⁶ mediated by Gli transcription factors³⁷. The cell surface receptor triggered signaling pathway Wnt/ β -catenin activated by T-cell factor/lymphocyte enhancing factor and fibroblast growth factors (FGFs) via Stat1/p21³⁷ are other relevant signaling pathways.

On the other hand, signaling associated with catabolic activity is largely related to proinflammatory cytokines, the most important of these being interleukin-1 (IL1)³⁸ and tumor necrosis factor alpha (TNF- α)³⁹. These cytokines act through the signaling pathways of c-Jun N-terminal kinases (JNK), p38 mitogen-activated protein kinase (MAPK) and nuclear factor kappa-light-chain-enhancer of activated B cells (NF- κ B)²⁰. The

effect of these cytokines in the chondrocyte phenotype can be direct activation of catabolic activity or downregulation of anabolic activity. Returning to the example of collagen type II content in the ECM, it is regulated by downregulation of the SOX9 gene lowering the transcription of COL2A1^{31,40}. Collagen II content is regulated also by the expression of MMP-13, the previously referred collagenase, which is known to be transcriptionally activated by IL1 through the signaling pathways JNK and p38 MAPK in conjunction with the constitutively expressed transcription factor Runx2⁴¹. IL1 is also known to activate expression of other cytokines such as IL6 which downregulates the COL2A1 and aggrecan gene expression via the JAK/STAT pathway and suppression of Sox9⁴².

Another important part of chondrocyte metabolism regulation is mechanotransduction⁴³, i.e. the ability of chondrocytes to sense the mechanical properties and forces acting in the cellular environment, which triggers several signaling pathways. As a tissue with inherently mechanical function and under dynamic mechanical environment, the cartilage ECM is highly responsive to mechanical stimulus¹⁷.

The cytoskeleton is a main part of the chondrocyte response to mechanical stress as well as in its phenotype regulation. Cell shape has been recognized to be connected to metabolic phenotype⁴⁴. Chondrocyte differentiation has been found to be dependent on cell shape⁴⁵ as well as on the maintenance of the appropriate phenotype and metabolic regulation⁴⁶. The actin cytoskeleton is a principal determinant of cell shape, and as such, is a main factor determining chondrocyte phenotype. Both in MSC derived cell progenitors and mature articular chondrocytes, a link has been found between the disruption of the actin cytoskeleton and the phenotype^{47,48}. Microtubules appear not to contribute much to chondrocyte shape and consequently, agents that disrupt those, do not affect differentiation⁴⁷. The previously referred anabolic effect of BMP and catabolic effect of IL1 have been demonstrated to be affected by the disruption of the actin cytoskeleton^{49,50}.

The rapid dynamic remodeling of the actin cytoskeleton allows cells to adapt and react to the application of forces⁵¹. In healthy cartilage, it was described that chondrocytes are under hydrostatic pressure⁵² and responding to either static⁵³ or cyclic⁵⁴ strain. Mechanically induced changes within the cartilage matrix⁵⁵ are the cue by which chondrocytes mechanotransduction is initiated, mechanoreceptors at the interface between the cell membrane and ECM⁵⁶ process mechanical signals, mainly through ion channels and integrins.

Chondrocytes experience membrane stretch during compression⁵⁷ and this stimulus is known to activate potassium channels⁵⁸. This stretch-induced matrix deformation, and associated cellular membrane deformation, regulate chondrocyte proliferation and differentiation, the signal being transduced by potassium channels as well as calcium channels⁵⁹.

Integrins are heterodimeric transmembrane receptors consisting of an α and a β subunits⁶⁰. Integrins naturally have a intracellular domain which interacts with cytoskeletal proteins⁶¹ and a extracellular domain that establishes interaction with ECM in cell-substrate interactions⁶². Forces acting on human chondrocyte constructs upregulate aggrecan and downregulate MMP-3 in a pathway involving the $\alpha_5\beta_1$ integrin as a mechanosensor and the release of the IL-4 cytokine⁶³.

The mechanical signals detected by the mechanosensors trigger a response through multiple signaling pathways, the most important being GTPase signaling via Rho-A and Rock^{64,65}. Rho and ROCK or Rho kinase are components in a phosphorylation cascade signaling pathway that has been known to act in the chondrocyte differentiation⁶⁶. Inhibition studies of ROCK signaling performed in monolayer cell cultures and using the Rho kinase inhibitor have shown increase in chondrogenic factors such as cell rounding associated to increased cortical actin organization, and increased glycosaminoglycan synthesis. ROCK-dependent changes in SOX9 messenger RNA (mRNA) expression seemed to be the underlying mechanism; furthermore, studies done in 3D culture systems seem to suggest that the SOX9 is not the sole responsible for the increased matrix gene expression⁶⁷. The various stages of chondrogenesis are represented in figure 6.

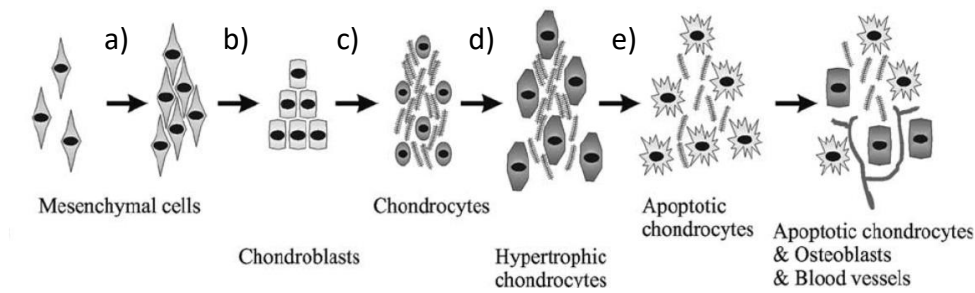


Figure 6 - Schematic representation of the differentiation pathway of chondrogenesis and endochondral bone; a) the proliferation and associated condensation of MSC is a major cue for the initiation of the differentiation process; b) the first step in chondrogenesis is the differentiation of MSC into chondroblasts; c) the differentiation into mature chondrocytes is associated with the secretion of ECM components; d) under non physiological mechanical or environmental cues the differentiation continues into hypertrophy; e) endochondral ossification is the terminal differentiation status associated with apoptosis of chondrocytes, degradation of ECM, vascularization and invasion of the tissue by osteoblasts⁶⁸.

2.1.3.3. Articular Cartilage biomechanics

Biomechanical studies of articular cartilage have been mainly motivated by the previously discussed interaction between mechanical stimulus and chondrocyte phenotype but also by the unusually high loads that this tissue is able to withstand. For example, it is known that knee and hip joints can hold loads of up to 10 times the body weight in routine tasks like walking⁶⁹. In particular, metallic hip prosthesis have been determined to suffer up to 18 MPa of compressive stress⁷⁰ in light physical activity.

The high loads experienced in a rotating joint and, to a smaller degree, in resting have implied high contact stress. To counteract these stresses and prevent friction, the tissue is capable of lubricating to a high degree⁴. Biotribology studies the interaction of two surfaces in relative motion, in particular, surfaces of biological nature and has been evolving in the study of articular cartilage. The mechanisms for lubrication presently accepted are biphasic lubrication of articular cartilage when the fluid support is enough to counteract the load and boundary lubrication when the fluid support is no longer enough to support the existing load⁷¹.

The friction coefficient (μ), a dimensional scalar metric, describes the ratio of the force of friction between two bodies and the force pressing them together, has been determined for articular cartilage in the joint of various animals to be in the range of 0.002 and 0.35, the later value being in conditions of low fluid present in the joint. A friction coefficient of 0.01 is considered to be the maximum value that occurs in physiological conditions, which is a very low value, suggesting very low friction⁴.

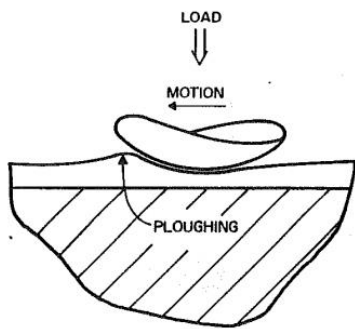


Figure 7 - Illustration of the ploughing effect present in a moving joint, adapted from Mow et al (1993) ⁴

Ploughing friction, which working principles are schematically shown in figure 7⁴, is a main mechanical phenomenon occurring in articular cartilage; it consists of the combination of a load with motion in an orthogonal direction. Joint cartilage is a relatively soft tissue allowing this type of mechanical phenomenon.

The compressive or Young's modulus is a measurement of the force needed to deform a body, defined as ratio between the uniaxial stress and the proportional deformation. The articular cartilage tissue has a compressive modulus of around 1 MPa ⁷² determined in confined compression assays, which vary greatly depending on location and subject, being measured as high as 6.3 MPa in a 63 year old male subject's ankle joint cartilage and 4.8 MPa in the same subject's knee⁷³.

The shear modulus on the other hand describes a body's response to shear stress being defined as the ratio of shear stress to shear strain. For articular cartilage the shear modulus is traditionally around 0.5 MPa while the Poisson's ratio varies between 0 and 0,42⁴. The Poisson's ratio is an adimensional value used to describe the behavior of a body's strain in the orthogonal direction to the one of an uniaxial stress.

It is important to note that these values are determined assuming linear elasticity which is only possible for cartilage under infinitesimal strain⁷². Strain in the order of 0.1 is still practically considered infinitesimal.

Table 1 - Load of the knee joint, forces presented in % of bodyweight (BW)

		Axial force (%BW)	Lateral shear force (%BW)	Anterior shear force (%BW)
Kutzner et al (2010) ⁷⁴ Note: Data measured by an instrumented tibial component	Two-legged stance	107%	1%	2%
	Sitting down	225 %	6%	11%
	Standing up	246 %	7%	10%
	Knee Bend	253 %	8%	11%
	One-legged stance	259 %	10%	-7%
	Level walking	260 %	11%	15%
	Ascending stairs	316 %	15%	17%
	Descending stairs	346 %	16%	18%

Ploughing friction is a main stress in articular cartilage and the lubrication response to this is theorized to be the referred Biphasic lubrication. This theory is based on the assumption that when under strain the water entrapped in the tissues molecular sized pores flows outwards producing a lubricating effect⁷¹. The low permeability of the tissue $10^{-15} \text{ m}^4/\text{Ns}^4$ is thought to, with the fluid flow, induce a high drag force that combined with the fluid pressurization allow for energy dissipation and load support⁴.

Table 2 - Cartilage Strains in Response to Dynamic Activity

Sutter et al (2014) ⁷⁵ Note: Measured by MRI after dynamic activity consisting of single legged jumps.	Tibia medial compartment average	Average: $5\% \pm 1\%$ Maximum (lateral) : $8\% \pm 1\%$
	Tibia lateral compartment	Average: $5\% \pm 1\%$ Maximum (medial) : $7\% \pm 1\%$
	Femur medial compartment	Average: $2\% \pm 1\%$ Maximum (medial) : $6\% \pm 1\%$
	Femur lateral compartment	Average: $1\% \pm 1\%$ Maximum (medial) : $3\% \pm 1\%$
Chan et al (2016) ⁷⁶ Note: Measured by MRI synchronized with physiologically relevant compressive loading by a pneumatic device.	Femur maximum principal strain	Male: $8.0\% \pm 2.2\%$ Female: $10.6\% \pm 4\%$
	Tibia maximum principal strain	Male: $9.5\% \pm 2.4\%$ Female: $8.7\% \pm 1\%$
	Femur maximum shear strain	Male: $7.4\% \pm 2.1\%$ Female: $9.8\% \pm 2.6\%$
	Tibia maximum shear strain	Male: $8.5\% \pm 2.4\%$ Female: $6.9\% \pm 0.9\%$
Liu et al (2017) ⁷⁷ Note: Measured by MRI before and after activity of walking on a treadmill for 20 minutes.	Tibia uncovered by the meniscus	Medial: $5\% \pm 3\%$ Lateral: $4\% \pm 2.4\%$
	Tibia covered by the meniscus	Medial: $2\% \pm 1\%$ Lateral: $3\% \pm 1\%$

The strain on cartilage presented in Table 1 is dependent on the region of the knee and also dependent on the surface, tibial or femoral. As shown by Liu et al⁷⁷, presented in table 2, the position in relation to the meniscus is also important in the load and subsequent strain felt by the tissue.

Most of the scientific works currently available that determine the effects of daily physical activity on articular cartilage employ a protocol of subject exercise followed by the use magnetic resonance imaging^{75,77} of articular cartilage, the interval between the two parts of the experiment allows strain to

diminish as shown by the greater strains measured by Chan et al (2016)⁷⁶. These authors used a method that allowed simultaneous application of a controlled load and measurement and obtained the higher physiological strain of 10.6% ± 4% for female maximum principal (axial) strain⁷⁶.

The direct measurement of loads in the joint is not possible by noninvasive methods, the most common method for measurement of loads on joints is the use of instrumented prothesis, the work of Kutzner et al (2010)⁷⁴, in which they used data obtained with instrumented tibia data in various common daily life stances and movements. These forces are adjusted to the weight of the subject and for that reason are measured in percentage of bodyweight. Mündermann et al performed a similar experiment using total knee replacement patient and obtained concurring results⁷⁸.

2.1.4. Articular cartilage disease and dysfunction

2.1.4.1. Articular cartilage lesions

When subjected to blunt trauma, immobilization, infection and other similar aggressions that may not mechanically tear or disrupt the tissue, articular cartilage is likely to suffer loss of matrix proteoglycans altering its mechanical properties. If the chondrocyte viability and the collagen backbone of the ECM remain relatively intact the cells can replenish proteoglycans, otherwise the injury will become irreversible⁷⁹.

It is possible that in small superficial injuries, in which cells and matrix are sufficiently damaged, a cascade of degeneration can be started. This cascade occurs due to limitations in the metabolic capacity of injured chondrocytes, impairing the proteoglycan and collagen production. The abnormal ECM production combined with increased hydration diminishes the mechanical performance of the damaged cartilage. This greater damage with further loss of ECM⁸⁰ of articular cartilage and subsequent transmission of the load to the subchondral bone increases the impact of loads on the already damaged tissue, resulting in a vicious cycle that contributes to the progression of the lesion condition⁸¹. Larger injuries with macrodisruption of the tissue may result in fissures or simply partial loss of cartilage thickness⁸.

The response to injury is greatly dependent on the severity and depth of the lesion. Cartilage lesions or defects can be divided in two main groups: chondral or osteochondral. The first is the one previously described where the lesion is limited to cartilage and the second corresponds to injuries that extend further into the subchondral bone⁸². The extent of injury is measured in clinical practice by the volume and surface area of the defect. Concerning the area, defects with diameter smaller than 1 cm² are likely to not affect the mechanical properties of the joint, and probably will not progress into larger lesions⁸². As a result of the avascular nature of the tissue, chondral lesions are known to not cause hemorrhage or fibrin clot formation or to provoke an immediate inflammatory response. The response to this type of lesion is limited to chondrocyte proliferation and increased synthesis of matrix macromolecules near the injury site, which is not enough to restore the smooth surface of hyaline cartilage in lesions of greater dimension⁸¹. Lesions of osteochondral nature have access to blood supply and cells including mesenchymal progenitors of chondrocytes, which supports some extent of repair ability⁸³. The invasion of the lesion by blood initiates a chain of events that include the formation of a hematoma, stem cell

migration, and synthesis of a ECM rich in type I collagen. The repaired tissue is not hyaline cartilage, but a lower quality fibrocartilage tissue with inferior stiffness, inferior resilience, and poorer wear characteristics⁸⁴.

Articular cartilage lesions are highly prevalent in society, with a greater prevalence among the elder population⁸² due to morphological changes associated with aging, often leading to osteoarthritis⁸⁵. A study conducted in 2004 reviewed 993 arthroscopies using the International Cartilage Repair Society (ICRS) scoring system⁸⁶ and concluded that 66% of the subjects showed articular cartilage pathologies within those 11% were full thickness chondral lesions. Another earlier and more comprehensive study comprising 31 000 arthroscopic procedures showed a concurring 63% incidence of cartilage defects⁸⁷.

The symptoms that are felt by patients range from joint swelling and pain to locking or pseudo-locking⁸⁸ of the joint. A study of symptomatology of 76 patients showed that the most common symptom is pain followed by swelling and locking⁸⁸.

2.1.4.2. Articular Cartilage disease

Osteoarthritis

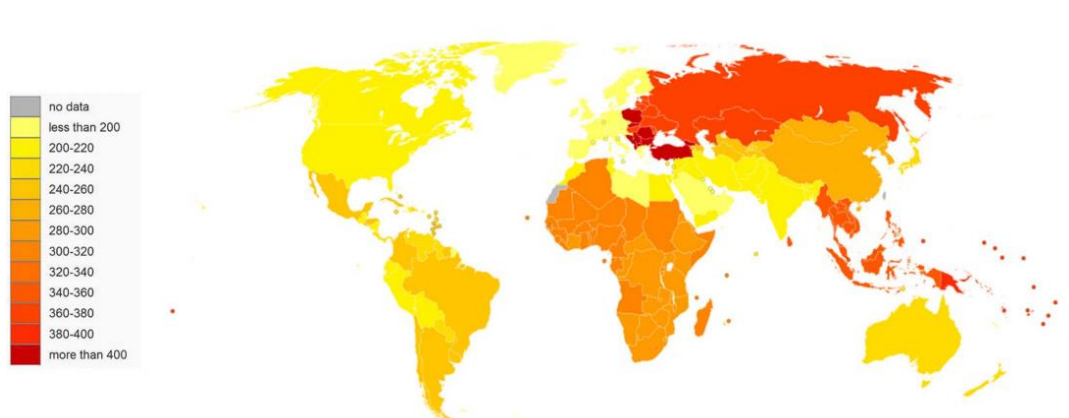


Figure 8 - Graphical representation of the morbidity of osteoarthritis worldwide. Data is of the age-standardised disability-adjusted life year rates by country per 100 000 inhabitants, from the WHO³².

Osteoarthritis (OA) is the most common form of arthritis and is estimated to affect 36.8% of the adult population in the United States⁸⁹. OA is characterized by a severe degeneration of the cartilage as it evolves with associated diminishing joint space and subchondral bone thickening⁹⁰. It is also associated with bone spurs and inflammation of the joint⁹¹, and the progression of the disease is also felt in the joint capsule synovium.

The early stages of OA tend to be asymptomatic for patients and only on more advanced stages, joint swelling and pain⁹¹ associated with inflammation are felt. The progression of the disease ultimately leads to irreparable joint damage⁹².

A type of OA that is particularly prevalent in younger populations⁹³ is post-traumatic osteoarthritis (PTOA). This sub-type of OA develops in approximately 50% of patients who experience a traumatic joint injury⁹³. Approximately 12% of all OA cases⁹⁴ are of post-traumatic type and this pathology usually

takes 10–15 years to develop⁹⁵, and thus, such timely clinical intervention can possibly prevent it. The factors that play a part in the development of OA are of mechanical, biological and structural nature, all contributing to the initiation and progression of the disease. PTOA's development is dependent on mechanical factors, but trauma is also associated with increase in the levels of pro-inflammatory cytokines in the joint, such as TNF- α , IL-6, and IL-1 β ⁹⁶, which are known to activate the catabolic activity of chondrocytes.

In all types of OA, inflammation is a major factor of pathogenesis. The autoimmune response involves both innate⁹⁷ and adaptive⁹⁸ immune responses. Inflammation is also connected to oxidative stress and catabolism of major ECM components like collagen and aggrecan. The degeneration of articular cartilage during OA is related with a vicious cycle similar to the described for articular lesion, in which damage elicits greater damage.

Inflammatory arthropathies

Inflammatory rheumatic diseases are more commonly known because of gout and rheumatoid arthritis, but also include juvenile idiopathic arthritis, systemic lupus erythematosus and seronegative spondyloarthropathies⁹⁵.

As all diseases in this group, rheumatoid arthritis is an autoimmune disease which is reported to affect 0.5% to 1% of the world population⁹⁹. Rheumatoid arthritis is typified by chronic systemic inflammation and arthritis in multiple joints and if left untreated the disease progresses towards the destruction of articular cartilage⁹⁹. Some of the major cytokines involved in these inflammatory diseases are TNF- α , IL-6 and IL-1 β ⁹⁹. Biologic drugs against TNF- α have been used as a strategy for the treatment of rheumatoid arthritis⁹⁵.

Gout affects approximately 4% of the population in the United States¹⁰⁰ and is the most common type of inflammatory arthritis. Similarly to chondrocalcinosis, the deposition of crystals in the joint is the primary cause for the disease, but in this case are uric acid crystals¹⁰⁰. Symptoms are managed using nonsteroidal anti-inflammatory drugs and colchicine. Moreover, lifestyle changes can also be prescribed aiming to reduce uric acid levels¹⁰¹.

Other diseases such as juvenile idiopathic arthritis, seronegative spondyloarthropathies and systemic lupus erythematosus are less common. The two first occur mostly in childhood. Juvenile idiopathic arthritis is in fact used to refer to any form of arthritis in a person younger than 16 years of age¹⁰². Seronegative spondyloarthropathies is a subtype of juvenile idiopathic arthritis and is associated with inflammatory bowel disease¹⁰³. Systemic lupus erythematosus is particularly characterized by the presence of anti-nuclear antibodies in the patient's blood stream¹⁰⁴.

Osteochondritis dissecans

Osteochondritis dissecans is a focal, idiopathic joint disorder that is of spontaneous and unknown origin and causes alterations in the subchondral bone. Such alterations entail a risk of disruption and loss of stability of articular cartilage, which ultimately can result in premature osteoarthritis in some of

the patients¹⁰⁵. The highest incidence of this condition occurs in the age group of 10 to 20 years old and in general affects 20 in each 100,000 woman and 30 in each 100,000 men¹⁰⁶, data obtained in the city of Malmo in southern Sweden.

Relapsing polychondritis

Relapsing polychondritis is a rare disease that affects articular cartilage as well as all other forms of cartilage and other organs containing proteoglycans, particularly, the eye and the heart⁹⁵. Symptoms include pain in joints as well as in other cartilaginous tissues like nose or external ear. It is also associated with local symptoms like in skin and hearing impairment and systemic symptoms like fever and weight loss¹⁰⁷.

Relapsing polychondritis is characterized by intermittent acute flares with an associated progression, possibly leading to complete destruction of the affected tissue¹⁰⁷. Autoimmunity against cartilage specific components is thought to play a role in the mechanism of the disease. Additionally, a genetic susceptibility to the disease has been found¹⁰⁸.

The most relevant morbidity and mortality of the disease is not related to articular cartilage but with cardiovascular effects (majority of patients death occurring due to respiratory failure)¹⁰⁹.

Chondrocalcinosis

Chondrocalcinosis is a joint specific disease which is characterized by the deposition of calcium pyrophosphate dehydrate crystals mostly in the pericellular spaces around chondrocytes in articular cartilage¹¹⁰. The condition can stay asymptomatic or produce an acute inflammatory response to the deposition of crystal that resembles gout¹¹¹ (also called pseudogout) or a chronic arthritis¹¹⁰.

The prevalence of chondrocalcinosis disease is high in elder people¹¹² with estimates of 7% to 10% in the population over 60 years old⁹⁵. Around 25% of the total of patients develop the acute form of the disease¹¹³, which leads to typical inflammation symptoms such as pain, swelling and warmth in one or more joints⁹⁵.

Cartilaginous tumors

Tumors of the cartilaginous tissue are a major class of the osteoskeletal tumors⁹⁵. There are both benign and malignant tumors of cartilage. The most common types of benign tumors are endochondroma and osteochondroma. The epidemiology of benign tumors is not well established as many cases are asymptomatic and those that show symptoms, generally include pain, osteochondral lesion or pathological fractures⁹⁵. Malignant cartilaginous tumors, also called chondrosarcomas, are divided in various types. Central primary chondrosarcoma is the most common and accounts for 20% to 27% of all cases of malignant tumors¹¹⁴.

In terms of treatment, benign tumors are generally surgically treated by excision or curettage, a medical procedure that consists of scraping the affected tissue, and if necessary, a bone graft is done⁹⁵.

In terms of prognostic, benign tumors of cartilage rarely evolve to malignant forms⁹⁵. Malignant tumors are divided in 3 grades of severity and higher grades imply more deviation from normal cartilage tissue phenotype¹¹⁵. Malignant tumors are also generally surgically treated¹¹⁶.

2.1.5. Current treatment methods

2.1.5.1. Bone Marrow stimulation

The mechanism of bone marrow stimulation is dependent on the invasion of articular cartilage by blood. This penetration of subchondral bone is still used despite being the oldest method for stimulation of neocartilage regeneration. This surgical strategy is used in full thickness defects and recapitulates naturally occurring processes with formation of the hematoma and subsequent mobilization of the mesenchymal progenitors to the lesion sites, aiming that the recruited cells will ultimately proliferate and differentiate to generate neocartilage⁸². The specific surgical techniques to achieve bone marrow stimulation are joint debridement and drilling, spongialization and microfracture.

Joint debridement is a technique based on the removal of cartilage fragments loose in the synovium, generally associated with lavage of the tissue. It is a technique that is combined with both drilling and microfracture as a first step of the procedure¹¹⁷. Drilling of the subchondral bone is frequently associated with this procedure and is one of the ways to achieve bone marrow stimulation⁸².

Spongialization is a more radical modification of debridement and drilling, in which both the damaged cartilage tissue and the involved subchondral bone are excised¹¹⁸.

Microfracture, the most common of these methods, is a modified drilling technique, which consists in the removal of all the affected tissue, maintaining the healthy surrounding tissue and the subchondral bone. After this, an arthroscopic awl is used to produce multiple microfractures, preserving the integrity of subchondral bone as much as possible and allowing the invasion of the tissue by blood¹¹⁹.

2.1.5.2. Mosaicplasty

Mosaicplasty uses a completely different underlying mechanism for the repair of chondral lesions. It consists on the harvesting of cartilage plugs from non-weight-bearing regions, which are used to replace the damaged cartilage. This method demands the previous preparation of the lesion area to receive the plugs to fill the chondral defect, creating a 'mosaic' pattern that gives the technique its name. The space between the plugs is covered with fibrocartilage provenient from the damaged cartilage¹²⁰. The morbidity in the cartilage source joint and tissue availability are main disadvantages¹²⁰. However, this technique was reported to have good results¹²¹.

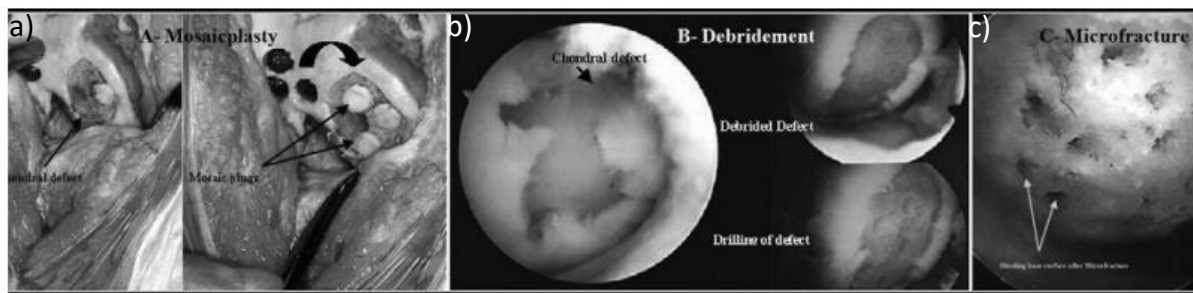


Figure 9 - Current surgical methods for articular cartilage regeneration; a) mosaicplasty; b) debridement; c) microfracture⁸²

2.1.5.3. Autologous chondrocyte implantation

Autologous chondrocyte implantation (ACI) is the first application of tissue engineering in orthopaedic surgery, originating in the 1980's¹²². This therapeutic approach consists in 3 main steps: firstly, harvesting of a piece of cartilage, like in mosaicplasty a low-weight-bearing joint is used; secondly, cells are isolated and expanded in laboratory; finally, the cell suspension is injected underneath a periosteal patch that covers the chondral defect.

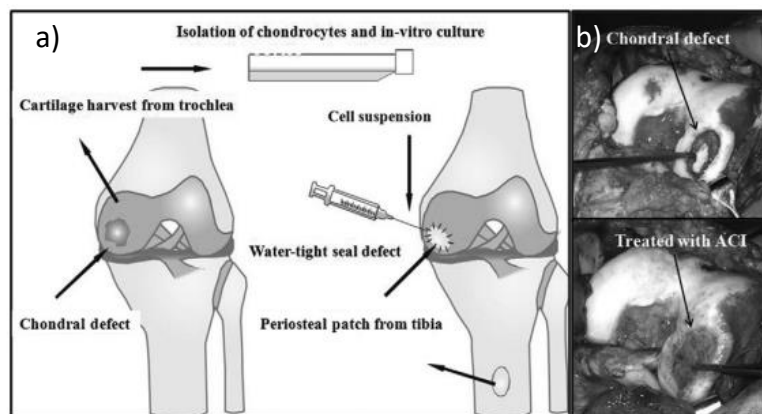


Figure 10 – a) Schematic representation of ACI, autologous chondrocyte implantation first cell based therapy method for chondral defect repair; b) photography of a prior and post treatment legion treated with ACI⁸².

This technique is thought to be a considerable advancement for the treatment of chondral defects. However, does not represent a definitive response to the patients' needs. Similarly, to the previous mentioned methods, ACI also presents drawbacks related to the quality of the neocartilage formed. Histological studies done following the procedure have found hyaline-like tissue, but the neocartilage produced is still not chemically identical to normal hyaline cartilage and fibrocartilage presence was observed in some of the treated joints¹²³.

Studies to assess the effectiveness of ACI in comparison with the more common microfracture technique have concluded that the first produces better results in terms of structural repair but the results are comparable¹²⁴. A 5 year follow-up program of patients treated both ways has also found similar long term results¹²⁵.

2.2. Articular Cartilage tissue engineering

2.2.1. The need for tissue engineering

The structural complexity of articular cartilage and the high prevalence of cartilage pathologies combined with the inefficiency of the current available clinical methods are the motivation for the need for novel articular cartilage tissue engineering strategies.

When discussing the physiology of articular cartilage, some characteristics have been highlighted, namely, the avascularity² and low cellularity⁸, which explain the low ability of the tissue for self-repair. Moreover, if left untreated, cartilage lesions tend to progress towards a osteoarthritic condition, the most prevalent joint disease⁸⁹.

The most important limitations of the current therapeutic methods are the quality of the repaired tissue produced by bone marrow stimulation; the cell availability for both mosaicplasty and ACI; and the low chondrocyte proliferative capacity for ACI procedures, in which the resulting tissue has been deemed only marginally better than other traditional therapies.

In conclusion, novel articular cartilage tissue engineering solutions are necessary to improve the quality and functionality of tissue produced, which will have a great impact in the life of the many patients suffering from joint diseases.

2.2.2. Cell Source for cartilage tissue engineering.

2.2.2.1. *Adult chondrocytes*

One distinct advantage of the lack of vascularization of cartilage is a greatly reduced immunogenic response. Therefore, engineered cartilage derived from chondrocytes of allogenic source have been implanted without evidences of immune reaction¹²⁶. Chondrocytes have been used in established therapeutic strategies such ACI but currently there is also success in chondrocyte use to produce engineered cartilage constructs. Major limitations regarding the use of chondrocytes is their low availability and reduced potential for cell expansion.

The use of juvenile human chondrocytes of cadaveric origin has an advantageous potential for ECM synthesis and have been shown to be not immunogenic¹²⁷. However, the availability of this cell type is naturally very limited.

Differentiated or mature chondrocytes are possible to obtain both from autologous or allogenic sources relative to the patient. Autologous chondrocytes can be obtained from low-weight-bearing joints in a similar way as done in mosaicplasty and with a similar associated morbidity. Mature chondrocytes produce a lower quality tissue in terms of characteristic ECM and structure when compared to juvenile chondrocytes¹²⁸.

2.2.2.2. Mesenchymal Stem Cells

Concerning articular cartilage tissue engineering strategies, mesenchymal stem/stromal cells (MSC) represent a good alternative to chondrocytes because of their superior availability, expansion capacity and ability to differentiate into cells of the osteoskeletal system, including chondrocytes. MSC-derived tissues include, for example, cartilage, fat, bone, and tendon¹²⁹. Additionally, the differentiation fate of MSC has been proved to be highly dependent on external cues¹³⁰.

MSCs can be obtained from several tissues including bone marrow, muscle, adipose tissue, periosteum, umbilical cord and synovial membrane¹³¹. However, the potential for differentiation towards the articular chondrocyte has been shown to be higher for bone marrow, synovium and periosteum-derived MSCs¹³².

The regenerative potential of MSCs is relevant and intrinsic to bone marrow stimulation surgical therapeutic techniques. The breach of subchondral bone is associated with the secretion of factors by the damaged tissue, allowing access and recruitment of MSCs to the site of lesion¹³³. As an alternative to ACI, the use of autologous/allogeneic MSCs injection instead of mature chondrocytes has seen success in inducing tissue regeneration and pain relieve¹³⁴.

The results obtained in the treatment with injected MSC suspensions are promising but presented similar shortcomings to those identified with chondrocytes, namely the minor quality of the repaired tissue. The tissue resulting from these procedures is often hypertrophic and lacks the mechanical properties needed to withstand the demanding mechanical loads felt in the joint.

The current paradigm in articular cartilage tissue engineering field is that in order to obtain hyaline-like tissue it is required to incorporate cells with biocompatible scaffolds and to recreate a biomimetic microenvironment in terms of chemical and mechanical cues that allow for the differentiation of these cells into the appropriate chondrocyte phenotype¹³⁵.

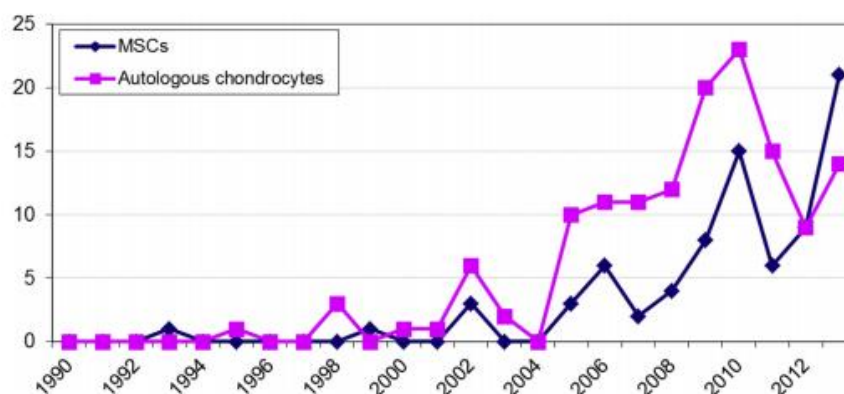


Figure 11 – Chart of the published clinical and preclinical articles using either MSC or chondrocyte for scaffold/cell osteochondral defect repair, showing a trend for MSC to become the preferred cell. ²⁵⁸

2.2.3. Scaffolds for chondrocyte differentiation

The choice of scaffold for osteochondral tissue engineering is essential to influence the cell-cell and cell-ECM interactions that modulate the MSCs' response to external cues, both of chemical and mechanical nature.

The spatial distribution of cells in a 3D configuration is an important factor for the chondrogenic process. The physical support for cells provided by 3D scaffolds allow cells to anchor and synthesize ECM. Other factors including material's chemical composition, biocompatibility and scaffold architecture and porosity have also been demonstrated to strongly influence in chondrogenesis^{135,136}.

The main types of scaffolds used in chondral and osteochondral tissue engineering are hydrogels, porous foams or 3D printed structures, and fibrous meshes¹³⁷.

The most commonly used scaffold type in articular cartilage regeneration settings is hydrogels, which are physiologically relevant due to their high water content that mimics the native cartilage¹³⁵. The main hydrogel materials include collagen types I and II, fibrin¹³⁸, hyaluronic acid¹³⁹, chondroitin sulfate¹⁴⁰, polyethylene glycol (PEG)¹⁴¹, alginate, and agarose¹⁴². These polymers can furthermore be modified to increase their potential to influence MSC fate or chondrocyte phenotype maintenance. One approach that is often used is the immobilization of growth factors such as TGF- β ¹⁴³ within the scaffold structure. Another possible scaffold modification is the functionalization with arginine-glycine-aspartate (RGD) sequences. For example, the inclusion of this cell adhesion moiety in PEG hydrogels promotes cell attachment and migration, increasing viability and the expression of chondrogenic markers¹⁴⁴. Another noteworthy modification of PEG-based hydrogels is the use of different combinations of ECM molecules creating unique cellular niches that could direct differentiation towards chondrocyte phenotypes associated with the different zones of cartilage tissue¹⁴⁵.

A current trend in articular cartilage tissue engineering is the use of biphasic, triphasic, and multilayered scaffolds to mimic the zonal varying properties of the osteochondral tissue¹⁴⁶. These composite structures can be composed of biodegradable polymers and bioactive ceramics that mimic the cartilage and bone components of the tissue, respectively¹³⁶.

2.2.4. Biochemical and environmental cues

The use of biochemical cues for chondrogenic differentiation of MSCs is informed by the knowledge of the metabolic regulatory effects of various molecules. Understanding how these molecules affect differentiation is crucial for a better control of the regulatory pathways associated with chondrogenesis.

The most important biochemical factors that have been used to promote chondrogenesis include TGF- β s, IGF, FGF^{147,148}, corticosteroids¹⁴⁹, and interleukins (IL), all of this discussed in the chondrocyte metabolism section 2.1.3.2. The most potent factors for the induction of MSC chondrogenesis belong to the TGF- β superfamily (TGF- β 1,2,3 and BMP)¹³⁵. These factors have also been found to amplify or to be required for the chondrogenic effects of mechanical loading¹⁴⁸.

Coculture of MSCs with chondrocytes have been demonstrated to produce engineered cartilage with improved mechanical properties (Young's modulus and dynamic modulus) as well as improved GAG and collagen contents¹⁵⁰. These effects are due to the secretion of soluble biochemical cues by

chondrocytes that stimulate MSC chondrogenesis¹⁵¹. Other studies have shown that this important relation works both ways since MSCs secrete paracrine factors which favor chondrocyte proliferation and ECM deposition¹⁵².

Another relevant environmental factor involved in chondrocyte differentiation is oxygen tension, which has even been deemed as a stronger chondrogenic factor than cyclic compression¹⁵³. As previously discussed in the Articular chondrocyte physiology section 2.1.3, the native microenvironment of articular chondrocytes is hypoxic (low oxygen tension) and previous studies have shown that low oxygen tensions (generally 2-5% O₂) are more suited for chondrogenic differentiation, allowing a reduction of tissue hypertrophy¹⁵⁴.

2.2.5. Mechanical Stimulation

As discussed in the articular cartilage biomechanics section the natural joint loading produces a variety of forces felt on the tissue that translate into physical stimulation of the chondrocyte, this includes osmotic loading, hydrostatic pressure, electrokinetic phenomena, stress, and strain¹⁵⁵. In terms of developmental biology of cartilage mechanical forces are also essential in activating the Indian hedgehog-parathyroid hormone-related protein (PTHrP) feedback loop, already introduced in the metabolism section, this signaling pathway is essential in the maintenance of phenotype and differentiation of articular chondrocytes³⁶.

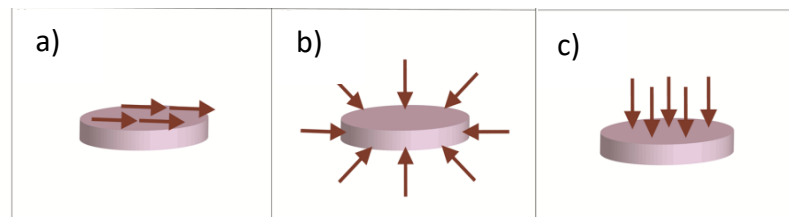


Figure 12 – Schematic representation of the three most common forms of mechanical stimulation used in articular cartilage tissue engineering, the red arrows represent the direction of the forces applied to the tissue engineering constructs; a) shear; b) hydrostatic pressure; c) direct compression; image adapted from¹⁵⁶.

The importance of mechanical cues in *in vivo* cartilage function and regulation have motivated the use and research of the use of mechanical stimulation in the context of articular cartilage tissue engineering. The use of mechanical stimulation with physiological level forces has various advantages in general it enhances the convection of nutrients and waste products through the tissue¹⁵⁷, it also allows the maintenance of chondrocyte function¹⁵⁸ and modulates chondrogenesis of MSCs¹⁵⁹. The response of MSC to mechanical stimulation is to a great degree dependent on timing, as the response of MSC is different in different stages of chondrogenesis¹⁶⁰.

2.2.5.1. Hydrostatic pressure

During physiological joint loading, the stress is felt by chondrocytes in a uniform way. The compressive load applied in the tissue imparts a pressurization of the fluid phase following the mechanism described in the biomechanics section, and according to the biphasic theory, it is mostly uniform all along the tissue. In reality, the stress is not completely uniform and gradients of pressure and of the associated stress exist¹⁶¹.

The physiological stress varies in most movement types from 3 to 10MPa⁷⁰ but can be as high as 18 MPa in the hip joint⁷⁰. These stresses are translated to hydrostatic pressure as described by the biphasic theory. The human walking cadence is typically 1 Hz¹⁶² and for that reason, when cyclic mechanical stimulation is applied, the frequency is this or as close as possible. The magnitude of hydrostatic pressure often applied in tissue engineering settings is within the physiological range.

The strategies of applying hydrostatic pressure in articular cartilage tissue engineering involve the design of bioreactors in one of two main forms. The first method employs the compression of a gas phase, which in turn, transmits the load to the tissue construct. This changes the gas pressure in contact with culture media, modifying the mass transfer from the gas to the culture media¹⁶³. The second strategy is to compress the liquid media directly. This is generally done in a bioreactor design that consist of a chamber filled with fluid that is compressed by a piston¹⁶⁴ or a pump with valve control¹⁶⁵. Temperature control at 37°C is essential to these bioreactor designs and both designs can be modified to allow for semi-continuous media perfusion¹⁶⁶. In Table 3 a collection of works available in the literature is presented.

Table 3 - Representative examples of studies targeting the effects of hydrostatic pressure stimuli for cartilage tissue engineering applications

Author	Cells/ scaffold	Magnitude	Frequency	Results
DuRaine et al (2015) ¹⁶⁷ Hydrostatic pressure chamber (Constructs in heat sealed bags)	bCHD self-assembled constructs	10 MPa	Static, 1h per day for 10 to 14 days	Activation of ERK, increase in GAG content, increase in compressive properties
Toyoda et al (2003) ¹⁶⁸ Hydrostatic pressure chamber (porpuse built, constructs placed in open vessels)	bCHD/ agarose gel	5 MPa	Static or Pulsatile 1 Hz 4h per day	Increase in GAG synthesis, 4-fold increase in levels of aggrecan mRNA
Correia et al (2012) ¹⁶⁹ High Hydrostatic Pressure Bioreactor (piston compressed media containing the constructs)	Nasal hCHD/ gellan gum hydrogel	0.4 MPa	Static or Pulsatile 0.1 Hz, 3 h/day, and 5 days/week	For chondrocytes pulsatile condition showed best results, 5 MPa physiological load better result for hASCs.
	hASCs/ gellan gum hydrogel	0.4 MPa or 5 MPa	Pulsatile 0.5 Hz, 4 h/day, and 5 days/week	

Table 3- Representative examples of studies targeting the effects of hydrostatic pressure stimuli for cartilage tissue engineering applications (continued)

Author	Cells/ scaffold	Magnitude	Frequency	Results
Candiani et al (2008) ¹⁷⁰ Hydrostatic Pressure Bioreactor (piston compressed media containing the constructs)	bCHD 3D porous scaffold	10 MPa	0.33 Hz 4 hours/day for 3 days	High pressure did not change viability and the collagen II/ Collagen I ratio was higher.
Ikenoue et al (2003) ¹⁷¹ Hydrostatic pressure chamber (Constructs in sealed bags)	hCHD/ monolayer	1, 5, 10 MPa	Pulsatile 1 Hz, 4 h/d for 1 or 4 days	Aggrecan mRNA upregulated in all stimulation, COLII only upregulated at loads of 5 and 10 MPa.
Parkkinen et al (1993) ¹⁷² Hydrostatic pressure chamber (Constructs in membrane sealed petri dishes)	bCHD/ monolayer	5 MPa	0.05, 0.25, 0.5 Hz, for 1.5 h/day or 20 h/day	Sulfate incorporation inhibited for lower time of stimulation but stimulated in longer time and 0.5Hz. Proteoglycan synthesis is proportionally related to sulfate uptake.
	bCHD/ explant	5 MPa	0.05, 0.25, 0.5 Hz, for 1.5 h/day or 20 h/day	Enhanced sGAG Incorporation compared to monolayer culture.
Mizuno et al (2002) ¹⁶⁵ Perfusion Bioreactor (with actuated valve back pressure control)	Immature bCHD/ collagen sponges	2.8 MPa	Static or cyclic 0.015 Hz, for up to 15 days	Sulfate incorporation into GAG 130% higher with static and 140% higher with cyclic stimulation in comparison to control. in general synthesis of ECM cartilage-specific components stimulated.

Table 3- Representative examples of studies targeting the effects of hydrostatic pressure stimuli for cartilage tissue engineering applications (continued)

Author	Cells/ scaffold	Magnitude	Frequency	Results
Wagner et al (2008) ¹⁷³ Hydrostatic pressure chamber (Constructs in sealed bags)	hMSC/ COL Type I sponges	1 MPa	1 Hz, 4 h/d, for 10 days	Chondrogenic markers mRNA aggrecan, COLII, and sox9, but increased col I mRNA levels also increased.
Angele et al (2003) ¹⁷⁴ Hydrostatic pressure chamber (Constructs in polypropylene tubes sealed by alminun caps with ruber septums)	hMSC/ aggregate	5 MPa	1 Hz, for 4 h/d, in day 1 or 7 days or just in day one	1-day treatment ineffective, multi day treatment increased collagen and GAG content
Miyaniishi et al (2006) ¹⁷⁵ Hydrostatic pressure chamber (Constructs in sealed bags)	hMSC/ pellet culture	10 MPa +TGF- β	1 Hz, 4 h/d, for up to 14 days	HP and TGF- β treatment and specially the combination of both, increased collagen II, aggrecan, and sox9 mRNA levels

2.2.5.2. Shear stress

As previously discussed, articular cartilage experiences shear stress during physiological movement. Fluid shear is a main part of the load absorption in the joint as the drag produced by the movement of the liquid through ECM channels allows for energy dissipation¹⁷⁶.

In general, shear is viewed as a negative factor on articular cartilage because it wears, tears and generally degrades the tissue over time. However, studies using low frequencies for dynamic and relatively mild loads have demonstrated good results in improving the properties of cartilage constructs. A good range of frequencies under 1Hz and magnitudes of stress smaller than 0.5 Pa has been found to favor chondrogenic differentiation^{156,177}.

Shear stress occurs in a parallel plane to the surface of the tissue and because of that causes a sliding shear between horizontal levels of chondrocytes and ECM. *In vitro*, generally using purpose-built bioreactors, shear stress is applied in one of two forms: fluid flow over or within the AC construct or through direct contact of the construct surface with an actuating object¹⁷⁸. Another option that is relatively common is low shear mixing solutions. Rotating microgravity bioreactors are commonly used to apply

this type of stimulus¹⁷⁹. Moreover, a more sophisticated form of applying shear stress stimuli have been recently introduced through the use of acoustofluidic perfusion bioreactors¹⁸⁰.

The loading regimen most successfully used for both fluid and contact shear application is an oscillatory shear stress, which better recapitulates what happens during physiological joint movement¹⁵⁶.

Table 4 - - Representative examples of studies targeting the effects of contact shear stress stimuli for cartilage tissue engineering applications.

Author	Cells/ scaffold	Shear Strain	Frequency	Results
Jin et al (2003) ¹⁸¹ Direct shear bioreactor. (composed of polysulfone chambers and prong like actuators that rotate in the axis of the bioreactor producing shear)	bCHD/ explant	0.5% to 6%+ IGF-I	0.1 Hz for 24h	Dynamic shear above 1.5% strain stimulated protein and proteoglycan synthesis, by maximum values of 35 and 25%, IGF-1 alone also stimulated biosynthesis, the combination of stimuli was even more effective.
Di Federico et al (2014) ¹⁸² Bioreactor with compression and contact shear	bCHD/ agarose gel	5% to 10%	1 Hz for up to 48 h	The combination of shear and compression did not significantly lower the viability of cells
Waldman et al (2003) ¹⁸³ Dual axis tester Mach-1™ (compression and contact shear)	bCHD/ Porous calcium polyphosphate	2%	1 Hz for 400 cycles every 2 days	The content of chondrogenic markers in the ECM increased following stimulation and after 4 weeks more tissue was formed and 40% more collagen and 35% more proteoglycan content compared to control,
Vainieri et al (2018) ¹⁸⁴ Bioreactor with compression and contact shear	bCHD/ polyurethane (in a model cartilage defect)	10% to 20%	0.5 HZ for 1 hour twice a day for 5 days	Chondrogenic response verified by mRNA ratios of collagen type II to type I and increased content of Proteoglycan

Table 5 - Representative examples of studies targeting the effects of contact shear stress stimuli for cartilage tissue engineering applications.

Author	Cells/ scaffold	Magnitude	Frequency/ duration	Results
Gooch et al (2001) ¹⁸⁵ Spinner flask bioreactor	bCHD/ fibrous polyglycolic acid meshes	80 or 160 rpm and varied stirrers producing Various shear intensities	1 day of stimulation	Higher mixing intensity GAG content up to 3 fold, mixing important in stimulation and mass transfer.
Vunjak-Novakovic et al (1998) ¹⁸⁶ Spinner flask bioreactor	bCHD/ fibrous polyglycolic acid meshes	50 RPM	2 weeks	High GAG and collagen content in constructs attributed to the effects of high initial cell density.
Mizuno et al (2001) ¹⁸⁷ Perfusion bioreactor (like the one in image 14e))	bCHD/ collagen sponges	0.33 mL/min	7 and 15 days	Collagen II increased up to 2.4 times GAG up to 3 times and proteoglycan 35%.
Raimondi et al (2006) ¹⁸⁸ Direct perfusion bioreactor	bCHD/ Polyesterurethane foams	0.5 ml/min, CFD calculated 4.6 to 5.6 mPa shear intensity	2 weeks	GAG content increased with perfusion and higher shear intensity produced higher sGAG content.
Carmona-Moran et al (2015) ¹⁸⁹ Perfusion bioreactor Note: Purpose built with a conical chamber and with a rotating scaffold support.	hMSC/ Polycaprolactone (PCL) beads	0.1 ml/min	8 to 14 days	The shear and perfusion combination induced an increase in Collagen GAG and proteoglycan content.
Tognana et al (2005) ¹⁵⁵ Rotating wall bioreactor Note: Constructs were cultured adjacent to either native cartilage or bone	bCHD/ hyaluronan benzyl ester non-woven mesh	15 to 30 rpm of the rotating wall	8 weeks	Integration with bone and ECM synthesis showed better results than coculture with cartilage explants. In general good results for chondrogenesis.

Table 5 - Representative examples of studies targeting the effects of contact shear stress stimuli for cartilage tissue engineering applications. (continued)

Author	Cells/ scaffold	Magnitude	Frequency/ duration	Results
Li et al (2014) ¹⁸⁰ Acoustofluidic bioreactor Note: Purpose built with microfluidic perfusion and ultrasound traps.	hCHD/ aggregates	890 to 910 kHz acoustic frequency and low shear perfusion	21 days	Hyaline like cartilage was formed with a dense proteoglycan and collagen ECM.

2.2.5.3. Direct compression

Direct compression (DC) is a widely studied form of mechanical stimulation in articular cartilage tissue engineering. Under physiological conditions, the dynamic mechanical environment includes various transient multi-axial compressive strains¹⁹⁰. In *in vitro* studies studying the AC constructs response to direct compression, the forces are generally simplified into uniaxial compression. There are several studies employing both static and dynamic compression of tissue engineered constructs. Despite the evidence of some discordant results, in general, strains lower than 10% have been described as beneficial in static and dynamic compression, producing AC constructs with higher quality than control conditions¹⁹¹. Concerning the effect of compression stimuli on the determination of MSC fate, 3.75% strain is thought to be optimal for bone differentiation while chondrogenic differentiation is favored in the range of 3.75% to 11.25%, and above this range, fibrous tissue is formed¹⁹².

Other than strain, stress is used for characterizing the magnitude of direct compression, which can be related to strain through the young modulus of the construct. In a self-assembly culture system since the forces are more directly felt by the cells this parameter is more commonly used. For self-assembly cultures a positive effect in the quality of the tissue is obtained for stress in the range of in the range of 3.3 kPa and 5 kPa¹⁹³.

Bioreactor designs for static DC are simple. Considering passive DC, the system generally consists of weights placed over the AC constructs, in which the weights are calibrated to produce the desired compressive stress to generate the strain required. The weights are removed during media change and otherwise kept acting over the AC construct¹⁹⁴. Bioreactors designed for dynamic loading generally use pistons, springs or linear actuators to dynamically load and unload the constructs.

Table 6 - Representative examples of studies targeting the effects of direct compression stimuli for cartilage tissue engineering applications.

Author	Cells/ scaffold	Strain	Frequency/ duration	Results
Wiseman et al (2003) ¹⁹⁵ Uniaxial strain apparatus ¹⁹⁶	eqCHD/ agarose scaffold Note: cells obtained from low and high loaded areas and different aged specimens	Static 0.8%, 15% dynamic peak	Sinusoidal 1 Hz, for 24h	Proteoglycan synthesis was stimulated only on young (5-month-old) specimen CHD.
Lee et al (2003) ¹⁹⁷ Uniaxial strain apparatus	canCHD/ Collagen II scaffold	Static 10%, 25%, or 50%	24h	Static stimulation downregulated protein and proteoglycan biosynthesis and depends on time and intensity. Dynamic stimulation upregulated this synthetic activity.
		Dynamic 10% ramp and hold + 3% sinusoidal	15 sec ramp and 0,1 Hz sinusoidal for 24h	
Hoening et al (2011) ¹⁹⁸ Uniaxial strain Bioreactor (integrated culture chamber) Note: purpose built by the authors	porCHD/ hydroxyapatite carriers	5%, 10%, and 20%	1 Hz, 3000 cycles/day for 14 days	Glycosaminoglycan or collagen content not changed in loaded and unloaded assays. 20% load showed best mechanical properties.
Stoddart et al (2006) ¹⁹⁹ Compression and contact shear apparatus (actuated by a roller)	Immature bCHD/ alginate (in culture) bCHD/ self-synthesized ECM (in stimulation)	0.5N	0.279 Hz for 8 h/day, or 2 times 30 min with equal length break twice a day, or same regime once a day	Continuous dynamic stimulation increased COLII mRNA only from 1 to 3h and further load time seem to lead to desensitization of the cells. Short intermittent loading stimulated proteoglycan synthesis while continuous decreased it.

Table 7 - Representative examples of studies targeting the effects of direct compression stimuli for cartilage tissue engineering applications. (continued)

Author	Cells/ scaffold	Strain	Frequency/ duration	Results
Grogan et al (2012) ²⁰⁰ Commercial Bioreactor with uniaxial loading and perfusion	Expanded hCHD/ alginate hydrogel (different age with healthy and osteoarthritic donors)	20% + perfusion	0.5 Hz for 1 h/day for 7 or 14 days	Both the compression and perfusion regimes used showed not to affect the mRNA content of the main chondrogenic markers. The GAG content diminished with the combination of stimuli. Biomechanical properties were also unaltered.
Zignego et al (2015) ²⁰¹ Uniaxial Compression bioreactor (custom built)	Expanded hCHD/ agarose hydrogel (50 to 80 years of age age with stage IV osteoarthritis donors)	3.1% constant + 1.9% amplitude sinusoidal	1.1 Hz for 15 min or 30 min	Untargeted metabolomics studies were performed, loading upregulated glycolysis and other central energy metabolic pathways. And the degradation of chondroitin sulfate was also upregulated.
Kisiday et al (2009) ²⁰² Uniaxial Compression bioreactor (custom built)²⁰³	eqMSC/ agarose hydrogel	7.5% constant + 2.5% sinusoidal	0.3 Hz in a 6h pattern with 45min of stimulation interspersed by 15 min interval. The patter was repeated 4 times with 24h intervals of free-swelling culture	GAG accumulation was not changed in alternate day pattern but in 12/h pattern changed by 2.8 times the value in culture solely with TGF- β .

Table 7 - Representative examples of studies targeting the effects of direct compression stimuli for cartilage tissue engineering applications. (continued)

Author	Cells/ scaffold	Strain	Frequency/ duration	Results
Schätti et al (2011) ⁵ Pin and ball bioreactor (Compression and contact shear) ²⁰⁴	hMSC/ porous polyurethane scaffolds+ fibrin hydrogel	10% constant+ 10% sinusoidal ($\pm 25^\circ$ rotation of the shear inducing ball)	1Hz for 1h/day 5 consecutive days/week for 3 weeks	The GAG synthetic activity was preserved in combination of shear and compression, avoiding hypertrophy. Just compression could not avoid this cell fate. Other chondrogenic markers mRNA content also increased in the combination regime.
Li et al (2009) ⁶⁸ Pin and ball bioreactor (Compression and contact shear) ²⁰⁴	hMSC/ porous polyurethane scaffolds+ fibrin hydrogel	10% constant + 5%, 10%, 20% sinusoidal ($\pm 25^\circ$ rotation of ball)	0.1 Hz or 1HZ	GAG content showed a dependence with intensity and frequency of compression, higher compression and 1Hz frequency had the best results. Same tendency for other chondrogenic markers mRNA.

2.2.6. Bioreactors for articular cartilage tissue engineering

Bioreactor devices are crucial for scalable and controlled tissue engineering approaches. As a result of cartilage biomechanical complexity, bioreactors are particularly valuable for articular cartilage tissue engineering because they enable the application of different types or physical stimuli. Since the main subject of this thesis is the design and production of a bioreactor able to provide mechanical stimulation to cartilage engineered constructs, it is essential to understand the current paradigm of bioreactor use in articular cartilage tissue engineering.

One of the key advantages of bioreactors is the possibility to cultivate cells/tissue constructs under a controlled environment. The most important operating conditions that normally are controlled in a bioreactor device are pH, temperature, oxygen tension and flow perfusion. As discussed in the previous section, different types of mechanical stimuli have been demonstrated effectiveness in enhancing MSC chondrogenic differentiation and maintaining chondrocyte phenotype. These stimuli have been applied using a wide range of commercial and “in-house” developed bioreactor systems.

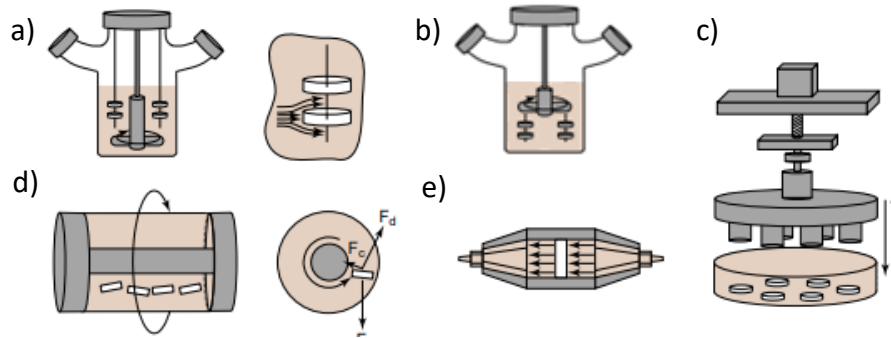


Figure 13 – Schematic representation of traditional bioreactors used for articular cartilage tissue engineering; a) spinner flask; b) rotating bead bioreactor; c) Uniaxial compression apparatus; d) rotating wall vessel; e) perfusion bioreactor. Adapted from Martin et al (2004) ²⁰³

A One of the main limitations limiting the tissue growth and ECM deposition in 3D tissue-engineered constructs is the supply of soluble nutrients and oxygen. Early in the development of tissue engineering, this problem became evident as it was observed that cellular spheroids larger than 1 mm in diameter contain a necrotic center surrounded by viable cells due to lack of nutrient and oxygen supply²⁰⁶. The poor deposition of GAGs in the central part of chondrocyte-poly (glycolic acid) scaffold constructs observed by Martin et al²⁰⁷ is another observation supporting the negative effects of poor diffusion. In AC tissue engineering, clinically relevant constructs need to have a thickness with few millimeters, as occurs in native articular cartilage. This gives rise to mass transfer problems, which vary among the different approaches since the internal diffusion on the construct is fixed to the properties of a certain scaffold as well as of to the state of development and cell density of the construct. However, external mass transfer can be considerably improved through enhanced convection, which results from introducing movement to the growth media using bioreactors. The main bioreactor configurations employed to mitigate this problem include stirred, rotating or perfusion bioreactors. Perfusion is a general mode of operation, but in the context of AC tissue engineering it is frequently used to designate bioreactors with no stirring but perfusion of media, this bioreactor architecture is frequently designated as perfusion bioreactors, and this designation will be used in the present thesis.

2.2.6.1. Fluid Flow shear inducing Bioreactors

The need for improved mass transfer phenomena during the generation of tissue engineering constructs combined with the mechanical stimulation of such constructs in the form of fluid flow induced shear stress towards enhanced chondrogenesis, increased the interest for bioreactor systems able to provide such stimuli. The main bioreactor types associated with fluid flow are spinner flask, rotating wall vessel, biaxial rotating and perfusion bioreactors²⁰⁸.

Spinner flasks have been commonly used to expand MSCs in adherent culture systems (e.g., microcarriers), resulting in enhanced mass transport which leads to higher cell densities²⁰⁹. Spinner flasks consist in a vessel with a gas exchange mechanism, a stirring mechanism, and in case scaffolds are used, they are generally fixed in supports pinned to the top of the vessel²⁰⁸.

Rotating wall vessels are composed of a hollow cylinder with a detached support for scaffolds, in which the cylinder is filled with growth media and rotates in its radial axis²⁰⁸. The rotation of this external cylinder produces a laminar flow that makes this the lowest shear stress option in dynamic culture systems.

Rotating bed bioreactor is similar to the spinner flask, but instead of the mixer producing movement of media around the scaffolds, the scaffolds rotate themselves.

Bioreactors for **perfusion culture** have been abundantly studied in the last decade with encouraging results regarding the formation of neocartilage tissue with improved quality²¹⁰. Such good results are attributed to a more efficient nutrient transport, leading to enhanced cell viability and uniform distribution throughout the 3D scaffolds²¹¹. Perfusion bioreactors allow the flowing of culture media through a chamber containing AC tissue engineered constructs. The flow renovates constantly the media in the culture chamber while inducing shear stress to the cells. The perfusion bioreactor architecture is generally composed by the abovementioned chamber designed to fit the geometry of the scaffold, a media reservoir and a waste container. Another possibility is the use of a closed loop system avoiding the use of a waste reservoir²¹⁰.

Importantly, high shear stress conditions have been associated with osteoblastic differentiation²¹² and cell migration²⁵, but shear stress in milder conditions have demonstrated to be beneficial in AC tissue engineering. For example, studies using human chondrocytes cultured in PLGA scaffolds exposed to mild fluid-induced shear stress conditions have found increased GAG retention in the ECM²¹³. Additionally, cartilage grafts cultivated on perfusion bioreactors has been found to be biomechanically similar to native cartilage²¹⁴.

The use of direct perfusion, forced through a porous scaffold has been shown to produce interesting results, particularly in the context of osteogenic differentiation²¹⁵. Forcing the fluid flow through small sized pores, produces a high shear environment which is not beneficial for chondrogenic differentiation or phenotype maintenance. Therefore, it is essential to establish an optimal perfusion flow rate for chondrogenic differentiation, to avoid harmful effects, in particular cell death due to high shear stress²¹². Direct perfusion bioreactors have also been used for MSC chondrogenic differentiation in electrospun nanofiber scaffolds, showing a improved phenotype in terms of morphology and synthetic activity²¹⁶.

The addition of a bypass to a direct perfusion system can be effective at lowering the pressure build up within the scaffold²¹⁷. Another mode of functioning of perfusion bioreactors that produces a more moderate shear environment is indirect perfusion. Indirect perfusion is done with either parallel or transverse flow. The effects of the direction of flow in indirect perfusion have been determined to affect the response of human MSCs in 3D constructs. Parallel flow has been shown effective in stimulating the production of FGF-2, but transversal flow improves mass transfer within the scaffold, allowing for a more uniform distribution of the factor²¹⁸.

Another current use of perfusion bioreactors in AC tissue engineering is cell seeding into 3D constructs, which proved to be a good alternative to static seeding methods like droplet or suspension placement and to other dynamic cell seeding methods using agitation and centrifugation²¹⁹.

2.2.6.2. Hydrostatic pressure inducing Bioreactors

Hydrostatic pressure bioreactors, previously introduced in the mechanical stimulation section, apply the hydrostatic pressure stimuli through the pressurization of the culture media directly or with the use of a pressurized gas. These bioreactors are divided between continuous and discontinuous operation mode. In discontinuous systems, constructs are in atmospheric pressure during culture and need to be transferred periodically to a pressurized chamber. In continuous systems, both cultivation and stimulation are performed in the same chamber, with a reduced interaction between the operator and the bioreactor system²²⁰. Furthermore, the hydrostatic pressure bioreactors are further divided by Zvicer and Obradovic²²⁰ into five categories. Within the discontinuous bioreactors, there are discontinuous systems with direct pressurization of the cultivation media by a piston and discontinuous systems with indirect pressurization by a compression fluid. Additionally, within the continuous bioreactor, the separation is in two categories depending on the use of static or perfused culture. Noteworthy, bioreactors for AC tissue engineering approaches can combine hydrostatic pressure stimuli with other forms of mechanical stimulation²²⁰.

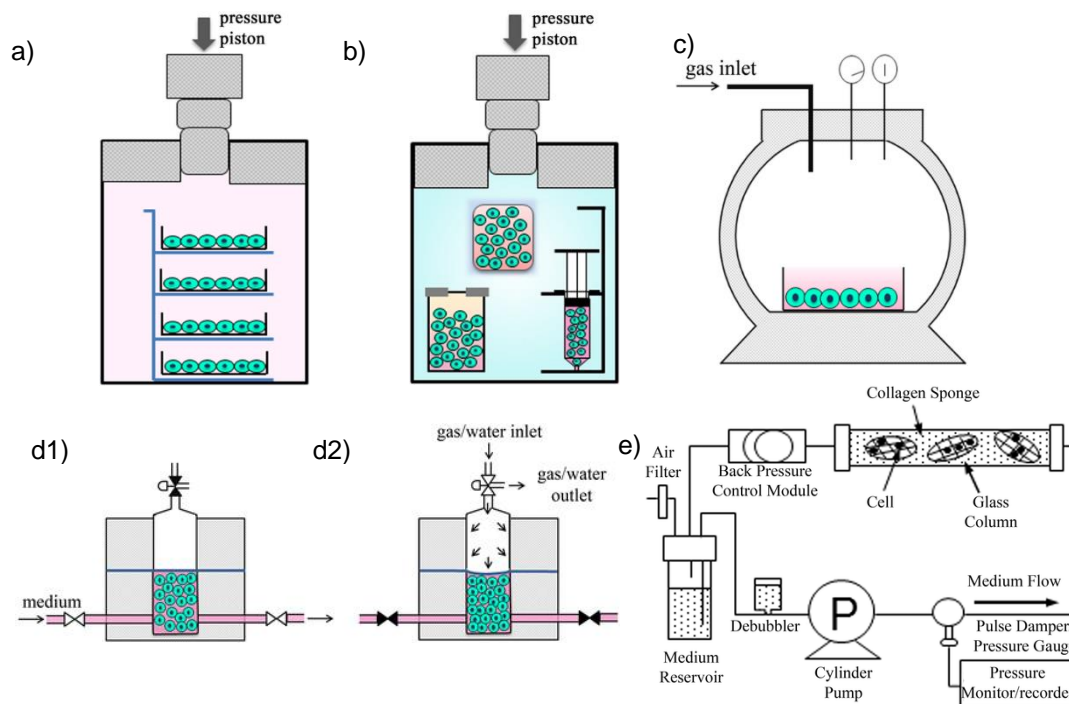


Figure 14 – Schematic representation of various bioreactor architectures for hydrostatic pressure; a) direct pressurization by a piston to the culture media; b) Indirect pressurization by a compression fluid the cell cultures are placed within a sealed bag or other closed vessel; c) Pressurisation of the cultivation media through injection of gas to the culture chamber; d1) Bioreactor with perfusion and a pressure chamber with a membrane in the interface with the culture chamber; d2) Pressurization by injection of fluid to the pressure chamber; e) Perfusion system that induces moderate hydrostatic pressure by use of an actuated valve and a pump. Adapted from Zvicer et al (2017)²¹⁴

Bioreactors employing hydrostatic pressure stimulation have been shown to have a significant effect in inducing cartilage formation. Studies with monolayer chondrocytes have shown improved results with dynamic stimulation¹⁶⁷, while recent studies with 3D constructs suggest a positive effect with static HP. Accordingly, immature bovine chondrocytes embedded in collagen sponges with static 2.8 MPa showed comparatively enhanced results¹⁶⁸. These results contradict several studies in which a greater

promotion of chondrogenic differentiation is observed in 3D tissue constructs obtained under dynamic hydrostatic pressure. A study using chondrocytes encapsulated in gellan gum hydrogels cultured with 0.4 MPa hydrostatic pressure under pulsatile dynamic or static for 3 weeks, showed improved chondrogenic phenotype with dynamic stimulation¹⁶⁹. Additionally, research studies using HP stimuli with magnitude of 10 MPa at the frequency of 0.33 Hz for 4 hours/day showed concurring results¹⁷⁰.

2.2.6.3. Direct Compression Bioreactors

As discussed above, compressive forces are a major factor on chondrocyte microenvironment and influence considerably the chondrogenic differentiation process and the maintenance of chondrocyte phenotype. For this reason, it is natural that bioreactors for dynamic compression stimulation are widely used in AC tissue engineering. The most common design of this type of bioreactors is composed of a vessel containing culture media, an apparatus for fixing scaffolds within the vessel and an actuator. The simplest design for application of direct compression to AC constructs is operated in a static mode and the actuator does uniaxial compression over the submerged tissue constructs, powered by electric step motors that can be computer-controlled^{221,222}.

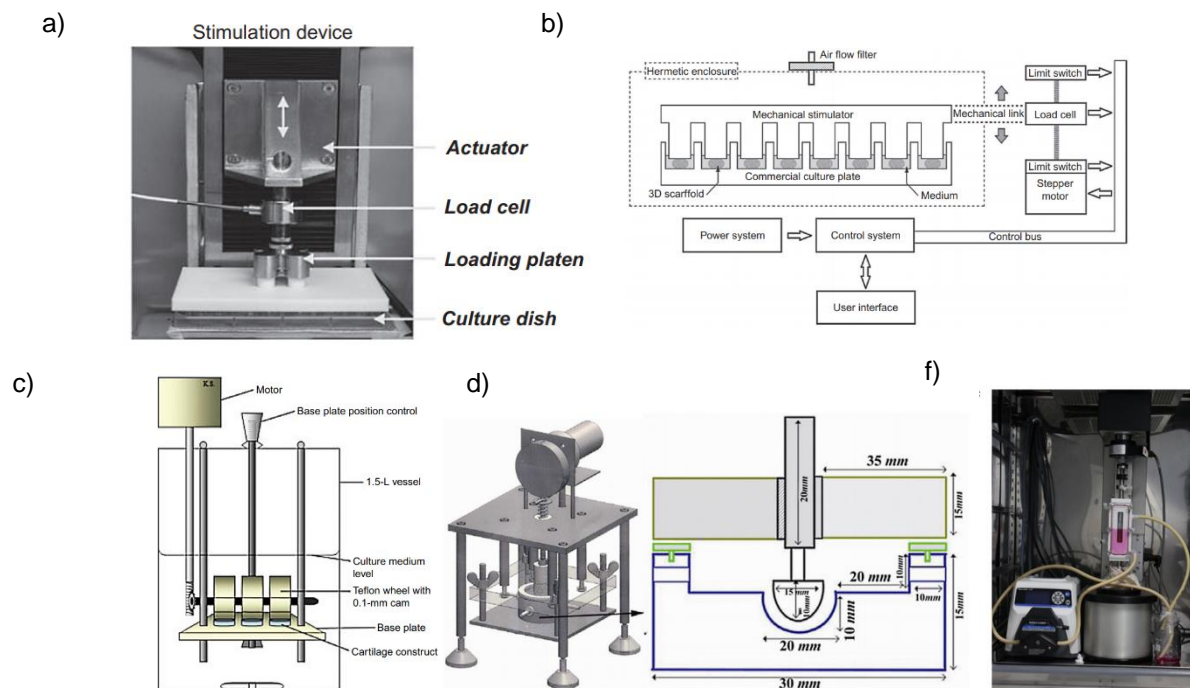


Figure 15 – Representation of various configurations direct compression Bioreactors; a) traditional loading apparatus with a culture dish that can be operated within an incubator adapted from Waldman et al (2006)²¹⁹; b) multiple well stimulation apparatus adapted from Correia et al (2016)²²⁰; c) stimulation apparatus to be used submerged in culture media, includes a screw driven compression actuator and rollers as actuators capable of rotating and as such inducing contact shear Shahin et al (2012)²²¹; d) Bioreactor combining perfusion with direct compression, the beads or sheet constructs are place in the well and the media perfuses in the greater chamber, the actuator is shaped as is the well like a semi-sphere adapted from Gharravi et al (2012)²²²; f) Comercial bioreactor BOSE ElectroForce® with perfusion and compression, adapted from Brunelli et al (2019)²⁰⁶.

Other less common but more capable systems introduce perfusion into the design^{224,208}, having the advantage of better supply of soluble factors and nutrients to the construct combined with a fluid induced

shear stress stimulation, which provides a closer mimicry of the native articular cartilage tissue. Moreover, other designs combine direct compression with direct contact shear stimulation²²³.

2.2.6.4. Bioreactor mimicking joint biomechanics

The current trend in the development of bioreactors for AC tissue engineering employs the use of various forms of mechanical stimulation in simultaneous to mimic as closely as possible the mechanical environment of the synovial joint and native articular cartilage tissue.

The combination of compression and shear stress has been targeted in several studies, including the works of Shahin and Doran²²³ presented in figure 16c) and Gharravi et al²²⁴ in figure 16d), which are early representatives of this tendency combining direct shear and fluid induced shear, respectively, with direct compression. Another design possibility that has been pursued is the use of a compression piston for compression in the z axis while moving the actuator in the x axis to produce a direct shear stimulation²²⁵ (a scheme of this bioreactor is presented in figure 16a)).

The abovementioned works achieved promising results in terms of increased GAG and collagen synthesis and, for that reason, more refined bioreactor designs have since been presented, highlighting this design philosophy.

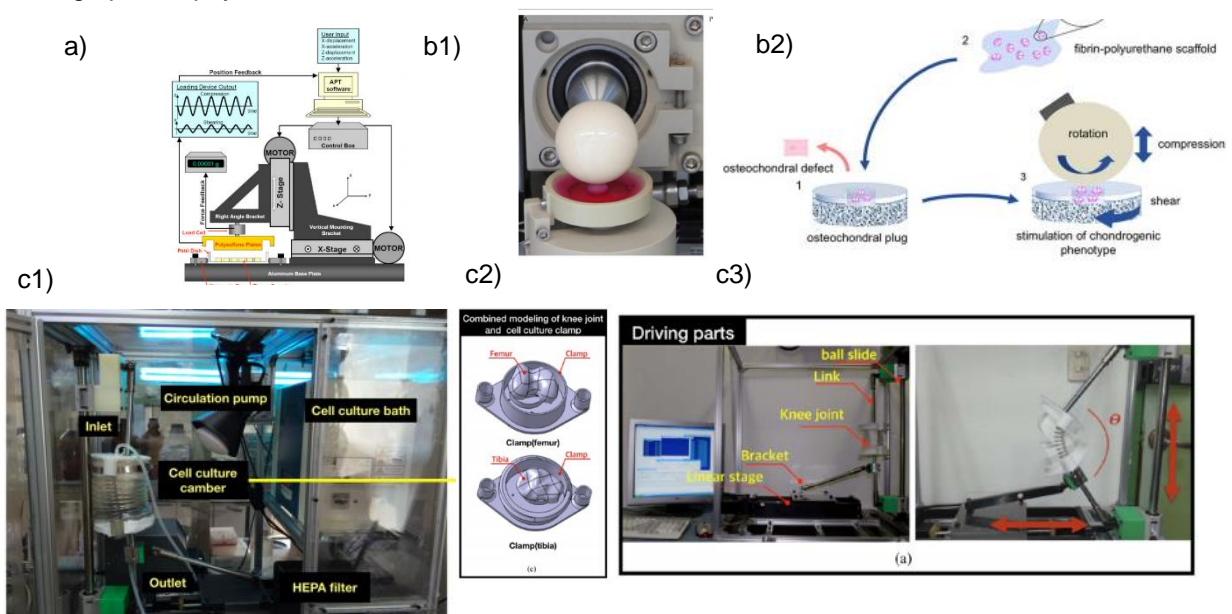


Figure 16 – Schematic representations and photographs of a selection of bioreactor designed to recapitulate the mechanical environment of the joint; a) dual axis actuating apparatus composed of a arm on rail that induces movement parallel to the plane of the construct inducing contact shear, this arm supports a compression actuator Bilgen et al (2013)²²³; b1) image of a typical pin and ball bioreactor design;b2) the bioreactor is composed of a pin capable of moving the ball actuator in the perpendicular plane to the plane of the construct, inducing compression, and the actuator the ball is capable to rotate producing contact shear. Vainieri et al (2018)¹⁸²; c1) cell culture part layout of the bioreactor;c2) model of the culture chamber and 3D printed joint, these two halves of the chamber join to form an articulating perfused chamber, allowing the movements to mimic the moving knee-joint;c3) Driving mechanism that allows for movement of the 3D printed joint within the chamber to move in the two anatomical axis for the knee-joint, Jeong et al (2019)²²⁴.

The work that might be considered the next step on the recapitulation of the biomechanical environment of articular cartilage is the multi-axial motion bioreactor developed by Vainieri et al¹⁸⁴ presented in figure 16b). The actuator of the bioreactor is a commercially sourced ceramic hip ball, which is pressed and rolled over the construct, producing compression and contact shear, respectively. This work was preceded by the work of Trevino et al²²⁷, which used a similar apparatus for stimulating the constructs, but was used to study the tribological properties of cartilage-on-cartilage interaction. The interaction required the use of two explants of native cartilage of bovine origin, one placed in the moving ball and the other in a receptacle like the one used by Vainieri et al¹⁸⁴. In general, this type of design is called pin and ball and is attributed to Wimmer et al²⁰⁴, which dates back to 2004.

Vainieri et al¹⁸⁴ performed a study on defect models produced from osteochondral explants of knee joints of calves. These defects were repaired with chondrocyte-polyurethane constructs and stimulated with a constant compression producing displacement of 0.4 mm or 10% to 14% strain or dynamic compression applied superimposed to this baseline strain producing up to 0.8mm or 20% to 26% strain in a sinusoidal manner with 0.5Hz frequency. The shear motion was induced by ball oscillation at $\pm 25^\circ$ and 0.5 Hz. The peak mechanical loads applied to the AC construct were approximately 0.35 MPa. This osteochondral model allowed to experimentally confirm that the use of this scaffold showed good results in terms of cell viability, low surface wear and typical chondrocyte gene expression¹⁸⁴.

The work of Jeong et al²²⁶ shows a completely novel approach of bioreactor design in the context of cartilage tissue engineering. This work goes further than any other before to mimic the knee-joint movement and biomechanical environment. As presented in figure 16c) the bioreactor is composed of a driving assembly that reproduces the movement of the knee-joint. The joints were 3D printed from a modeled femur and tibia using a biocompatible material (MED610). The surfaces of the joint were coated with a silicone and a 3 mm hole was done for the installation of a scaffold. These bone models were attached to a driving system that allows it to move in two directions, as the movement of the knee joint as two degrees of freedom. These printed joints were enclosed in a culture chamber that allowed bending movement and were placed under perfusion. Thus, this bioreactor system incorporated multiaxial compression, contact shear and fluid induced shear as mechanical stimulation signals. The authors considered this bioreactor system as a possible replacement for the use of animal models in AC tissue engineering studies or disease modeling, and that can also provide an improved model for rehabilitation and to tailor the treatment according to the position of damaged cartilage²²⁶.

3. Materials and methods

3.1. CAD design

The 3D models produced during this work were used to represent and analyze the different design concepts investigated during the ideation and design process but, also used as input to the 3D printing of each component in the prototyping part of the work.

The software used to produce said 3D models was Solidworks 2018 student edition. This software is a solid modelling CAD (computer-aided design) software that includes also CAE (computer aided engineering capabilities). The CAE capabilities of the software were used in their fluid flow simulation function, which will be discussed in the following section.

The workflow of producing a 3D model in Solidworks consists in first producing a 2D sketch and extruding this design's features into a 3D space, this extrusion can be done linearly, rotationally around a chosen axis or along a previously established 3D profile. The other main form of modifying the 3D model is to produce a 2D sketch and extrude from this a cut of an already modelled 3D part.

Solidworks also has the virtual assembly functionality, that is doing virtual integration of components in a visual model of the assembled components that can also be used in the CAE capabilities of the software.

For assembly of the components it is necessary to define the spatial relation of the said components, this means defining what in software are called "mates", this can be for example coincidence of geometric features, distance, concentric circular profiles, or more complex like a simulated screw/ thread relationship. The use of the assembly mode is not only important to produce the assembled models presented in this work, and used in the fluid dynamics simulation but, were also important in the design process allowing for adjustment of components design based on the interaction with other components without the need for actually constructing the said parts.

3.2. Computational fluid dynamics

As discussed in the previous section Solidworks is not exclusively a CAD program but also includes CAE tools, within these tools is a Fluid simulation plugin. This plugin was used for simulating the flow within a culture chambers of the bioreactor.

The flow pattern and the flow characteristics of the fluid in the culture chambers are necessary to inform the design of the bioreactors because as previously discussed fluid induced shear stress is a main factor in determining cell fate of MSC and chondrocytes, and for that reason is a main cue in articular cartilage tissue engineering.

The fundamental basis for solving CFD problems are the Navier–Stokes equations, these equations use the of Newton's second law adapted to fluid flow and are an evolution of the simpler Euler equations that consider inviscid flow, while the Navier-Stokes equations consider the viscosity of the fluid²²⁸, the remaining equations consist of mass, momentum and energy conservation laws²²⁹. In CFD application

this equations are reformulated or discretized, various methods exist for discretization but Solidworks fluid flow uses the finite volume method²³⁰.

The finite volume method consists on dividing the flow domain into control volumes, generally referred to as cells and the variable of interest is evaluated at the centroid of each cell. The differential equations that are associated to each control volume are integrated and interpolation is then used to describe the variation of the variable in evaluation between control volume centroids²³¹. For the division of the fluid domain Solidworks instead of using the more common body fitted algorithms, to define fluid flow domain around solid objects commonly composed of tetrahedral shaped cells, uses a Cartesian-based mesh. A Cartesian mesh is composed of cuboids adjacent to each other oriented along the cartesian coordinates. The cells intercepted by the surface of the solid body are called “cut-cells” and are treated differently depending on the boundary conditions of the problem²²⁹.

The use of Solidworks flow simulation is simplified by the fact that it is done in the same software as the CAD models, dispensing the export and import of files between different software.

The use of the CFD plugin starts with the design of the parts and assembly as described previously. The next step is to create a new simulation in the Fluid flow tab of the program, for this the wizard option was used that directs the user in the creation of a new CFD simulation. The unit system used was centimeter, gram, dyne (cgs) because it better fits the scale of the problem, the wall roughness was defined as 25 μm , this value was obtained from the work of Hartcher-O’Brien et al²³² that determined the roughness of 3D printed parts by the fused deposition modelling, the method used in this work. This data is not specific for the material used in this work but, it was the best approximation found. Finally, temperature was defined as 37° C, the culture temperature generally used, as will be discussed in a following section of this work, and 1 atm of pressure. The mesh and fluid domain were chosen automatically by the program and were verified by the tools of this program to fit the domain of interest. The number of fluid cells created is 30799. The boundary conditions used and the number of iterations to solve the problem are resumed in the following table.

Table 7 – Synthesis of the frontier conditions and number of iterations by CFD assay

Frontier Conditions	Number of iterations before solution convergence
$Q_{in} = 2 \text{ mL}$ $Q_{out} = 2 \text{ mL}$ $P_{\text{at the fluid surface}} = 1 \text{ atm}$	150
$Q_{in} = 1 \text{ mL}$ $Q_{out} = 1 \text{ mL}$ $P_{\text{at the fluid surface}} = 1 \text{ atm}$	118
$Q_{in} = 0.5 \text{ mL}$ $Q_{out} = 0.5 \text{ mL}$ $P_{\text{at the fluid surface}} = 1 \text{ atm}$	118

The simulation goals chosen were the dynamic pressure, the velocity, the force and shear stress as global goals, the local goals for the surface of the scaffold were average velocity (including the separate x,y,z components), total force acting on the walls and shear stress.

3.3. Prototyping

Prototyping the designed bioreactor was the ultimate goal of this master thesis work, for this the chosen method was 3D printing. The beginning of this process was to convert the Solidworks file format to stereolithography (STL) file format that could be read by the 3D printer, the following 3D printing will be discussed in the following section.

3.3.1. 3D Printing/ Additive manufacturing

3D printing is a manufacturing process that can produce a three-dimensional object from a CAD model. In general 3D printing adds material layer by layer, and for this reason it is considered an additive manufacturing technique²³³, in opposition to traditional manufacturing processes like machining or forging that remove material.

The particular technique of 3D printing used in this work is Fused deposition modelling, which is the most common consumer level technology for 3D printing. This technique consists of a thin thermoplastic filament that is fed into a machine where the extrusion head melts the filament in a thickness of typically $250\ \mu\text{m}$ ²³³ this extruded filament is deposited according to the position of the extrusion head. This method is considered one of the most cost effective and simpler methods of 3D printing, but is limited on the z axis resolution by the thickness of the extruded filament and also by the extended time to print larger sized parts²³³.

The 3D printer used in this work was the Makerbot model Replicator 2x, pictured in the following image. The filament used was white ABS or Acrylonitrile butadiene styrene of 1.75 mm diameter and density $1.03\ \text{g/cm}^3$ of the brand Velleman. This thermoplastic, ABS, is appealing for cell culture applications because it is chemically inert and not affected by biological agents²³⁴ and can be suitably sterilized using ethanol²³⁵.

In early 3D printing experiments was used as bottom surface to receive the first extruded layer the specialized adhesive tape (shown in the figure). For printing in such a surface, it is necessary to do so with first printing rafts. Rafts are light printed elevated surfaces, printed to be the substrate for the printing of the part. These

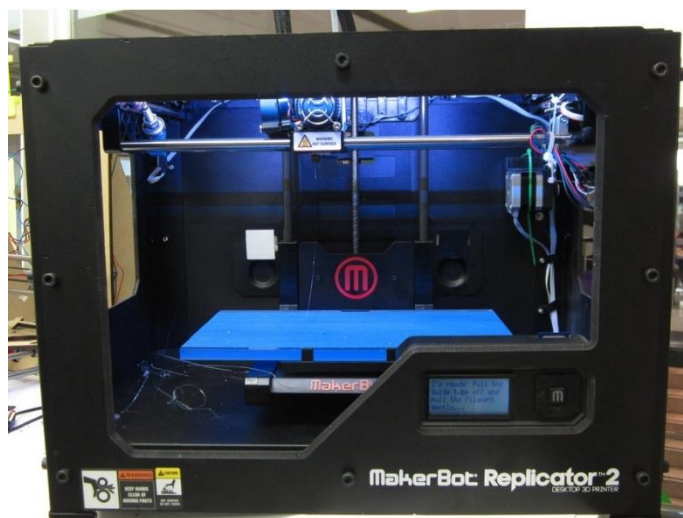


Figure 17 – Image of the 3D printer used in the prototyping phase of this work, the MakerBot Replicator 2x; image obtained from pinshape.com.

rafts were printed in the same material as the part which made the rafts strongly bound to the part making it impossible to fully remove the rafts. Other than the problem of removing the rafts from the part it was also extremely difficult to remove the printed parts from the build plate of the 3D printer, these two problems occurred mostly to the larger parts needed for the final bioreactor design.

Because of the problems found printing directly on the specialized tape over the heated bed of the 3D printer it was decided to attempt to print over a glass surface. A small glass plain was fixed using tape to the build plate and the z axis restricted to take in account the increased height of the build plate. This solution produced smoother pieces and did not demand the use of rafts, this allowed the pieces to be easily removed from the bed.

One problem that was noted was that the glass was not perfectly level creating some difficulties in calibrating the machine and possibly small warping in the parts. The difficulty in calibrating the machine was mostly noticeable for larger pieces and it had the side effect of in some instances the filament not adhering to the build plate and the 3D printing process needing to be restarted and the machine recalibrated. Sometimes the restart recalibrate cycle needed to be repeated up to 5 times until the print proceeded with no problem. Despite of this limitations, the better quality parts are considered worth the complications associated with this modification of the 3D printer.

The polymer had a tendency for clogging of the extrusion head of the 3D printer, in one instance this clogging broke in the filament within the extrusion head assembly, to solve this it was required to disassemble the machine and by heating the assembly with a heat gun to remove the fragment of filament. To solve this chronic occurrence, it was decided to operate the machine in colder extruder temperature, at 210° C a value below the recommended by the manufacturer for ABS (220° C to 270° C).

Table 8 - 3D printing parameters

Material	Acrylonitrile butadiene styrene (ABS)
Printing Infill	10%
Layer height	0.20 mm
Extrusion head temperature	210° C
Build plate Temperature	100° C
Speed while extruding	40 mm/s outlines; 90 mm/s infill, insets, top and bottom

3.3.2. Actuation Control/ Drive

For the construction of the actuator control and driving system the materials used were: Arduino mega 2560 microcontroller board, USB cable to connect the board, power source VT-20250 from V-TAC, a A4988 stepper motor driver, a model MT-1704HS168A stepper motor from Motech motor, jumper cables and a 50 µF capacitor. The code for the microcontroller was created in the Arduino specific programming environment Arduino IDE, that includes the Arduino specific C++ programming libraries.

4. Results and discussion

4.1. Design Objectives

As previously stated, the objective of this thesis work is to propose, design and prototype a bioreactor for articular cartilage tissue engineering. The overall goal for the bioreactor here presented is to produce tissue with hyaline like properties, with clinical and research relevance. As discussed in the introduction the requirements for the production of tissue engineering constructs of articular cartilage are multiple and of varied nature and need to be taken into account as input for the design of the bioreactor.

The basic needs of any bioengineering culture system of maintaining culture conditions are present but are associated with the need of relevant stimulation of the tissue constructs, in this case with mechanical cues.

The nature of the AC constructs needs to be taken in to account as well as the need to keep the culture free of microbiological contamination through passive methods of sterility maintenance, but also the possibility of sterilization of the bioreactor by some practical method prior to operation.

Table 9 – Synthesis of the design Objectives for the Bioreactor

Mechanical Stimulation	Compression: 10% to 20% strain 1Hz frequency
	Hydrostatic Pressure: 5 MPa to 10 MPa
	Shear: to be determined by CFD
Culture Conditions	Temperature: 37° C Oxygen Tension: 3% ²⁴² to 5% ¹⁵⁴ Humidity: 100%
Construct Size	1 cm ² to 10 cm ²
Scalability	Capable of parallel integration of culture chambers
Construction	3D Printing

4.1.1. Mechanical stimulation

Mechanical stimulation has been previously discussed in the introduction section, with particular focus on its role on the differentiation of MSCs into mature chondrocytes or the maintenance of chondrocytes with the correct phenotype, (stimulation of ECM synthesis). Mechanical stimulation is considered an important factor to produce a good quality tissue, that can be used in a potential clinical setting or as an in vitro model useful in research applications.

The types of mechanical stimulation that were proposed in the final design or intermediate designs are hydrostatic pressure, shear (fluid induced, or contact induced) and direct compression. These three main forms of mechanical stimulation are relevant in articular cartilage, and are suggested to be applied, either solely or in combination, on ranges that mimic the physiological conditions for articular cartilage.

Various research works (Li et al⁶⁸) combined compression and contact shear, or (Gharravi et al²²⁴) perfusion with compression and (Mizuno et al¹⁶⁵) perfusion with hydrostatic pressure. These studies presented positive results and are the basis for the decision to introduce in this work the combination of mechanical stimulus of different nature.

The magnitude of mechanical stimulation and frequency of dynamic stimulation are project variables that should also be set in the beginning of the design process. The following decisions were taken on the design of the bioreactor concerning mechanical stimulation:

- 1) **Dynamic stimulation** has shown consistent results that are better than those for static simulation^{165,171,169,168}, for this reason dynamic stimulation studies seem to dominate the current research in this field, especially for hydrostatic pressure and compression stimulation.
- 2) **Frequency of stimulation** the bioreactor should be able to work within the physiological range at values around 1 Hz¹⁶² the general walking cadence of a human.

The magnitude of the various forms of mechanical stimulation is a more debatable question as there are studies that employ different magnitudes.

- 3) For **direct compression** the magnitude of the stimulus is already well studied. Physiological **strain** exerted on the articular cartilage of the knee (Table 2) range is between 4% and 11%, the research works compiled in Table 7 show that in general research on direct compression uses strains that are in the upper physiological range or above it, generally in the range of **10% to 20%**, the design of the bioreactor should then be capable to produce a **direct compression** within this range, as most results indicate that it is the range, both for MSC^{5,68} differentiation and to stimulate the maintenance of chondrogenic markers in chondrocytes¹⁹⁵.
- 4) Measurements of **hydrostatic pressure** and shear stress exerted over the cell population in vivo are not available, this is not possible to measure in a noninvasive way just like measuring the forces exerted in the joint (table 1). The various works using hydrostatic pressure (table 3) resulted on varied levels of success, a hydrostatic pressure in the range of 1 MPa to 10 MPa, the work of Correia et al¹⁶⁹ showed that the resulting cartilage constructs are of lower quality when pressures lower than 1 MPa are applied, in this case 0.4 MPa. The application of hydrostatic pressure with magnitude of 1MPa to 5 MPa have good results at increasing the expression of aggrecan^{168,171,174} but higher pressures of 5 MPa to 10 MPa were needed for significant increases in the expression of collagen type II¹⁶⁸ and increase of the ratio of composition of Collagen type II over collagen type I¹⁷⁰, this ratio

when low is associated with the loss of the chondrocyte phenotype²³⁶. In conclusion the current scientific consensus indicates that a hydrostatic pressure in the range of **5 MPa to 10 MPa** would be ideal in the bioreactor design.

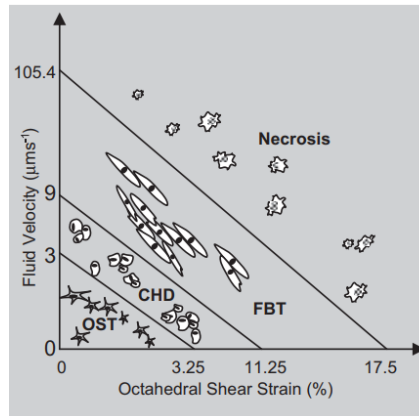
5) Direct Compression can be theoretically described by the biphasic theory. According to this theory the way compression is manifested in the cellular level, is in part through the pressurization of the liquid entrapped in the tissue¹⁶¹. Because of this applying by expressly different methods **hydrostatic pressure and direct compression was considered redundant in this work** and will not be proposed in any of the following design ideas, in the literature there were no works using this combination of express stimulus found.

6) **Fluid Induced Shear:**

The works that focus on **fluid induced shear** by mixing or perfusion are particularly hard to compare because they are generally characterized by the operating conditions in either rotations per minute (rpm) for spinner flask and rotating wall architectures or in volumetric flux values for perfusion, generally in mL/min, these values are not easily comparable between each other. Even the same rpm or the same volumetric flux for different geometry or different scaffolds with different fluid flow characteristics result in different hydrodynamics making comparison of systems difficult. The idea of introducing mixing was not explored at length as a possibility for the design of the bioreactor as it is an architecture that demands a great volume of media to be feasible and is not particularly suited for the stimulation of AC constructs, furthermore chondrogenic media is costly and great volumes of it can rapidly become prohibitively so.

The use of perfusion will be the most explored way to induce fluid induced shear but, the problem of obtaining a relevant target value for the shear stress/ volumetric flow in the literature remains. The only feasible way to obtain the shear stress produced in the surface or within the scaffold is the use of computer simulation of fluid dynamics (CFD), combined with experimentation, to determine operation conditions able to achieve relevant values of shear stress to induce a chondrocyte phenotype similar to the one of hyaline cartilage.

There are published works that use the published data of various published “basic science” works on the response of chondrocytes or MSC constructs to mechanical stimulation, to simulate the cell response. One of the most extensive such modulation is that done by Stops et al²³⁷. This work aimed at achieving a physical modulation of the scaffold deformation and the fluid flow in the interstices of it by finite elements (FE) simulation and CFD. Additionally, the authors using a model of the cell response to stimulation in the conditions determined by FE and CFD simulated the fate of the MSC and ultimately obtained a simulation of the cell composition on the scaffold.



Modified Pendergast *et al.* (1997) Mechano-Regulatory Model (cell necrosis added)

Figure 18- Mechanical regulatory model of Pendergast *et al.* (1997)²³⁸ modified by Stops *et al.* (2010)²³⁷ to include necrosis. Octahedral shear strain is the shear strain (described in the biomechanics section) as simulated the FE mesh cells in octahedral shape. Fluid velocity in this case refers to the velocity felt by the cells, in the case of porous scaffolds this is the interstitial fluid velocity.

In general, these conditions of fluid velocity and octahedral shear strain are dependent on the characteristics of the scaffold used in a much greater degree than on the geometry of the culture chamber, as such the perfusion volumetric flow would need to be changed and adapted depending on the scaffold used because the microenvironment that surrounds the cells is determined by the scaffold properties.

One presumption of the design of the bioreactor is that it should have compatibility to various types of scaffold and for that reason not one fluid induced shear parameter can be determined in general but needs to be determined in a case by case basis.

4.1.2. Culture conditions

As previously discussed oxygen tension is a major factor in articular cartilage tissue engineering conditions, In normal conditions the oxygen tension *in vivo* is on the range of 2% to 7%, in addition to this it has been determined that hypoxia through hypoxia inducible factors promotes the expression of chondrogenic marker genes like those that code for the ECM components²³⁹. The effect of hypoxia in the regulation of phenotype is reported to affect the chondrocyte, preventing hypertrophy²⁴⁰, but also chondrogenesis of MSCs^{241,242}. In conclusion for MSC chondrogenesis, and also for chondrocyte culture, the optimal range of oxygen tension is within the 3%²⁴² to 5%¹⁵⁴.

The remaining culture conditions that are not AC specific are the remaining atmosphere parameters such as CO₂ tension and humidity, humidity generally is kept at 100%, as saturation prevents the evaporation of media²⁴³, CO₂ tension is crucial to maintain the pH of the culture.

Temperature of culture of human, and generally animal, cells is commonly the average temperature of the human body of around 37°C, this temperature has been verified to be the best for chondrogenic

marker expression and the general metabolism for chondrocytes, between the temperatures of 32°C, 37°C, and 41°C even though good results were also obtained for culture at 32°C²⁴⁴.

The design of the bioreactor could incorporate the capability to control all these parameters but, that would entail a greater level of complexity in the amount of systems that needed to be designed and in the control equipment and software that would need to be developed. That was not possible to achieve in the scope of this thesis. As such these capabilities are allocated to an incubator, this allows greater simplicity in the design but creates the conditions that the designed bioreactor must fit in an incubator in a practical way and all electrical systems must be compatible with the conditions inside the incubator.

4.1.3. Scaffold and tissue construct and Cell type

One of the propositions of this thesis work was the possibility of culture and stimulation of 3D tissue engineering construct aiming at the development of AC tissue constructs. Culture in 3D mimics more closely the 3D microenvironment native to articular cartilage. Therefore current consensus is that 3D culture is important to the production of good quality tissue constructs²⁴⁵. For this reason, culture methods that were relatively common earlier like monolayer cell culture are now often discarded when envisaging the design of the bioreactor.

Various scaffold types and material are used to promote the development of cartilage like tissues. These were briefly discussed in the section of the introduction pertaining to scaffolds. In general hydrogels are considered an interesting type of scaffold, as their characteristics are compatible with clinical application in minimally invasive surgery with *in vivo* crosslinking of the polymers²⁴⁶.

In terms of material composition, scaffolds can be composed of proteins, polysaccharides, or synthetic materials. Collagen and Fibrin are the most important protein materials for scaffold in AC tissue engineering, polysaccharides are most notably Hyaluronic acid and alginate and Polyethylene glycol is an example of synthetic material.

The design objective of the bioreactor is to be capable to operate with various types of scaffold with minimal alteration of the apparatus setup.

Another important consideration to make is the versatility of size of construct to be produced in culture by the bioreactor.

Since one of the main focuses of this work is to design a bioreactor capable of producing clinically relevant AC constructs the information that should inform the construct size is the size of the defect on clinically relevant cartilage lesions.

The current treatment methods that have been discussed previously have clinical indication depending on various factors, within these are the severity, location, age of the patient and most relevant for the current discussion the size of lesion²⁴⁷.

Microfracture is one of the oldest and still currently most common surgical procedures to repair AC, despite of this it is limited in the size of defect that can be repaired to lesion sized between 2 and 3 cm², patients with lower physical requirements or older age can be treated with bigger sized defects often cannot be treated by microfracture. Osteochondral Autograft Transfer or mosaicplasty can effectively treat lesion in the range of 1 to 4 cm² or with multiple grafts up to 9 cm², the limitation of size

of defect that can be treated by this method is greatly associated to the morbidity of the source joints of the grafts. Autologous chondrocyte implantation is of the traditional methods the most capable being able to treat lesions of up to 10 cm² in area.²⁴⁷

In conclusion lesions of surface area between 1 and 10 cm² are of current clinical practice relevance, this should as such be an indication of the size of construct to pursue in the design of the bioreactor.

In terms of cell type to use chondrocyte or MSC, the bioreactor design should be capable of operating with both as these do not respond in fundamentally different ways to the mechanical stimulation, furthermore as discussed in the section concerning the chondrocyte metabolism, the biomolecular mechanisms related with the chondrocyte phenotype maintenance are largely coincident with the mechanisms associated with chondrogenesis.

4.1.4. Maintenance of sterility

Any cellular products that demand a long period culture are potentially subject to microbiological contamination. MSC and chondrocyte constructs have a relatively long culture process including a potential cell expansion stage before differentiation. Therefore culture time can be from some weeks and up to a few months²⁴⁸.

The European good manufacturing practices²⁴⁹ (GMP) state that this sort of medicinal product, a advanced therapeutic medical product (ATMP), must have special attention in assuring aseptic conditions and validating that aseptic conditions are present. This is also valid for strictly research application, as any microbial contamination can affect the results obtained and turn the data obtained unusable, or even the experimentation practically impossible.

Any cell or tissue construct aiming to be used as therapeutic product must pass a strict validation process. Therefore, closed culture systems are preferred instead of open culture like flask-based methods. The operator interaction is a main source of contamination and as such should be limited as much as possible. The ideal bioreactor then should be a closed vessel with the most automation possible, if it is to be compliant with GMP.

In conclusion to assure sterility the proposed design should be a closed vessel with as much automation as possible.

4.1.5. Scalability

A production of tissue engineered constructs for implantation considers as discussed before, constructs with up to an area of 10 cm², moreover autologous cell source is a preferred method. Even if AC is a tissue with no vascularization and because of that low immunogenic response to allografts, autografts are preferred still to avoid the possibility of immune response against the graft. Patient specific constructs are preferred.

In addition to that, GMP demands that different patient therapeutic constructs should have no possibility of contact between each other, this prevents the use of the same shared culture media to culture for more than one patient's specific cell and tissue therapeutic product.

In conclusion, the scale up of the production by increasing the size of the culture chamber is not desirable, for a single patient and to comply with GMP constructs of different patients should not be cultivated in the same culture chamber.

Since vertically upscaling is not useful the other option is to do horizontal upscaling. So instead of increasing the scale of an individual culture chamber, increasing the number of culture chambers is envisaged in the project. For this effect the bioreactor design should possess the capability for parallel integration of culture chambers to allow for multiple constructs to be cultured simultaneously.

4.1.6. Construction methods

The use of 3D printed or extruded thermoplastic for the construction of bioreactors is currently appearing with various works currently published using this technique^{250,251,252}.

The use of 3D printing is booming in various applications of biotechnology and the use of this technique in the construction of bioreactors is now appearing in the literature. The use of this method of construction is advantageous for rapid prototyping as it is relatively fast to go from project to prototype, demands low manhours of work and not much expertise to produce faithful to design components. This technique is also possibly done by using commercially available commodity materials and equipment, like commercially available 3D printers and polymer filament for extrusion, all relatively inexpensive and easily available. These characteristics are beneficial for allowing clinical and research application, in contexts where other means do not exist.

For all these reasons it was decided to use 3D printing to construct most of the components of the bioreactor.

This method of construction also has some disadvantages like the ability to withstand high pressures, limiting the application of hydrostatic pressure as a mechanical stimulus. This downside is thought to be counterbalanced by the streamlining of the prototyping process allowed by 3D printing.

The use of thermoplastics also has the disadvantage of being generally incompatible with autoclavation, at least when relatively small and delicate pieces are at hand, even if the temperatures are not enough to melt the polymer, the humidity and temperature environment affects the shape and structural integrity of the components. For these reasons other methods, generally less effective, for sterilization must be applied.

4.2. Ideation for the Bioreactor design: Integration of different mechanical stimulus with perfusion

This chapter describes the rationale for selection of the type of perfusion to be explored and ideation of the possible strategies to integrate fluid induced shear stress with other mechanical stimuli. As discussed in the design objectives section, one of the main objectives of design is to include various forms of mechanical stimulation, perfusion is one of the forms of mechanical stimulation that is already decided that will be included, mostly due to the several advantages it entails.

Two other forms of mechanical stimulation were considered, those are compression and hydrostatic pressure. As already discussed, these two forms of mechanical stimulation are treated as redundant and as such they were treated as mutually exclusive. Contact induced shear was also considered here, as a non-redundant mechanical stimulus, because it is a better recapitulation of the physiological mechanical environment of native articular cartilage.

Combination of fluid perfusion with hydrostatic pressure, direct compression or contact induced compression will be further discussed on this chapter as it allows to study synergistic effects of different types of mechanical stimulation.

4.2.1. The choice of Perfusion

The choice of perfusion is a starting point for the design of the bioreactor. All the suggested designs here present some form of perfusion. The advantages of perfusion have been discussed in various parts of the present work. These advantages are the improvement of mass transfer to and from the tissue construct, savings of media volume needed to fill a chamber (in comparison to agitated vessel bioreactor designs), lower need of operator interaction (in comparison to static culture), and perhaps most importantly, precision on providing controlled fluid induced shear stress when aiming at mechanical stimulation.

The next design choice to be answered is the form of perfusion. Perfusion is generally divided in two forms depending on the way the flux is directed. If the flux is directed through the scaffold then it is designated direct perfusion, in the case of perfusion only occurring in the chamber, i.e. the fluid moves on the surface of the scaffold then it is called chamber or indirect perfusion.

Direct perfusion is limited to two options of the direction of flux, it can theoretically be done through the bigger surface (top) of the scaffold or through the smaller surface (lateral), the first option is much more common.

Indirect perfusion or chamber perfusion has two general directions of perfusion, either the flow direction is orthogonal or parallel direction to the surface of the scaffold.

Various of these options were explored in conceptual designs that will be discussed ahead.

Another point that was previously referred is that in the case of direct perfusion, very high pressure build up within the scaffold may occur that can be mitigated and controlled by the use of a bypass²¹⁴. The pressure loss of the fluid flow is particularly important in direct perfusion through the smaller cross section of the scaffold, as seen in figure 19 b).

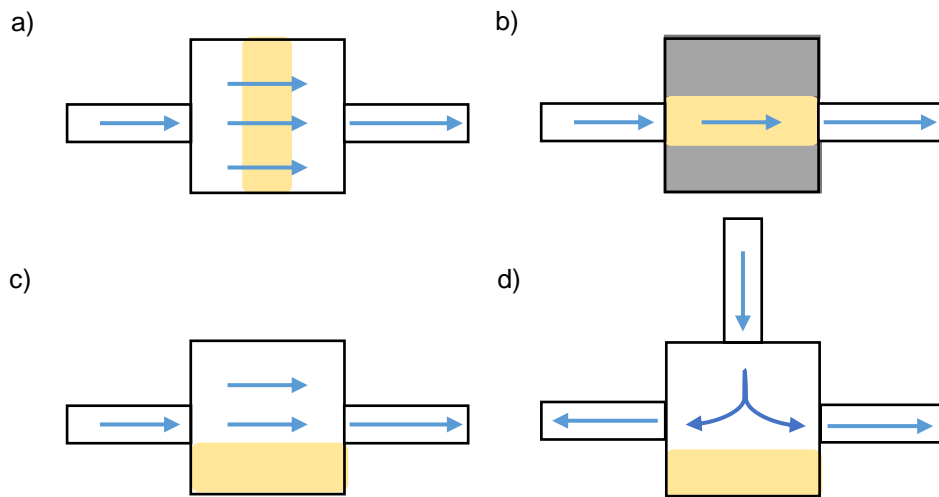


Figure 19 - Schematic representation of the main possibilities for perfusion; a) direct perfusion on the big surface of the scaffold; b) direct perfusion on the smaller surface of the scaffold; c) chamber perfusion; d) orthogonal chamber perfusion; the → (blue arrow) represents the direction of flux, the yellow box represents the scaffold.

4.2.2. Integration of perfusion with hydrostatic pressure

The use of various forms of hydrostatic pressure integration were considered, these include the piston liquid compression, pump + valve, pressurized gas compression of the culture media.

These forms of action are not necessarily original as various works have used these bioreactors architectures to apply mechanical stimulation on AC tissue engineering constructs, some examples were already presented in the introduction. An example of a system including perfusion and pressurization by a gas or liquid is showed in image 14 d) and a system with perfusion and pressurization driven from the combined action of the pump and valve, as shown in figure 14 e).

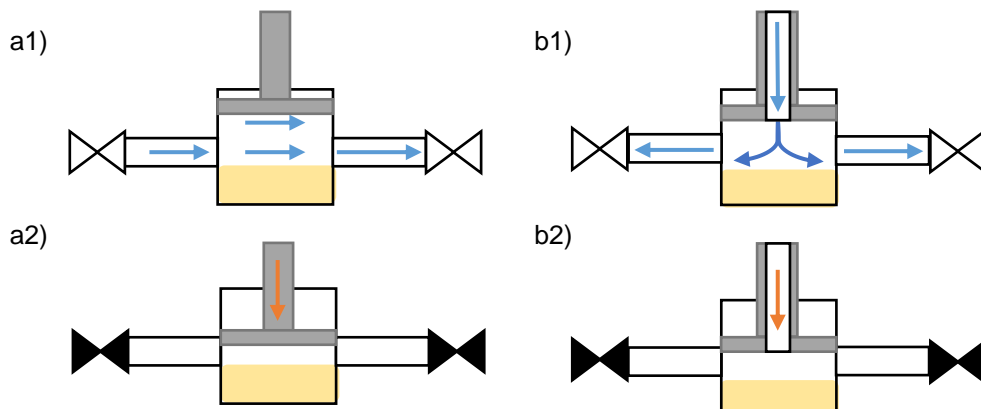


Figure 20 – Schematic cut representation of concepts for integration of perfusion with hydrostatic pressure actuated by a piston; a1) bioreactor with parallel perfusion including actuated valves and a piston for pressurization, in the unpressurized state; a2) same bioreactor in pressurized state with the piston pushed down and the valves closed; b1) bioreactor with orthogonal chamber perfusion, in this concept the entering fluid flow is incorporated within the piston shaft; b2) same bioreactor in the pressurized state; the → (blue arrow) represents the direction of flux, the yellow box represents the scaffold, grey represents the piston, ; the → (orange arrow) represents the direction of movement of a component, the valve symbol when filled in black is in the closed state otherwise is open.

These design concepts with perfusion and hydrostatic pressure actuated by a piston, are composed of a culture chamber that contains the tissue engineering construct fixed, a perfusion system and the actual pressurization of the media is done by the combination of compression by a piston and the required action of closing the media flow by the means of actuated valves. This system could incorporate a dynamic compression by a programming of the actuator of the piston and valves.

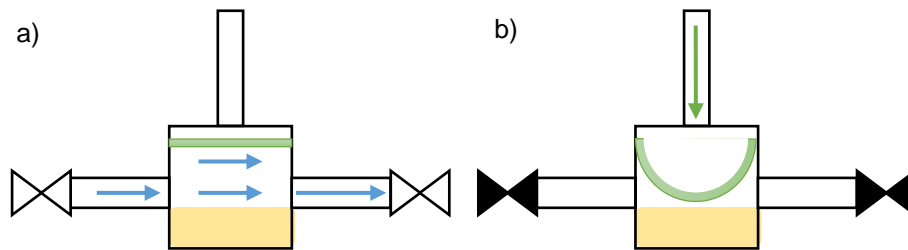


Figure 21 – Modification of the piston actuated hydrostatic pressure perfusion bioreactor instead using a membrane and a compressed fluid that can be air, pumped water or another fluid; a) system in the unpressurized state; b) system in the pressurized state with the membrane being stretched by the pressure fluid transmitting pressurization to the culture chamber; the → (blue arrow) represents the direction of flux, the yellow box represents the scaffold, green represents the membrane, ; the → (green arrow) represents the direction of flow of the pressurization fluid, the valve symbol when filled in black is in the closed state otherwise is open.

This general system for pressurization could be modified to use a pressurized fluid instead of using an electrical actuator moving a piston. This second option of method for pressurization has the advantage of lowering the amount of specialized moving parts, facilitating liquid sealing, sterilization and GMP approval. On such case, the pressurization can be done by of-the-shelf components like air compressors or pumps. The work of Chen et al²⁵⁰ is based on this concept and it demanded the use of a stainless steel pressure vessel to withstand the necessary pressures, going against the preferred construction method for this work. Most importantly this is a design concept already explored and already available in the literature losing the novelty value.

A more innovating idea would be to incorporate direct perfusion with hydrostatic pressure. One possibility to achieve this is to adapt the previous concept of using a membrane to separate a pressure chamber from the culture chamber, using a flexible membrane of some nature.

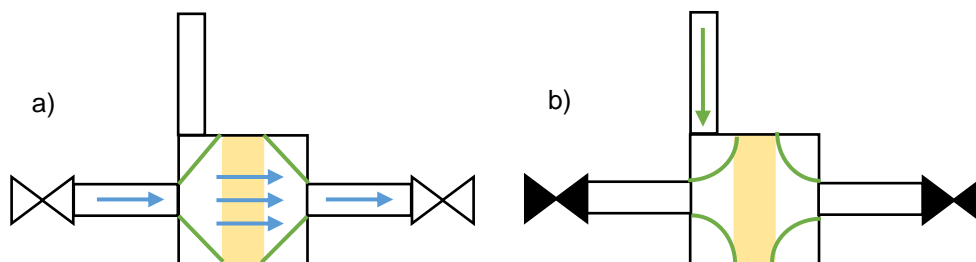


Figure 22 - schematic cut representation of a bioreactor concept including direct perfusion and hydrostatic pressure induced by a compressed fluid; a) bioreactor in the unpressurized state, it contains a biconical shaped chamber within a cubical shaped pressure vessel, the chamber is made of a flexible membrane material, the inner chamber is the culture chamber that contains the fixed scaffold; b) bioreactor in a pressurized state, when pressurized fluid is injected in the outer pressure chamber the flexible culture chamber shrinks increasing the hydrostatic pressure felt by cells in the construct. the → (blue arrow) represents the direction of flux, the yellow box represents the scaffold, green represents the membrane, ; the → (green arrow) represents the direction of flow of the pressurization fluid, the valve symbol when filled in black is in the closed state otherwise is open.

The need to withstand the hydrostatic pressure of up to 10 MPa would be demanding for both the pressure chamber demanding the use of expensive construction methods and materials and possibly not being viable to be prototyped in a timely manner. Additionally, the benefits of direct perfusion in articular cartilage are not clear and for that reason this final direct perfusion idea may not be useful to pursue, even though other concepts proposed ahead use this form of perfusion. Furthermore, in comparison with piston actuated systems, in compressed fluid actuated systems the response to pressurization is more limited (slower) so the dynamic stimulation protocols with physiological frequency 1 Hz may not be feasible.

In conclusion the limitations of the use of hydrostatic pressure turn this form of stimulation a complex problem to produce a functioning prototype, despite this bioreactor concepts being easily integrated in a parallel system, allowing easy horizontal scale-up.

4.2.3. Integration of perfusion and Direct compression

The demands of the high hydrostatic pressure needed for stimulation of articular cartilage constructs make the use of direct compression more attractive from the standpoint of the construction methods needed to produce a prototype.

The idea of a flexible culture chamber proposed for the application of hydrostatic pressure is interesting for other forms of mechanical stimulation because it allows the isolation of the culture chamber from the stimulation mechanisms, this is a form of producing a leak-proof system and diminish the probability of microbiological contamination without the need of many complicated sealing options involving O-rings.

The idea of the flexible culture chamber was then adapted to a direct compression bioreactor. This concept can also be easily expanded with a modular design.

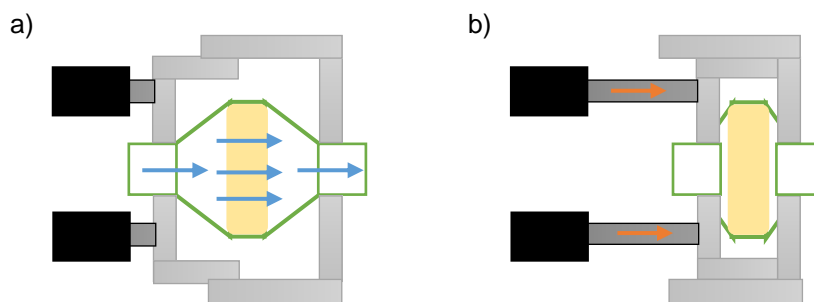


Figure 23 – Bioreactor design incorporating direct perfusion and direct compression, with a flexible culture chamber and an outside box structure that in the compression state presses against the culture chamber walls and through this compresses the cell construct; a) bioreactor in the non-compressed state with direct perfusion culture; b) bioreactor in the compressed state in which the linear actuators push the outside box walls to compress the scaffold; the → (blue arrow) represents the direction of flux, the yellow box represents the scaffold, grey represents the mechanically actuating parts; the → (orange arrow) represents the direction of movement of a component, green represents the membrane that forms the biconical shaped culture chamber, black represents the linear actuator.

4.2.4. Integration of perfusion with direct compression and contact shear

In this configuration the mechanical stimulation would include fluid movement induced shear stress and direct compression by an actuator perpendicular to the scaffold surface. Direct contact shear compression could be achieved by using a second uniaxial actuator system, adding a second movement, in axis parallel to the scaffold surface, allowing another form of mechanical stimulation, contact shear. As already discussed in various sections of this work contact shear is both relevant in terms of the mimicking the natural environment felt by articular cartilage in the synovial joints and proved effective for mechanical stimulation in the context of AC tissue engineering. As such adding a capability to produce direct shear stimulus would greatly enhance the bioreactor design.

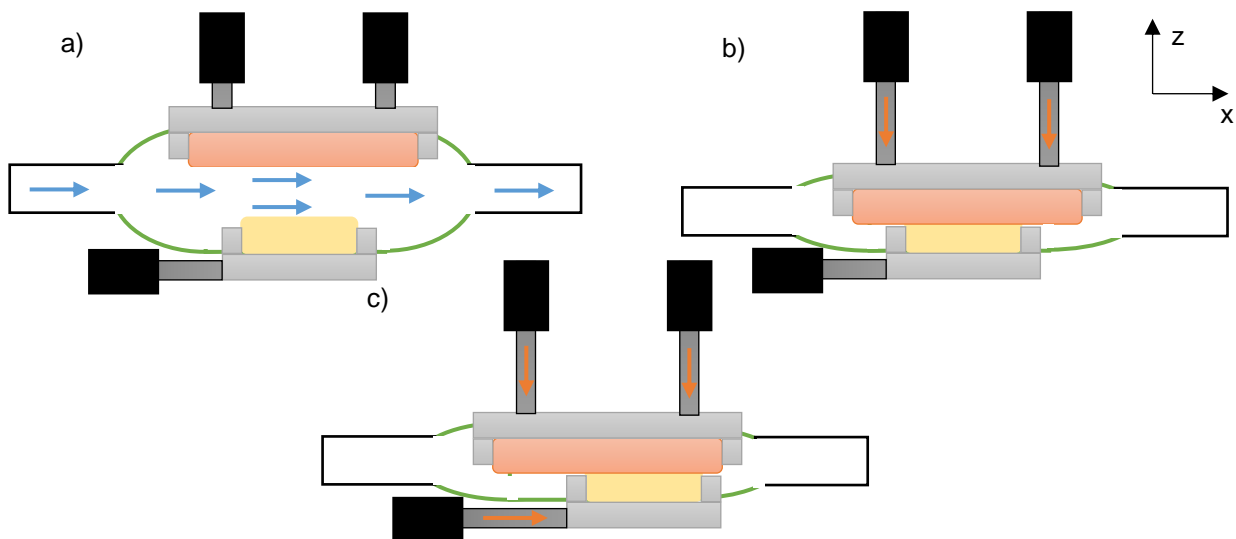


Figure 24 – Schematic cut representation of a chamber perfusion, direct compression and contact shear bioreactor concept, the concept is composed of a culture chamber constituted by a flexible cylinder in which perfusion is made, this chamber contains a scaffold and a soft material actuator fixed opposite each other; a) Indirect perfusion operation of the bioreactor with no mechanical stimulation other than perfusion; b) Direct compression operation, the z axis linear actuators push the actuator against the scaffold producing the deformation of the scaffold; c) the contact shear is produced by activating the x axis linear actuator moving the scaffold in relation to the actuator, producing drag between both surfaces; the → (blue arrow) represents the direction of flux, the yellow box represents the scaffold, grey represents the mechanically actuating parts, ; the → (orange arrow) represents the direction of movement of a component, , green represents the membrane that forms the biconical shaped culture chamber, black represents the linear actuator and orange box represents the soft material actuator.

This bioreactor concept would be very capable in terms of mechanical stimulation possibilities with perfusion, direct compression and contact shear, being capable to faithfully replicate the physiological mechanical environment of native cartilage and produce mechanical stimulation suitable for maintaining chondrocytes in culture with the hyaline like phenotype, as well as direct the MSC to chondrogenesis. Importantly from a scientific study standpoint it would be capable of isolating the 3 forms of stimulation, allowing for separate control which allows them to be studied separately.

The short comings of this design concept are of practical nature, this system utilizing various linear actuators is not practical for construction and operation and is not cost effective, more than that it is also not practical to integrate in parallel various of these chambers to make simultaneous culture of various tissue constructs. The flexible chamber would be subject to constant stress in multiple axis with constant stretching and for that reason finding a material with the correct characteristics of flexibility and durability

would be difficult, but the limitations of time associated with a master thesis make it impractical to follow this design any further.

4.3. 3D modeling for ideation and concept of novel bioreactor designs

Considering the objective of combining fluid induced shear stress and other mechanical stimulation and after a brainstorming process, three bioreactors configurations were closely modeled using CAD software. These designs are designated on this work as: two-scaffold contact bioreactor, the rotor Bioreactor and the Cam Bioreactor. The ideation process for the two-scaffold bioreactor is presented in the two design iterations, the second iteration includes a CAD model. The rotor bioreactor was designed in CAD and the main considerations of this design are also presented. Finally, the Cam design that is the final design prototyped in this work is discussed on a greater length. The Cam bioreactor and its five main design iterations are discussed, and the CAD models are presented for each iteration. The problem of dimensioning of the Cam design actuator is addressed through a mathematical approach here developed.

4.3.1. The two-scaffold contact bioreactor

The design concept discussed on the previous section of integration of perfusion with direct compression and contact shear, despite of all its downsides, was interesting in advancing the ideation process for the development of the bioreactor design. In particular on the idea of integrating two scaffolds in the same stimulation apparatus. Indeed, if one soft actuator is required to direct contact shear, it is only logical that the actual scaffold is used as actuator, under culture. Therefore, the first design idea to be investigated in this work using 3D modeling it was the two-scaffold contact bioreactor, described in this section. Despite the apparent similarities of this configuration and the final design suggested not being obvious, there are key elements that are conserved from these two configurations that will be mentioned on the final subsection of this chapter.

In order to understand whether the challenges posed by the previous design could be overcome, while replacing the soft actuator by a construct, the conceptual design was developed on two steps. First a simplified design, not considering contact shear, but only direct compression was considered. In an adaptation of the design presented in figure 23, two scaffolds can be included in such design and serve as a mutual actuator of sorts.

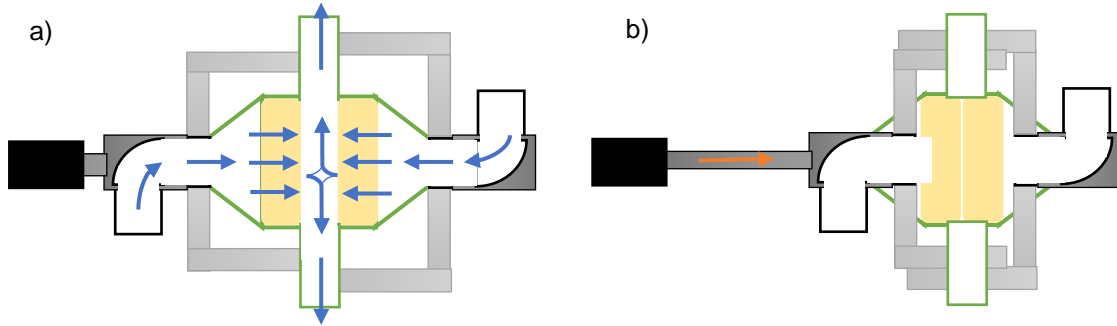


Figure 25 – reactor design concept including direct perfusion and mutual compression of two articular cartilage constructs, this design includes a culture chamber that contains two constructs, this chamber is flexible allowing the stretching and contraction that elicits the compression of the constructs against each other; a) direct perfusion operation of the bioreactor before compression action; b) compressed state of the bioreactor the linear actuator pushes the structure of the outside box that because of this pushes the construct against the other construct that remains static; the → (blue arrow) represents the direction of flux, the yellow box represents the scaffold, grey represents the mechanically actuating parts, ; the → (orange arrow) represents the direction of movement of a component, , green represents the membrane that forms the biconical shaped culture chamber, black represents the linear actuator.

Secondly, the design complexity was increased, evolving the concept to incorporate the idea of using a pendulum motion stimulation. The type of movement provided by a pendulum has the potential to mediate contact shear using simpler mechanisms for creating a rotating motion. The required apparatus will be also mechanically simpler, requiring a simpler construction using only a motor with or without some distributing component like a belt or gears to promote translational movements. The compression stimulation is produced by the movement of a linear actuator that pushes the top scaffold holder against the lower scaffold and the lower scaffold holder rotates in a pendulum like movement sliding over the other scaffold producing contact shear.

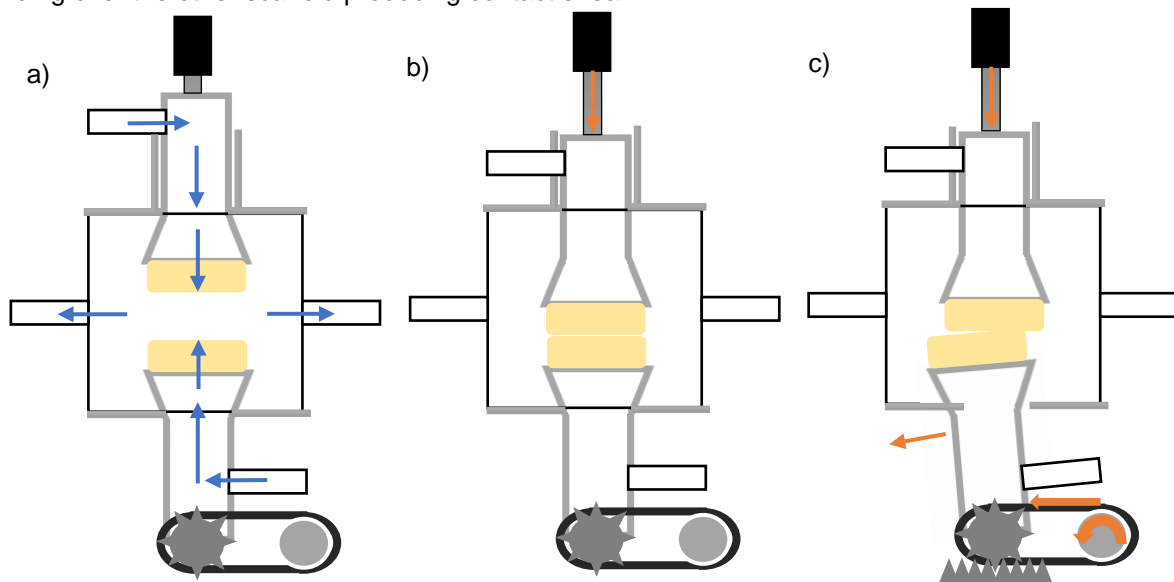


Figure 26 – Cut schematic representation of the joint mimicking bioreactor concept; a) direct perfusion operation similar to the one presented for the previous design concept, in the state without compression and contact shear; b) bioreactor state where the linear actuator is causing compression of both cell-scaffold constructs; c) stimulation state where an electric step motor is activated to trough a belt rotate a gear that is associated with the lower scaffold holder, this gear travels through a gear rack that produces a linear motion that is transmitted to the scaffold holder that moves in a pendulum like motion producing surface drag between the two constructs; the → (blue arrow) represents the direction of flux, the yellow box represents the scaffold, grey represents the mechanically actuating parts, ; the → (orange arrow) represents the direction of movement of a component,

This mechanism needs greater amplitude of movement that would not be allowed by the previous chamber design constraints. This design is inspired in the anatomical movement of the joint. However, contrary to previous work by Jeong et al²²⁴, which aimed at doing a direct mimicking of the form of the joint anatomy; the design here proposed aims at a specific mechanical stimulation, for this reason the design is informed by the tissue engineering needs instead of the anatomy of the joint.

This design suggested on Figure 26 was modelled in SolidWorks™, as represented on Figure 27. This design represents an evolution to the bioreactor concepts considered in the previous section, where the bioreactor represented in figure 24 is the most comparable as it possessed similar capabilities. This bioreactor is capable of culturing two different constructs per chamber while the earlier design could only hold one.

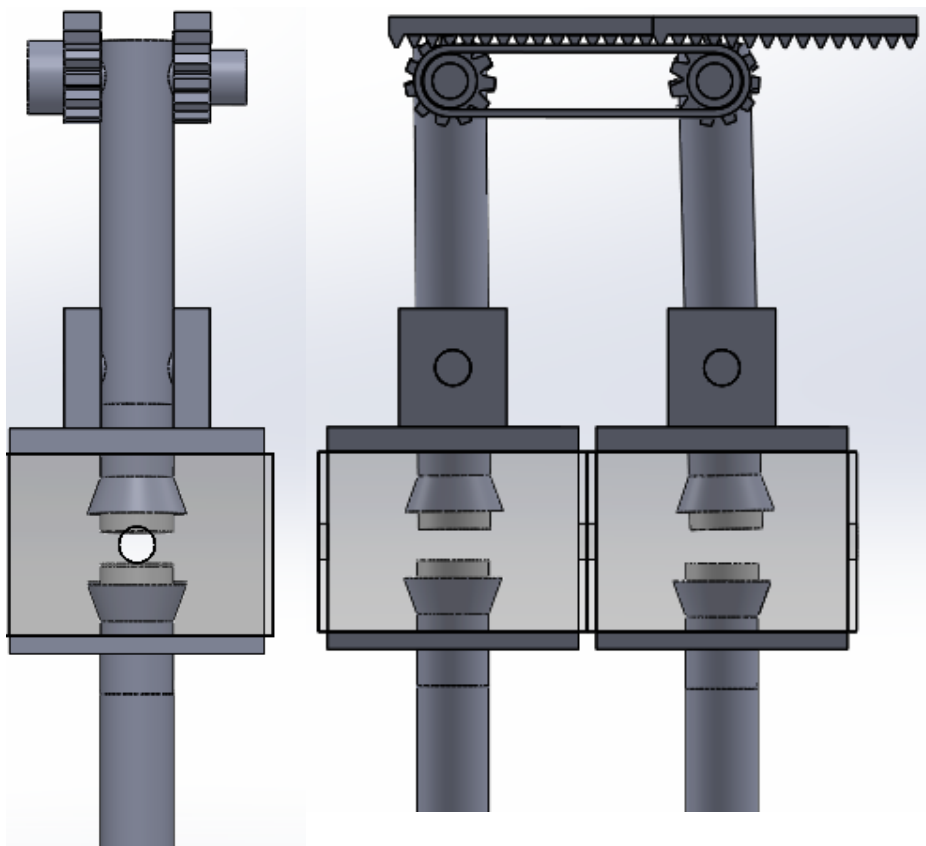


Figure 27- Two different profile views of the 3D model of the joint mimicking bioreactor concept design, produced in Solidworks

The other major advantage of this design concept is that it, in comparison to the previous propositions, is capable of various forms of mechanical stimulation (direct compression, fluid induced shear, contact shear), but without totally losing the possibility of parallel integration of various chambers sharing many of the features of the apparatus. The linear actuator could be potentially shared by various chambers with minimal redesign, and the belt used in the contact shear mechanism could easily be associated with various culture chambers.

Regardless of the advantages identified for this design, the difficulties for its practical implementation are several. The first difficulty is the design of the means to fix or clamp the constructs in the holders, this is a complex problem because of the varied array of forces acting on it, having the perfusion media pushing the scaffold in one direction and the compression pushing it in the opposite direction while the contact shear pushes the scaffold in the orthogonal orientation. The second difficult problem to address is sealing the gap between the scaffold holders/ actuators and the culture chamber. Note that sealing for the case of the uniaxial compression side actuator would be a relatively simple issue to address, as this type of seal using O-rings is relatively common and allows movement. Possibly, a double seal would be more effective at preventing leaks and contamination, but the “shear side” actuator has a more complex dual axis movement that cannot be sealed with some sort of O-ring sealing solution and a more complex solution would be necessary. These difficulties are too important and are considered to outweigh the benefits of the design.

The designs using two scaffolds add a new possibility of contact between two different AC constructs, possibly better mimicking the natural environment, but the question of the feasibility of the flexible culture chamber is still dubious. While the second design iteration overcomes the problem of the flexibility or durability of the flexible material to be used on actuator, it increases the complexity of the sealing solutions, needed to avoid leaks of media in part joints during the parts movement, over different wide freedom ranges, required to provide adequate mechanic stimuli. The capability to simultaneous culture of two constructs also loses some of its appeal for autologous applications, as GMP will not allow the culture of two different patient’s constructs in the same chamber. Still culturing two different constructs may be clinically useful as it allows the choice of the one with better characteristics but, may also just be an unnecessary expense and effort as one of the tissue engineered constructs would be always wasted. The cost benefit would need to be studied in more depth, but it is mostly a clinical question so outside of the scope of this work.

These considerations, together with the difficulties of practical implementation, led to further investigations of this bioreactor configuration being forfeited in favor of other developments.

4.3.2. Rotor Bioreactor design

The shortcomings of the previous design could not be easily solved, at least in keeping the design philosophy as is, for this reason the designs considered on this and on the next section evolved to explore different geometries in the bioreactor design.

In the bioreactor design explored on this section, the strategy to promote perfusion is revisited. In other words, it addresses the following question:

-Can other geometries or forms of perfusion be useful in the design of a bioreactor for AC tissue engineering?

This in practice means a step back to a strictly perfusion bioreactor design that had been previously described in section 4.2. The mechanisms to promote perfusion presented in the 4.2.1 section were not yet questioned to this point of the current document, as all the already presented bioreactor concepts share the same basic concept of perfusion, with a static construct submerged in flowing media. Another possible form to promote perfusion is to maintain a static culture media and a construct that moves through it. This could be done in a linear fashion with a go and return pattern, with cell-scaffold construct moving forwards and backwards in a linear motion. Still, as previously discussed, a mechanical system for rotation is generally simpler than a linear motion system, for this reason this type of geometry is preferred.

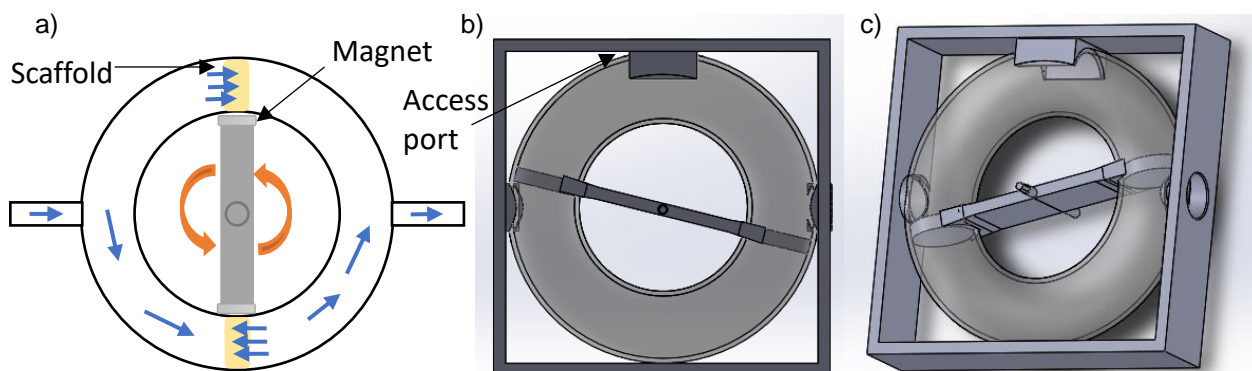


Figure 28 – The rotor bioreactor concept, a perfusion system, a) schematic cut representation of the rotor bioreactor concept, it is composed of a donut shaped culture chamber, a rotor with two “arms” in the centre of the donut, this arms are magnetically clamped to magnetic scaffold holder, this rotor rotating makes the scaffold travel in the culture chamber in a circular pattern; b) top-down vision of the 3D model of the bioreactor; c) profile of the bioreactor. → (blue arrow) represents the direction of flux, the yellow box represents the scaffold, grey represents the mechanically actuating parts, ; the → (orange arrow) represents the direction of movement of a component

The current design concept only provides perfusion induced shear stress as a relevant mechanical stimulus for the cell constructs. Therefore, it does not fulfill the aim to promote a combination of several types of mechanical stimuli. Despite this design concept having such lower capabilities, it has other advantages that support some discussion and can promote approaches to be integrated on further designs. Namely, this design is capable to self-pumping by the movement of the scaffold within the media on the chamber, this allows the system to be completely closed and for that reason it has the best characteristics for avoiding microbiological contamination. Another advantage, that this system has

in relation to the previously presented concepts, is the possibility of easy parallel integration of multiple chambers. The modelled design has the feature of allowing chambers to fit together at the same rotation shaft, allowing integration of as many chambers as the electric motor in use is able to withstand, or changing the motor a virtually unlimited number of chambers is possible.

Despite of these advantages, this bioreactor design is limited by not being able to provide other mechanical stimulus, and also the feasibility of a magnetic latching system, for holding the scaffolds. For this reason it was considered an insufficiently capable design to reach the project objectives. Still, some of the ideas on the parallel integration and the general rotating design explored for this design will be employed in the final design presented in this work.

4.4. The Cam design: ideation and modelling

The origin of his design is the design discussed at the end of section 4.3.1, the concept of the pendulum as the motion inspiring the mechanical stimulation device was not fully explored by that design but it gave rise to the inspiration of this design.

The pendulum's motion profile forms a circle so in a mechanical stimulation of a construct this type of movement will have a combination of contact shear with compression, the same combination

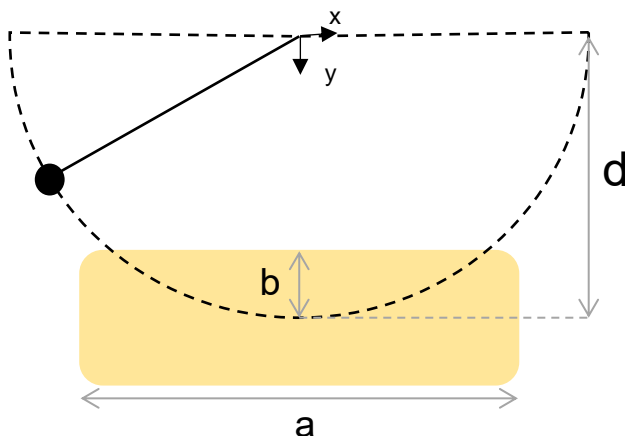


Figure 29 – Representation of the motion profile of a mechanical stimulation device with the pendulum type motion profile; a – scaffold face length; b – maximum deformation of the construct; d – diameter of the motion profile.

obtained in various previous design concept with more complex mechanical components.

This type of mechanical stimulation has the two mechanical stimulus, contact shear and direct compression, these are delivered by the same movement, being impossible to separate and use separately each of this stimulus, which is a disadvantage in a research setting where it will be important to study each stimulus independently or in combination with varying force intensities for each of the stimulus type.

To produce this type of mechanical stimulation only one motor is necessary and

is a purely rotational motion. This approach simplifies the design of the mechanical stimulation apparatus. In a similar way to the rotor design concept presented in the previous section this concept allows for relatively simple integration of various culture chambers with the same mechanical stimulation, provided a sufficiently powerful electric step motor is used.

An interesting point in this type of motion is that with this style of mechanical stimulation the cross-section of the cell-scaffold construct does not feel an homogenous strain, with the strain being a maximum in the center of the scaffold and symmetrically from there diminishes until reaching an equal minimum value at both side edges. An infinitely large diameter of the motion profile (d) would mean a completely homogeneous stimulation profile with strain being equal along the profile of the scaffold.

However an infinitely large motion profile would imply an infinitely large equipment, and as previously stated there are size limitations that are due to the need to fit in an incubator for culture.

The design of the cam action is dependent in a great degree to the choice of the motion profile diameter (d) and this choice depends on the choice of variation of strain along the profile of the scaffold that is considered adequate. For this design choice a mathematical approach of the problem was developed.

Considering the referential represented in figure 29 was the basis of the calculations, with (0,0) coordinates being placed in the center of the motion profile. The profile of the pendulum motion was described as a semi-circumference by equation 1.

The deformation at any point is defined by the position of the surface minus the deformation at a given x coordinate value, the symmetric of local deformation to a given x value was called ΔX and is described in equation 2.

$$y = \sqrt{d^2 - x^2} \quad (1)$$

$$\Delta X_x = - \left((d - b) - \sqrt{d^2 - x^2} \right) \quad (2)$$

The average deformation along the x axis is the average of the values for each x value, in the dominion if $-a/2$ to $a/2$ and was designated $\Delta \bar{x}$.

$$\Delta \bar{x} = \frac{1}{a} \int_{-\frac{a}{2}}^{\frac{a}{2}} \sqrt{d^2 - x^2} - (d - b) dx \quad (3)$$

This integral was solved using integration by parts and the result is shown in equation 4.

$$\Delta \bar{x} = -d + b + \frac{1}{a} \left(\frac{a}{2} \sqrt{d^2 - \left(\frac{a}{2}\right)^2} + \frac{d^2}{2} \left(\arcsen \frac{a}{2d} - \arcsen -\frac{a}{2d} \right) \right) \quad (4)$$

Numerical solving the equation for calculation of d given a certain $\Delta \bar{x}$, a and b, was performed in excel with the results being synthetized in figure 30.

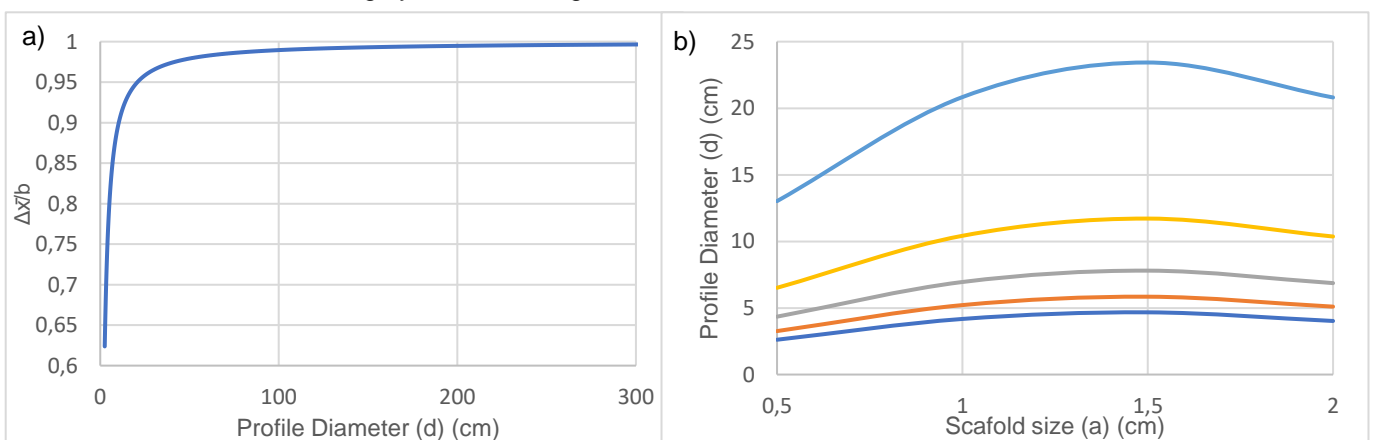


Figure 30 – Charts for the dimensioning of the pendulum style actuating system; a) chart of $\Delta \bar{x}/b$ with dependence on the profile diameter in cm, with $b=0.04$ cm and $a=2$ cm it is valuable at indicating the trend in increasing the size of the apparatus versus the benefit of increasing the homogeneity of the stimulus; b) chart of Profile diameter (d) in cm needed to achieve a certain ratio $\Delta \bar{x}/b$ depending on scaffold size (a) also in cm, the ratios studied were $\Delta \bar{x}/b$ - 0.75, - 0.80, - 0.85, - 0.90, - 0.95.

As can be understood from the tendencies of the previous charts the uniformity of the $\Delta\bar{x}/b$ compressive stimulus depends on the profile diameter in a logarithm like fashion, so as the profile increases the benefit in uniformity of stimulus also increases but with a diminishing return. A similar conclusion can be taken from the chart in figure 30 b), the higher the $\Delta\bar{x}/b$ demanded the higher the profile diameter needed, a curious tendency is that a maximum diameter needed occurs for scaffold size with a values between 1 cm and 1.5 cm.

For simplicity the choice was made to dimension the pendulum arm for a fixed a and $\Delta\bar{x}/b$, and this requires that an adjustable positioning system for the scaffold be created to adjust the position, adjusting in the process the deformation (b), with the side effect of a changed $\Delta\bar{x}/b$.

The development of the cam design as previously referred is started from the design of the joint mimicking design. This represents an evolution of previous designs discussed. Namely uses direct perfusion and rotation as a strategy to apply mechanical forces on the scaffold and considers the soft surface to interact with the scaffold, but the use of a second scaffold is not considered. The details of the cam design as well as intermediate versions made to reach a final design are presented in this section.

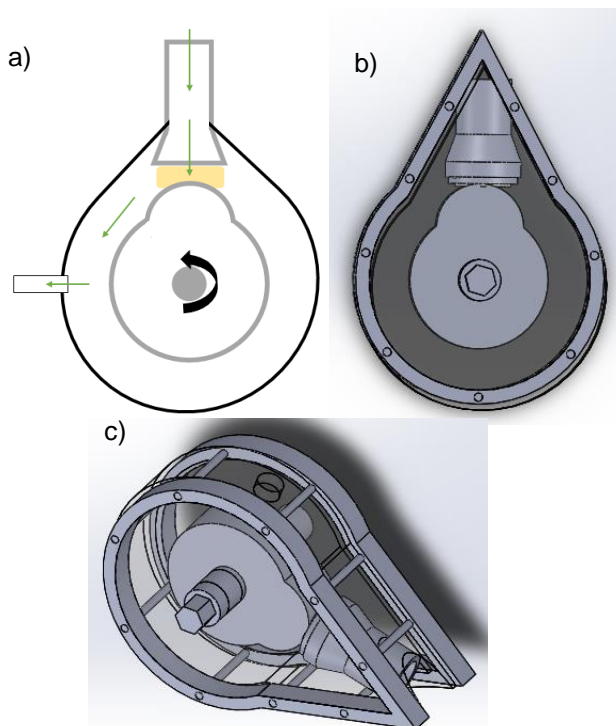


Figure 31- First iteration of design of the Cam Bioreactor; a) schematic top-down view of the bioreactor design with the cam in the middle of the culture chamber, the rotation of the cam produces a combination of contact shear and direct compression, perfusion is still designed to be direct; b) top-down view of the model for the design; c) profile view of the model.

The pendulum was reinterpreted as a cam, a common mechanical component in various types of machinery, like the internal combustion engine. The cam while not in operation is rotated away from the scaffold, and direct perfusion is done, when the stimulation apparatus is in operation the cam rotates over the construct doing a motion profile like that described for the generic pendulum.

The limitation of fixating and of sealing the scaffold given such a complex combination of forces remains and associated with limited need for direct perfusion this feature was left, but the two chambers with media present in this design will remain until the final design.

The two separate chambers system is interesting in the tissue engineering of articular cartilage because cartilage is a tissue greatly linked to the underlying bone,

as discussed before some therapeutic techniques require not only a chondral but an osteochondral graft. The engineering of osteochondral constructs as opposed to solely chondral constructs benefits on the

use of two separate media system. These two separate media systems can contain in the bigger chamber chondrogenic media while the smaller chamber contains osteogenic media, developing a stratified construct with bone characteristics in one side and chondral characteristic in the other. This architecture has a great value of novelty as this is a very uncommon architecture for cartilage tissue engineering bioreactors. The only work in articular cartilage tissue engineering found that uses this dual perfusion independent in the two faces of the construct is the work of Spitters²⁵⁴, but in this work only perfusion was applied and the overall objective was to study oxygen diffusion in the native tissue.

The cam design concept was developed interactively:

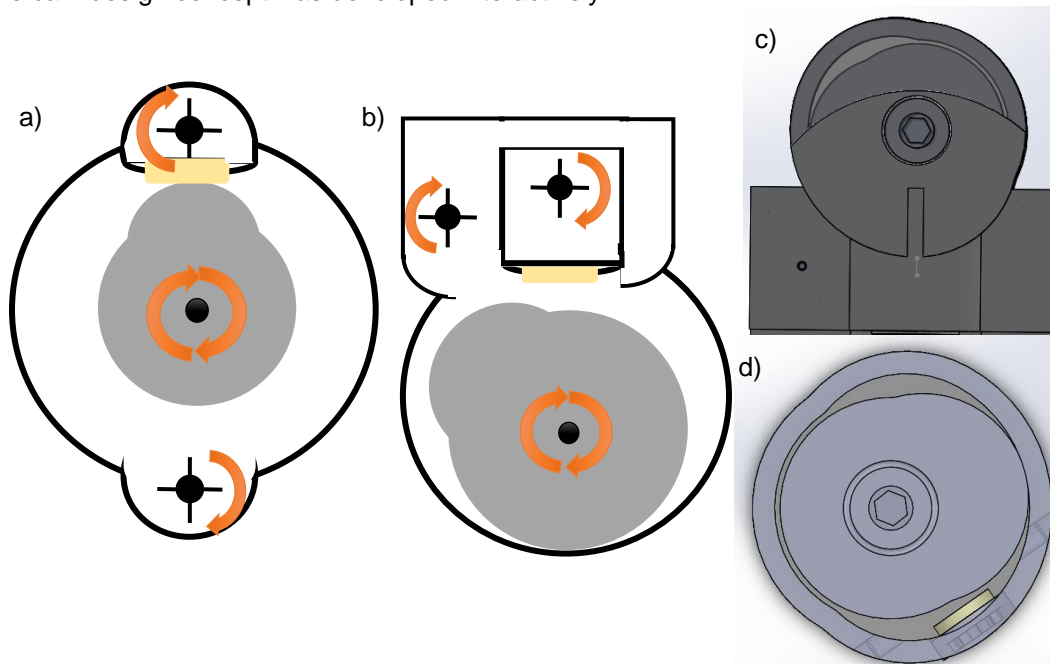


Figure 32 – Early designs for the Cam Bioreactor; a) Early design that proposed the use of two separate agitated chambers, the two agitators are represented in both the upper and lower end of the bioreactor, the cam remains in the centre of the bigger chamber; b) Second design in which the chambers are moved to one end, the bigger chamber contains a smaller media volume and the bigger agitated chamber should act as a pump producing perfusion in the bigger chamber; c) top-down view of the bioreactor model for the two mixing chambers initial design; d) detail of the bigger culture chamber containing the cam actuator; the → (orange arrow) represents the direction of movement of a component.

1) First Iteration:

The first iteration of the two chambers design was the one represented in the figure 32a), it consisted of two agitated chambers one connected to each side of the construct, one of the two chambers included the cam actuator. This design evolution made evident that due to the required size of the stimulation apparatus, previously described the cam needs to be in the 5 cm to 10 cm scale. These dimensions turns the main chamber too large, up 100 mL which makes it impracticable considering the required volume needed in expensive chondrogenic media, moreover this design does not provide necessarily good mixing properties. The next design schematically represented in Figure 32b) is a first attempt to limit the need of media to fill the bioreactor, improve the mixing and improve the control of the flow in the bigger chamber. The main chamber pictured in the 3D model in figure 32d) is dimensioned as small as possible. Those changes allow the cam to move over the scaffold providing direct compression to the mechanical stimulation phase, while in a solely perfused culture phase can be placed away from the

construct, allowing media flow to be minimally disturbed. The side opposite of the scaffold is as close to the cam actuator as possible without the creation of surface drag.

Both these designs have the lack of a mechanism for adjusting the position of the scaffold in relation to the actuator. The lack of such a system takes away much of the flexibility of the bioreactor, without adjusting the position only scaffolds with the size and depth as designed could be correctly mechanically stimulated, or alternatively the cam would need to be substituted depending on the scaffold, but this still could not correct tolerances, errors in the construction of the actuator and variations on the scaffold dimensions.

2) Second Iteration

The second iteration addresses the next design problem which is precisely the design of a mechanism for accurately positioning the tissue engineering construct.

The mechanism that inspired the design of the positioning and adjustment system for the AC construct was the micrometric screw. The micrometric screw uses the translation of rotational movement into linear movement, to measure distances by measuring the rotation of a well calibrated screw.

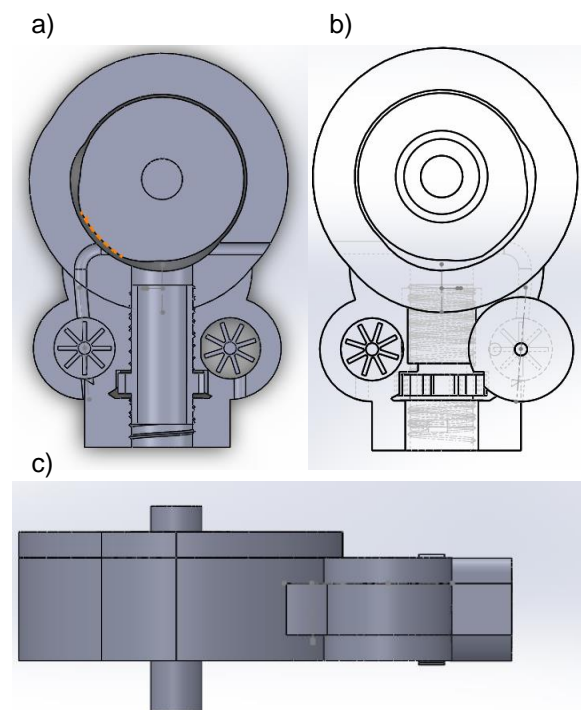


Figure 33 – Second evolution of the design of the cam bioreactor, including the screw design position adjustment system and revised perfusion/ agitation system. a) cut view of the model showing the internal channels that provide fluid flow into the main chamber, and the internal part of the two pumping chambers on the lower part, on each side of the secondary chamber; b) wire frame view of the bioreactor showing the agitators/ turbines in the pumping chambers as well as the channels to move the culture media within the bioreactor and the thread in the secondary chambers that would allow precise positioning of the scaffold; c) profile view of the design.

The bioreactor design presented in figure 32 is the first attempt at integrating a scaffold positioning system with use of a screw and thread system.

The basic idea of this bioreactor concept is that there are two culture chambers, the main chamber is the one that contains the actuator cam, the secondary chamber pictured in the lower part of the bioreactor is cylindrical shaped, this chamber would be capable to move closer or further away by adjustment depending on the scaffold and stimulation characteristics intended. This movement is done by the screw that is designed into the outside of the cylindrical chamber and the thread that exists in the outer cylinder, so rotating the whole chamber would adjust the linear position of the cell-scaffold construct attached to the secondary chamber.

This design evolution also has a major change to the way the mixing/ pumping chambers are designed, the two similar pumping chambers can be seen in each side of the secondary culture chamber.

Preliminary CFD done using the Solidworks CFD plugin showed that the previous chamber

design was ineffective at translating the mixing into pumping of the media to perfuse the main chamber, for this reason the pumping / mixing chambers were modified to be more constricted and have a functioning more similar to a centrifugal pump, the pumps would be connected to the culture chambers by means of purpose designed channels in the bioreactor and external tubing.

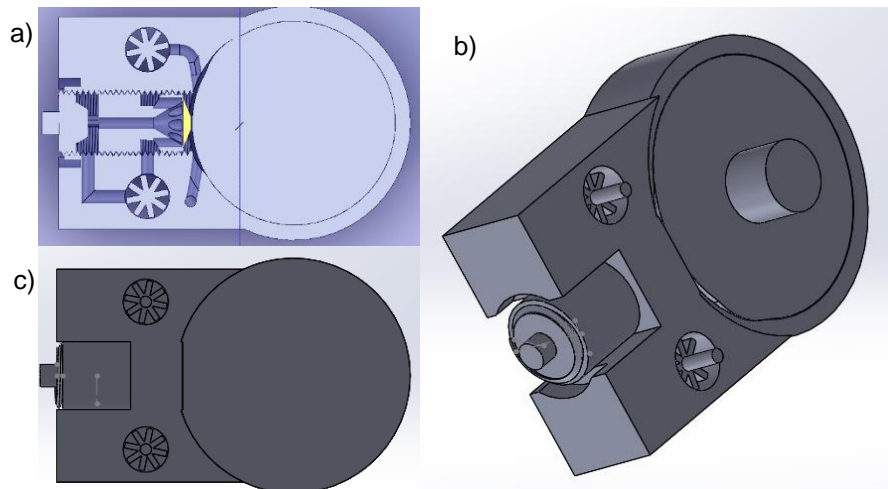


Figure 34 – Third evolution of the cam bioreactor design; a) top-down cut view of the bioreactor, the internal fluid flow chambers are visible as well as the complexity of the redesigned secondary chamber separated in two sub-chambers one for incoming and another for outgoing media; b) profile view of the modified bioreactor body design and where the modified main chamber is visible with further reduced space for fluid volume; c) top down view of the bioreactor with the exposed pumping chambers.

3) Third Iteration:

In the third iteration, the next evolution of the bioreactor design is concerned with introducing a fluid system that needs no external tubing and has all the fluid flow within it. The main chamber perfusion channels are partially visible in figure 34a) and are connected to the pumping chamber in the upper part of the image, this channels are contained within the bioreactor body and one of the channels is direct to the main chamber while the other needs to wrap around the secondary chamber and is only partially visible (on the lower part of the image). The secondary chamber has suffered a major redesign, one of the greatest motivations for this design is the economy of culture media needed to fill the bioreactor. The cut image shows very clearly the how small are the chambers compared with the previous design. The volume of the main chamber being greatly reduced to include only the space around the tissue construct with most space occupied by the actuator, but still with enough space for the actuator to be in a position of not in contact with the scaffold-cells construct. The secondary chamber was redesigned also with the aim of reducing the media volume, (in comparison the previous design), but also to allow a way of conducting fluid flow exclusively in internal channels.

The use of internal channels is motivated by the reduction of entrance ways to the bioreactor, with reduced gaps the probability of a microbiological contamination is reduced despite the increased complexity demanded by this design specially given that the secondary chamber is supposed to rotate in relation to the pumping chamber to adjust the position of the scaffold.

The secondary chamber design opposite to the design used in the previous iteration of the bioreactor uses both the rotating component and the stationary component as part of the walls of the

chambers, the scaffold is fixed to the rotating component and a truncated conical shaped chamber is located in this component where the construct is placed, this culture chamber has entering diffuser type channels on the lateral surface of the cone and the exiting is done through the truncated vertex of the cone. Both the entrance and exit of media are associated to donut like chambers that allow connection to the pumping chamber independently to the rotation of the component with a tolerance to allow forward and backward linear motion.

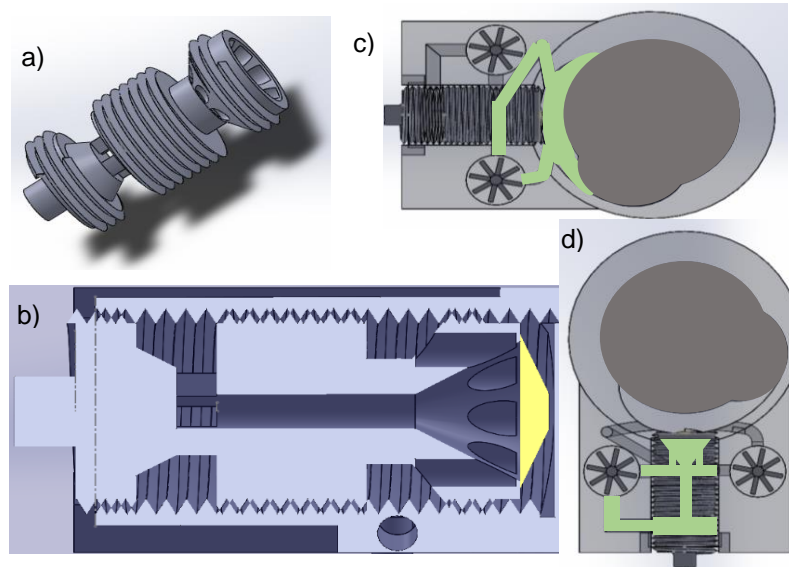


Figure 35 – Illustrative images of the fluid containing areas of the third evolution bioreactor design; a) 3D model of the rotating component of the secondary chamber, on the top right the conical culture chamber is visible with the diffuser like entrances, the entrance chamber is visible just below that as a donut like shaped cut of the component and lower is the exit chamber; b) cut of the 3D model of the secondary chamber including the rotating component in the middle with the represented scaffold in the top of the conical culture chamber, the static component of the secondary chamber that is fixed to the bioreactor body is represented in the outside, and the two smaller entrance and exit chambers that are limited by the conjunction of the rotating and stationary component, the sealing designs are not present since the design evolved before this were designed; c) channels of flow of media to the perfusion of the main chamber; d) channels of perfusion of media for the secondary chamber. The green painted areas represent the fluid filled areas.

This design is the last main design before the final state in the ideation/ design process of the bioreactor. In general it is a very complex design with many moving parts and difficult sealing solutions, that may be excessive for the actual needs.

Designing an O-ring sealing solution for a rotating + linearly moving chamber is not only complicated but also generally uncommon. In the design of the secondary chamber presented in figure 35 these seals would be needed not once but five times, one for the separation of the two culture chambers and two for each of the entrance/ exit chambers, this could be possibly reduced to 3 seals if it was considered fine to have media leaking in the central thread screw area. The question if this leak would not be problematic is important to the design, the question being if having possible regions of stagnated media would be acceptable.

In general the main chamber in all the previous designs has a small amount of media invading the small space between the actuator sides and the wall of the chamber, this media would be mostly stagnant and also under near contact between two surfaces in relative motion, this could possibly cause

localized heating possibly denaturing proteins (relatively unlikely due to the low velocities of operation) and in general damaging biomolecules in the media, with possible formation of unwanted sub-products. The possible heating would not be a problem in the case of the secondary chamber but the stagnant media would still be present.

These interconnected problems will have two separate solutions: in one hand there is no practical need for the cam actuator to be completely submerged in culture media, secondly the internal screw/thread system is not the only solution to the position adjustment system.

The main chamber was designed to be completely full with media since the inception of this general cam bioreactor stimulation concept. This design choice was a feature inherited from the previous designs and was thought to be useful for potential application of hydrostatic pressure. The idea that hydrostatic pressure would be needed or practical to use in this design had not been discussed to this point, but it warrants discussion.

The need for separate hydrostatic pressure and direct compression in tissue engineering of articular cartilage has been discussed in various sections of this work and seems to be a relatively uncontested fact, what can be discussed and has also been previously discussed is the need to combine both in the same stimulation protocol. Literature of both being applied in simultaneous is not available and this combination is not even discussed in the literature as a possibility. One possible explanation for this apparent lack of discussion is the already proposed redundancy of both stimuli. By the biphasic theory of articular cartilage biomechanics⁷¹ the fluid and within solid phase of the tissue is essential for its mechanical characteristics, one of the most important parts of this is the pressurization of the fluid within the porous tissue, or (in tissue engineering) a microporous scaffold, which is preferred for AC tissue engineering, direct compression should likewise produce pressurization of the interstitial fluid. So, in conclusion hydrostatic pressure is in this work treated as redundant with direct compression.

The reason for filling the bigger culture chamber with media being void and no new reasons arising this design feature was abandoned. The next option which is used in the final design proposed for the bioreactor is to keep the chamber in a upright position as pictured in figure 35 and design a small chamber in the bottom of the main body of the stimulation apparatus capable of holding only enough media to completely cover the construct, and the media is kept at atmospheric pressure.

The internal thread and screw for the scaffold holder and secondary chamber position correction system that was present in the last two evolutions of the design is interesting in the sense that it is completely self-contained, space efficient and requires few moving pieces. The problems with the design nevertheless turn it very difficult to implement for two main reasons, one that is inherent to the design and as been already discussed is the complexity of the sealing solution required to avoid media leaking and diminish the likelihood of contamination. The other reason is due to the means available to construct the bioreactor prototype, since most pieces of the bioreactor are to be 3D printed. The limitation of resolution of the 3D printer make the thread and screw impossible to print, as these are very fine structures. For other construction methods this problem would persist because the only other practical way to produce such a shape would be machining, and machining a piece this size so finely would be difficult and expensive turning this design feature more impractical than useful.

4) Forth Iteration:

To solve the design problem of the construct position adjustment system a new solution needed to be developed. The use of the screw/ thread type system is still considered a good general idea as it allows to precisely convert rotational movement into linear movement. This general strategy can be implemented in various ways, the final and best solution was a push/ pull system.

The push/ pull construct positioning system consists of a screw based adjustment of position of a platform that is itself connected to the secondary chamber and adjusts its position and associated to it the position of the scaffold.

The position adjustment system consists of two of the shelf screws and two also commercially available nuts. These nuts are fixed with a gear that is fixed to a platform, this gear is itself connected to a gear system that allows for multiplication of the rotation of the knob gear with which the operator interacts. This multiplication of the rotation allows for a greater precision in the final rotation of the nut and the associated linear movement, allowing a finer control of the position of the tissue engineering construct, and that implies a greater control of the strain inflicted on the scaffold. This system is detailed in figure 36.

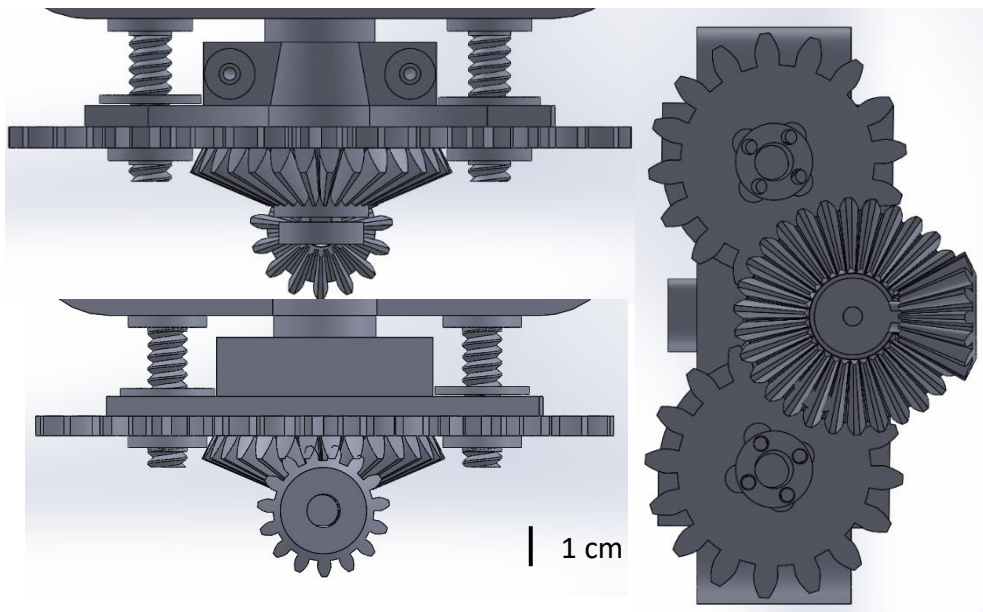


Figure 36 – Detail of the final model for positioning system of the tissue engineering construct, to adjust the strain produced by the action of the mechanical stimulation apparatus. (screw is only a illustrative model)

To determine the precision of this system it is important to take into account the effect of the thread and the effect of the the multiplication by the gears.

The screw available in the laboratory and wich was used for the constuction is of standard M8, this standard has a thread pitch of 1 mm, by definition of pitch this means that every complete revolution means a linear movement of 1 mm. So a 1° rotation is equivalent to a linear motion of 0.033 mm.

The two bevel gears have a 15 and 30 teeth respectively so have a gear ratio of two, the smaller gear fixed under the bigger bevel gear is fixed to it so the ratio is 1 as they rotate dependently of one another. The small gear has 8 teeth while the bigger gear has 16 so the gear ratio is again 2. In conclusion in total the gear ratio is the multiplication product of the individual gear ratios wich is 4. This means that 4° of rotation of the knob or smaller bevel gear produce a movement of 0.033 mm, or a more practical 10°

produce a movement of 0.083 mm. this result means that the scaffold position using this system is accurately adjusted.

The next design feature to be addressed was the pumping system to produce perfusion. It was discussed previously in the last design evolution the interest of having a closed system with as few external features as possible. This was applied to the design of the pumping system in the last design evolutions, and the pumping system was integrated in the body of the bioreactor. This solution was not fully advantageous because it lowered the flexibility of the design, so in this final design it was preferred to use a different design philosophy. The culture chambers were designed to have internal channels to direct the media flow to the culture chambers, but a design provision was made to allow the use of an external pump by creating locations where a tubing fitting can be placed and connected to an external pump. This system also allows the connection of a purpose built pump.

The type of pump to be used and designed was also a focus of this final design evolution. The type of design used in the previous bioreactor concepts were an evolution of a mixing and not necessarily pumping option, this design was to have an agitator type of propeller with multiple baffles. Preliminary CFD using the Solidworks internal plugin showed that this architecture was very ineffective in pumping and generally generated very vigorous mixing inside the pumping chamber. This very vigorous mixing is not only a loss of power to an ineffective result but a possible problem as it can create an increase in the temperature of such a small liquid volume (scale of 0.5 to 2 mL), that can possibly have consequences for the biomolecules present in the media, or change the temperature of the cell construct to a value that can compromise the viability of the cells.

The next possibility of design was to design a proper centrifugal pump with a turbine type design. This design solved the problem of the efficiency of the pump but kept another problem that was present in previous design evolutions and that was the design of a functioning sealing that prevented leaking in a high velocity rotating shaft of the pump. This type of design was investigated and in general the use of an O-ring based sealing was discarded because of the small size of the components and the complexity

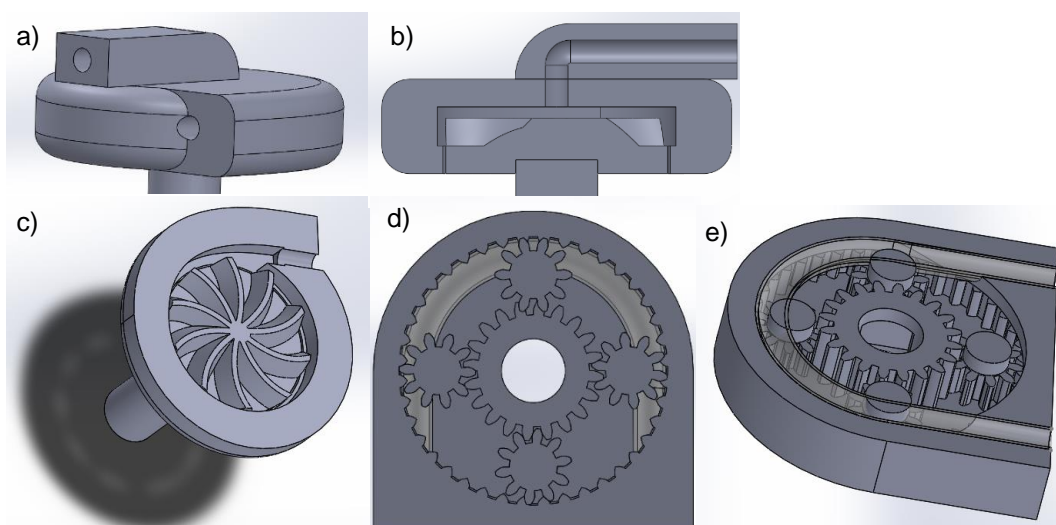


Figure 37 – a) centrifugal pump design; b) centrifugal pump vertical axis cut; c) centrifugal pump horizontal axis with the detail of the turbine cut; d) peristaltic pump with the tubing in yellow translucent; e) cut of the centrifugal pump with the detail of the pumps actuating gears.

of such designs, a magnetic option was also investigated but was considered also to complex given the available time and in general the scope of this work.

The last investigated option is the design of a peristaltic pump specific for the bioreactor, which could also be connected to an external pump. The peristaltic pump design is a bearingless option that uses gears as bearings. These gears contain a cylindrical section that deforms the tubing producing the pumping effect.

The design of the pumping solution for the bioreactor is not pictured in the final model of the bioreactor because it was not possible to further refine the design of the perfusion pump and for that reason it was decided that an external pump would be the provisory solution for the perfusion of the bioreactor.

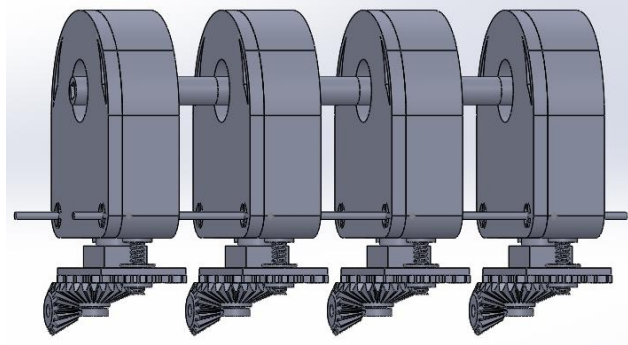


Figure 38 – Model of a potential form of parallel integration of the bioreactor.

5) Final Design:

In the final model of the bioreactor presented below the features that have been discussed are incorporated, namely the culture chamber in the bottom of the bioreactor, the modified positioning system and the locations to attach tubing fittings connecting to a purpose built or other pump. Other smaller modifications like simplification of the chamber design with unnecessary shapes removed addition of an adaptor in the bottom of the body of the bioreactor to fix various bioreactors by means of a small metal rod, as depicted in Figure 38.

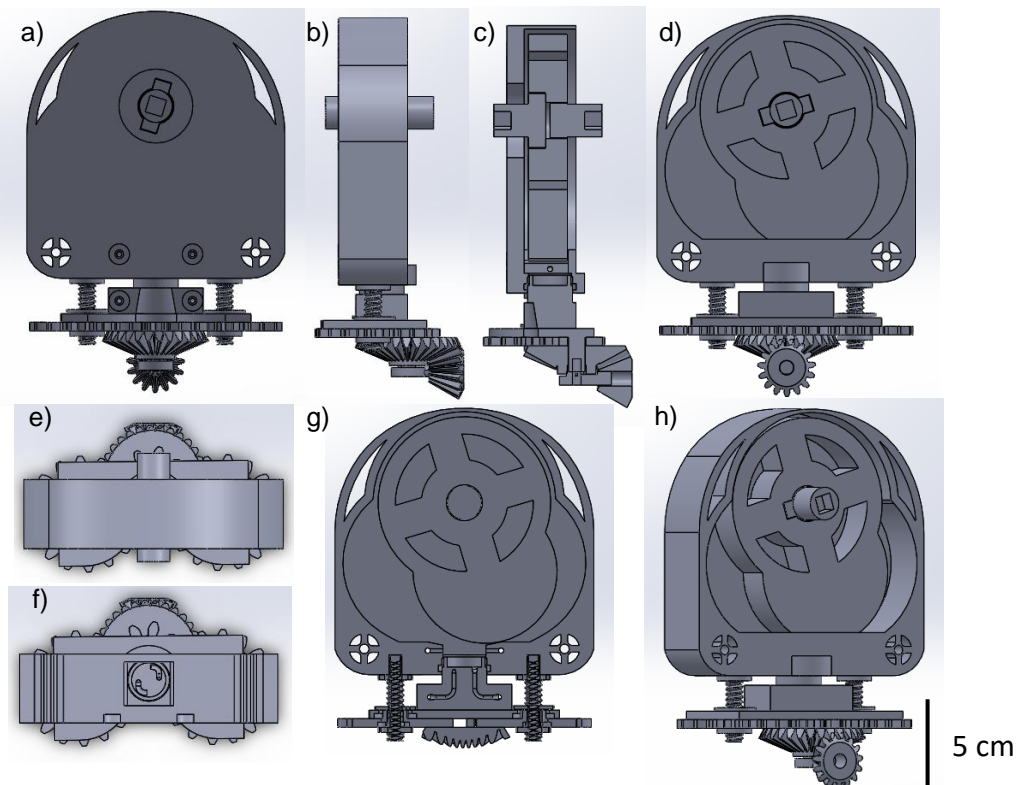


Figure 39- 3D models of the final bioreactor design; a) back view of the bioreactor showing the spot for entrance and exit tube fitting fixing on each of the chambers; b) lateral view of the bioreactor; c) cut of the lateral view of the bioreactor, on the top it shows the detail on the fixing of the actuator to the axel, lower the cut of the culture chambers is visible; d) front view of the bioreactor; e) top view of the bioreactor; f) top view cut of the bioreactor exposing the view of the culture chamber; g) frontal view cut of the bioreactor showing the internal channels for fluid flow into and out of the two chambers; h) profile view of the bioreactor.

4.5. Computer fluid dynamics modeling

The effect of the various forms of mechanical stimulation has already been discussed in detail, in particular the effect of fluid induced shear by perfusion is dependent on the velocity of the fluid interacting with the tissue engineering constructs.

To obtain a preview of the effects of various volumetric flows of perfusion in the bioreactor CFD modelling was done. This allows to, in some degree, have a beforehand idea of the effects of the fluid perfusion on the cell fate.

CFD is a branch of the fluid dynamics subject of the physics of continuous bodies, the objective of CFD is to use numerical analysis to solve problems of flowing fluids, this technique is associated frequently with mechanical engineering but is becoming more commonly applied to biotechnology and bioengineering. In particular on the subject of AC tissue engineering various works have been done using CFD, the work of Gharravi et al²²⁴ already referred used CFD as an aid in the design of the bioreactor, Mahmut et al did CFD simulation in rotating-wall perfused-vessel for articular cartilage tissue engineering²⁵⁵, another example is the work of Silva et al that applied CFD to a perfused bioreactor²⁵¹.

The basis of CFD are the Navier-Stokes equations, these equations are a formulation of mass, momentum and energy conservation laws and are discretized to be applied to computational fluid dynamics.

As already discussed in the materials and methods section for the present work the internal plugin for Solidworks was used for CFD, this was chosen because of its simple interface without losing to much of the accuracy of the results, and with the integration of the CAD modeling greatly simplified by both parts of the process being done in one self-contained software.

The first assay of CFD was done using as frontier conditions a volumetric flow rate of 2 mL/s entering and leaving the culture chamber and atmospheric pressure at the surface of the media. The fluid mesh included 30799 cells and 274 iterations were needed before convergence of the solution was obtained.

The stated goals for the calculation were dynamic pressure in the fluid, average velocity, force, shear stress and localized in the scaffold surface the velocity, force and shear stress. The results are graphically presented in figures 40 and 41.

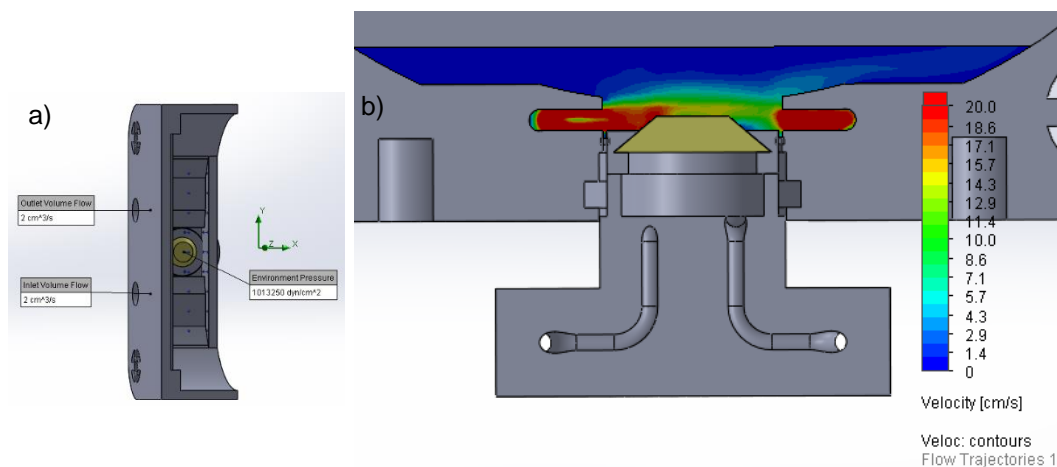


Figure 40 – Graphical representation of the results of CFD for 2mL/s; a) Boundary conditions graphical synthesis; b) central cut of the chamber fluid velocity contours.

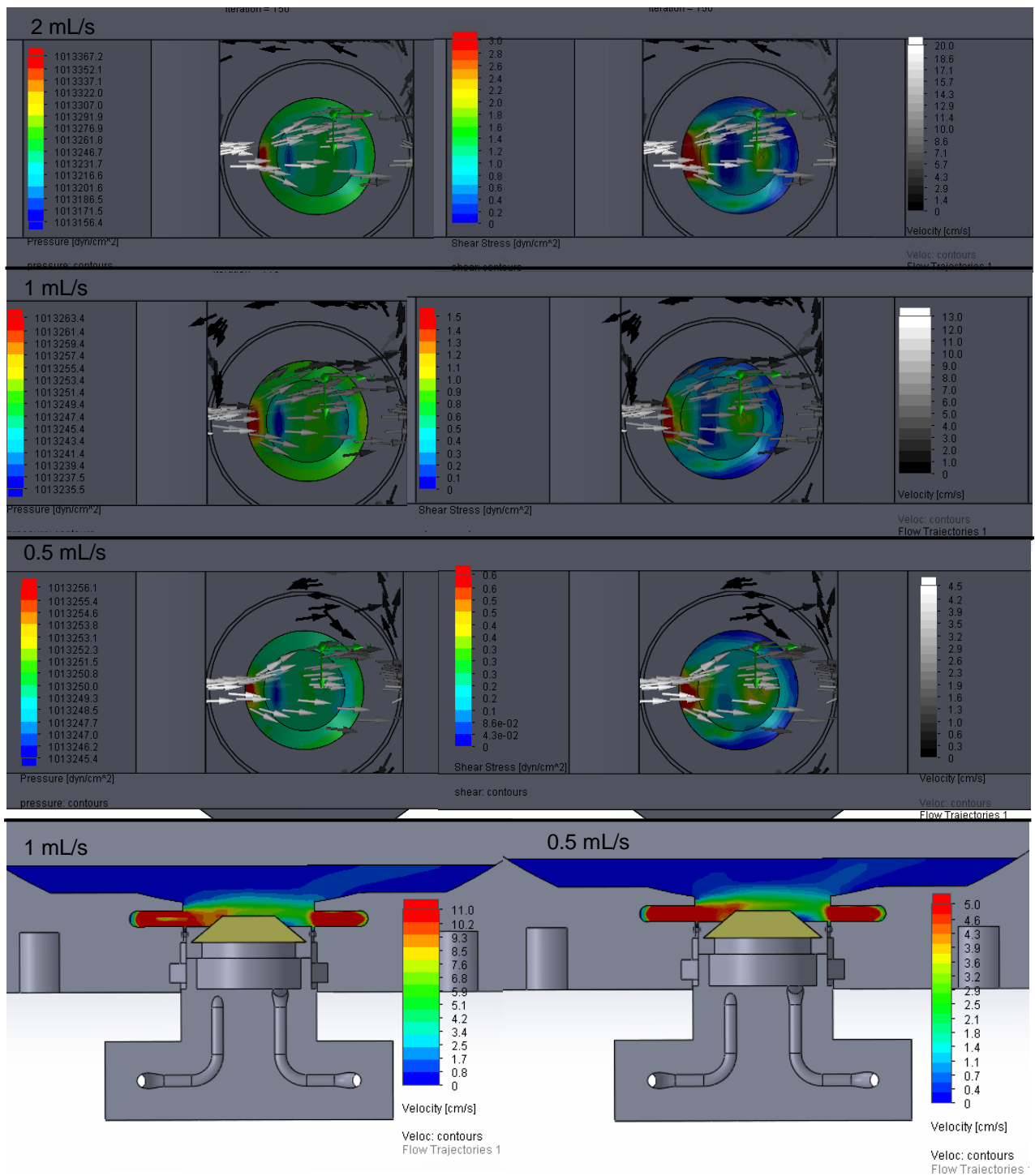


Figure 41 – Graphical representation of the results of CFD produced in the Solidwoks flow simulation plugin; results obtained for 0.5 mL, 1 mL and 2 mL as signalled, on the right the results of total pressure exerted over the construct are represented on the right is the intensity of Shear stress exerted on the surface; the two contours chart bellow represent the velocity of the fluid in a cut at the middle plane of the culture chamber.

As could be expected the general distribution of both shear and pressure on the scaffold does not change visibly depending on the volumetric flux of media but the general intensity does, and exactly the same can be said from the cut charts the velocity of the fluid also respects this logic. Naturally for the highest volumetric flow of 2 mL/s the shear on the scaffold reach a peak of 3.0 dyn/cm², for 1 mL/s it lowers to 1.5 dyn/cm² and for 0.5 mL/s it peaks only at 0.6 dyn/cm². The pressure doesn't differ significantly from the atmospheric pressure meaning the dynamic pressure is insignificant in comparison to the static pressure, which is the expected result, the charts for the surface pressure are mostly interesting for the demonstration of the conservation of the flow form independent of the volumetric flow.

The data presented in figures 40 and 41 defines the flow pattern of media in the culture chamber, which is interesting by itself, but this data is not useful for determining the intensity of the fluid induced shear felt by cells within the tissue engineering construct. Cells within a porous scaffold are not directly exposed to the environment of the culture chamber but are exposed to the environment present in the interstitial spaces of the scaffold, to have some idea of the cell response data must be obtained to indicate what would be the conditions in such interstitial spaces.

The pore size is dependent of scaffold type and within specific scaffold types and materials can be changed by changing the condition of production like the conditions of polymerization of a hydrogel²⁵⁶. The optimal pore size for a Articular cartilage scaffold however as been determined to be around 200 μm ²⁵⁶. To do a simple exploration of the microenvironment with such a pore, to the scaffold used in the previous computational assays were added 3 pores of 200 μm in the center axis and the velocity within these was simulated.

The velocity calculated within this simple pore simulation was for 2 mL/s around 3×10^{-5} mm/s, for 1 mL/s was 2×10^{-5} mm/s and for 0.5 mL/s approximately 1×10^{-5} mm/s. From image 42 the range of fluid velocity in a 10% strain operating bioreactor was determined to be from 0 to 6×10^{-4} mm/s, to be in chondrogenic conditions, for this reason all the volumetric flow conditions tested should contribute fluid induced shear in the correct range for chondrogenesis of MSC.

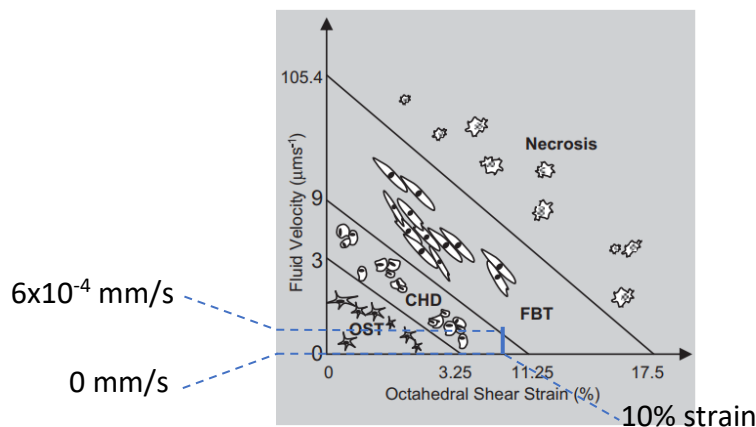


Figure 42- Mechanical regulatory model of Pendergast et al (1997)²³⁸ modified by Stops et al (2010)²³⁷ to include necrosis, the markings show the expected compression in operation conditions for the bioreactor and the associated interval of fluid velocities that are associated with chondrogenic differentiation of MSC.

It is important to note that the mesh used for these calculations was chosen automatically by the program, for that reason the results may be less accurate, to obtain better results manual refinement of the mesh should be done, this is most important for the results obtained for the simulated pores as they represent a constriction on the flow.

4.6. Prototyping

Prototyping of the bioreactor design was done by 3D printing of the parts designed in Solidworks, and according to the final design presented in the ideation and design section.

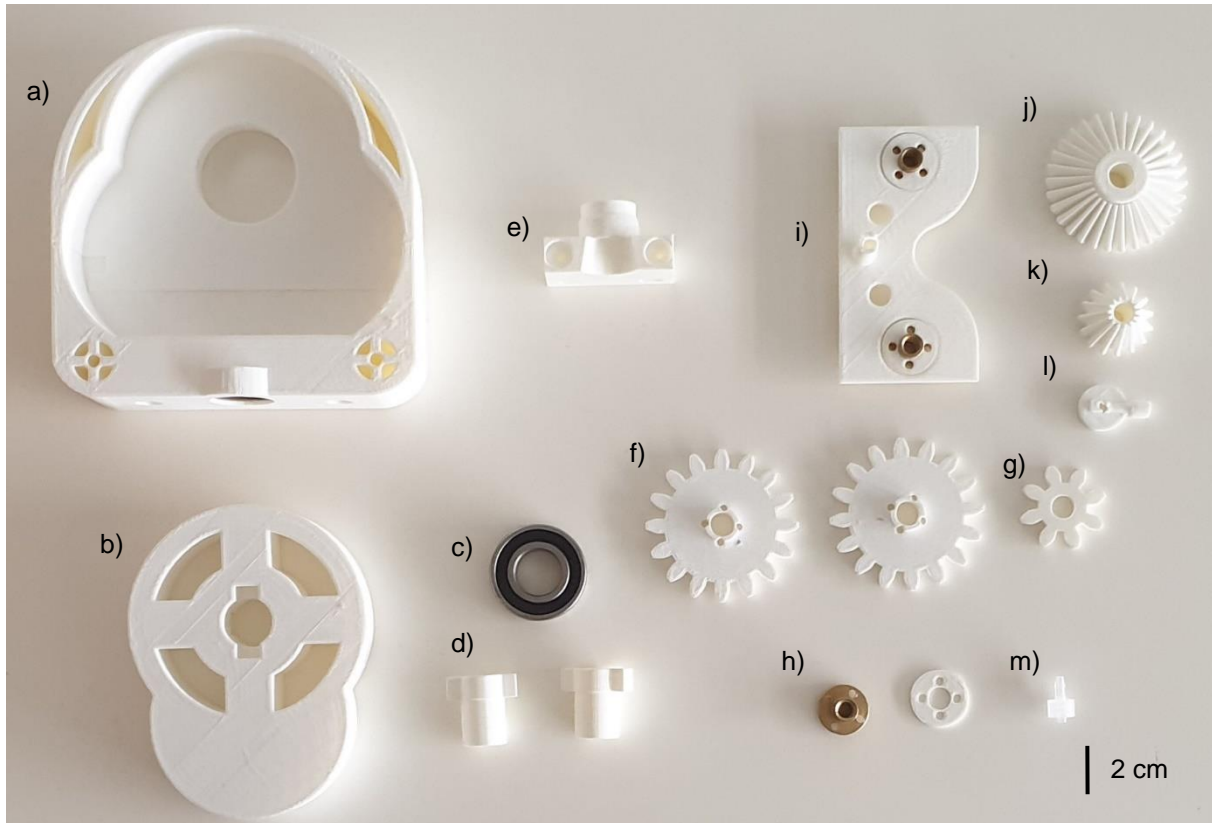


Figure 43 - 3D printed components of the bioreactor; a) main Bioreactor chamber; b) Cam actuator; c) Ball-bearing for the actuator axle; d) Actuator axle parts; e) Secondary chamber; f) bigger flat gear; g) smaller flat gear h) Nuts; i) Positioning system base; j) bigger bevel gear ; k) smaller bevel gear; l) bevel gear support; m) tubing fitting.

In figures 43 and 44 the results of 3D printed parts are presented, in general good results were obtained in the 3D printed parts. Many of them required various attempts, notably the main chamber was a multi-attempt effort due to its dimension close to the limits of the capabilities of the 3D printer in terms of part dimensions. After various attempts including one failed overnight attempt it was decided to break the part in two more sensible sized parts that could be printed more easily and faster, allowing for various attempts faster and with less expense of 3D printing filament.

The parts were tested for leaks and none were found, which was one of the most likely points of failure of 3D printing.

Another place where some errors were made was in taking into account the tolerances needed due to the inherent error associated with the printing, errors associated with this demanded repeating the printing of the axle of the actuator and demanded some parts to be grinded down to better fit in position.

The gears of the construct positioning system are sufficiently precise to be of relatively smooth action. The point of connection of the base to the two bigger gears was a point of difficulty in design and demanded experimentation and various attempts to make work.

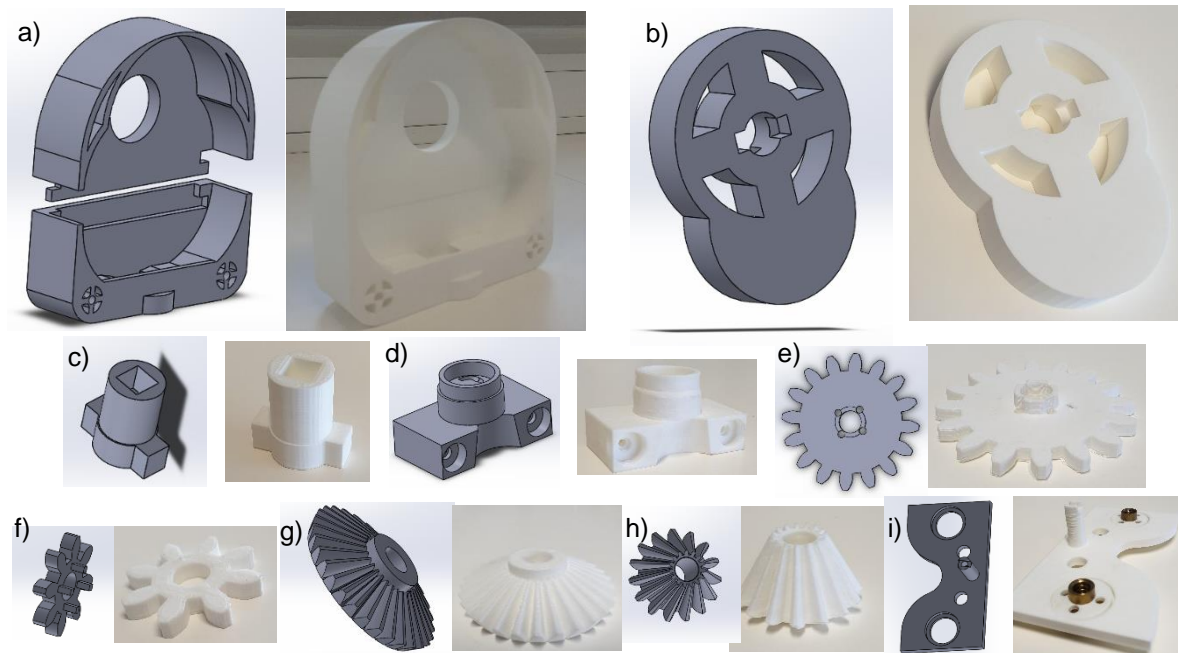


Figure 44 – Close comparison of the main components' models and 3D printed parts; a) main Bioreactor chamber; b) Cam actuator; c) Actuator axle parts; d) Secondary chamber; e) bigger flat gear; f) smaller flat gear; g) bigger bevel gear; h) smaller bevel gear; i) positioning system base.

One defect that is inherent to 3D printed parts by the fused deposition modeling type, the one used in this work, is that long (tall while printing) parts that are also relatively thin tend to warp due to the fast cooling of the polymer which introduces some defects in the parts. Another common defect occurs when the interior honeycomb structure interacts with the printing pattern introducing small dents in these tall parts with a circular section. These two referred defects happened mainly in the cam axel and to a lower extent to the secondary chamber.

The Pumping system was not finished even though an early prototype of a purposefully built peristaltic pump was 3D printed , it was in an immature state and could not currently be incorporated in the bioreactor design, so for early use an external pump would need to be used, and for that reason the location for the tubing fittings was designed.



Figure 45 - 3D printed peristaltic pump initial prototype.

The final state of the prototype is as seen figure 47, some of the most important parts of the bioreactor were prototyped, but since the stimulation control was not finished it was not possible to work on the integration and connection of the motor to the actuating cam, which was essential to study the effectiveness of the main feature of this bioreactor design the mechanical stimulation system. Another part that is not present is the cover of the main chamber, this is not essential for the functioning of the bioreactor design but it would be necessary if actual tissue engineered constructs were to be cultured, as previously discussed a closed culture chamber is preferred to diminish the likelihood of microbiological contamination.



Figure 46 - Final Bioreactor prototype

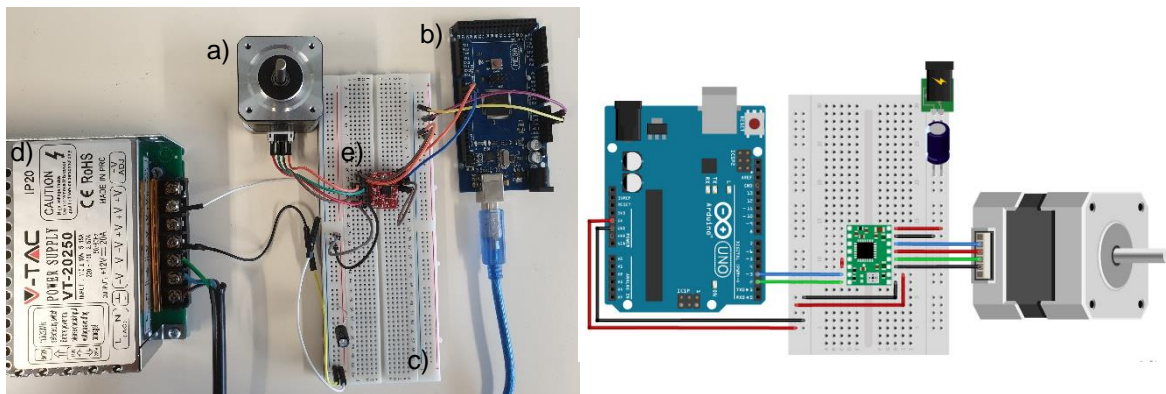


Figure 47 – Photography of the proof of concept circuit for controlling the actuating movement; a) step motor; b) Arduino board; c) Breadboard; d) Power source; e) step motor driver integrated circuit board; schematic representation obtained from makerguides.com and shows the wiring diagram for the circuit used.

The Arduino based circuit for control of the electric step motor that drives the actuator of the bioreactor was based on a similar circuit schematics²⁵⁷. The circuit is controlled by an Arduino microcontroller board that allows programming of the action of the actuation of the bioreactor, the board through a driver circuit controls the step motor to perform the programmed motion cycles. The circuit was mounted on a breadboard as a proof of concept at the current stage. A next necessary stage to implement this in a practical bioreactor would need to be made more permanent, one option would be to simply solder the connections in place, but a more practical and flexible option would be to use a shield circuit board that would mediate the connection, some of these boards even allow for relatively simple integration of user interface options as they are designed for consumer oriented products like 3D printers.

Programming of Arduino controller board is done in a specific programming environment “Arduino IDE” which uses a specific C++ library and is programmed in that language’s syntax. Individual programs in this context are generally called sketches.

Arduino programming can be done at a low level by directly setting the values of the Arduino pins, in the analog pins to a current value within their range, in the digital pins to a low or high setting. This would mean needing to define the two logical variables needed to activate the driver circuit, the two other connections of the Arduino board to the driver are just for powering the logic circuit part of the driver. These two variables are the direction and step, and this would need to be written as high or low directly. To simplify the program the Accel library’s specific functions for controlling stepper motors were used, allowing more high-level programming avoiding the need to write directly the variable values for specific output pins.

The strategy for controlling the movement is to use the internal clock of the Arduino as indirect indication of the current position of the rotation motion. The function `stepper.setpSpeed()` of the Accel stepper library sets the rotation speed in terms of steps per second, it is known that the stepper motor used as 200 steps per rotation, so full rotation would take 1 second at 200 steps/s, so with base on the speed set and the number of steps and the wanted angle of action of the motor, in this case is 90°, the time the motion takes can be calculated. This is where the internal clock of the Arduino board enters the

process, the actual change of direction is done by a conditional operation, if the correct interval of time as passed change the direction of rotation, else keep the rotation direction.

```

sketch_aug08a$
// Include the AccelStepper library:
#include <AccelStepper.h>
// Define stepper motor connections and motor interface type.
//Motor interface type must be set to 1 when using a driver:
#define dirPin1 2
#define stepPin1 3
#define motorInterfaceType 1
#define actionangle 180

// Create a new instance of the AccelStepper class:
AccelStepper stepper = AccelStepper(motorInterfaceType, stepPin1, dirPin1);

// Stores last time direction changed
unsigned long previousMillis = 0;
//rotation speed steps per second
int SPDL = 100;
// Initial direction
int DIR = 1;
//Angle within wich the motion occurs
int ANG = 90;
// Interval between direction changes
//const long interval = (ANG/360)*(200/SPD)*1000;
//200 is the number of steps per complete rotation
const long interval = 1000;

void setup() {
  // Set the maximum speed in steps per second:
  stepper.setMaxSpeed(1000);
}

void loop() {
  //check time
  unsigned long currentMillis = millis();
  if (currentMillis - previousMillis >= interval) {
    // save the last time rotaion direction changed
    previousMillis = currentMillis;

    if (DIR == 1) {
      //Set the speed in steps per second:
      stepper.setSpeed(SPDL);
      DIR = 2;
    } else {
      //Set the reverse speed in steps per second:
      stepper.setSpeed(-SPDL);
      //Step the motor with a constant speed as set by setSpeed():
      //stepper.runSpeed();
      DIR = 1;
    }
  }

  stepper.runSpeed();
}

```

Figure 48 - Arduino sketch code in the Arduino IDE application, this code is designed to drive the step motor in a rotation that is exact to the travel needed in the bioreactor and then turn back and do the same movement in the inverse direction.

These experiments made at proof of concept of the mechanical actuation control system, but it was not possible to further integrate the system into the bioreactor. An attempt to adapt this circuit and controlling sketch to control more than one step motor failed and caused the drivers to burn and be unusable, other pieces may have been damaged but no further investigation was possible. For this reason, the developments of this line of work were halted and were not possible to restart due to time constraints. The cause of the failure of the circuit was likely human error in doing the connections, possibly some error in the polarity of the power source, no reason was found that would make this circuit not convertible to control more than one stepper motor.

5. Conclusions and future work

As this master thesis work is finalized, it is possible to conclude that the initial goals and the ambitious design options pursued were not totally achieved. The beginning goals and the way they were pursued can be characterized as too broad and unfocused, this can be understood by the number and variety of design possibilities that were considered and described in this work. On another perspective, the variety and discussion of this broad spectrum of solutions to solve the problem of a bioreactor capable of mechanical stimulation relevant for articular cartilage tissue engineering is possibly the most important part of this work. This ideation process is the most extensive and can be considered the most successful part of this work.

The final design proposed is capable and has some novelty value, as no direct comparison is available in the literature. Possibly the most comparable design are the ones done by Vainieri et al¹⁸⁴ (2018), Shahin et al.²²³ (2012), Bilgen et al²²⁵ (2013). The comparison is mostly because these designs are capable of direct compression and contact shear stress combination mechanical stimulation. The work of Vainieri et al¹⁸⁴ used the pin and ball bioreactor architecture, this bioreactor has been described as a good recapitulation of the physiological loads felt by AC in vivo, but it is not capable of introducing perfusion. The lack of perfusion presents limitations on the culture of tissue engineering constructs, especially on the mass transfer to and from the construct limiting the density of cells and the size of construct possible with a non-perfused bioreactor is limited. Additionally, lack of perfusion also demands more direct contact of the operator with the cell-scaffold constructs introducing greater contamination risk. This limitations are also associated to the designs used by Shahin et al.²²³ and Bilgen et al²²⁵ but, in the first, the entire apparatus for mechanical stimulation is submerged in the media demanding a great volume of media for a relatively small construct. The only work found that combined perfusion with this combination of mechanical stimulation loads is the work of Jeong et al²²⁶ but, as previously discussed this work, it has different aims to the ones proposed in the present work, being designed to mimic as faithfully as possible the biomechanics of the diarthrodial joint of the knee and demanding a much more complex setup.

The final design concept for the bioreactor is considered capable given the original design objectives proposed. The summary of the design objectives is present in the following table.

Table 10- Synthesis of the design objectives comparison with the capabilities of the final design

Mechanical Stimulation	Direct compression: designed for strains around 10% ✓
	Hydrostatic Pressure ✗
	Shear
	Contact Shear: capable ✓
	Fluid induced shear: within the relevant values for AC tissue engineering (verified by CFD) ✓
Culture conditions	Size compatible with an incubator; dimensions of 22 cm by 15 cm ✓
Construct Size	Maximum of 3.1 cm ² , within the clinically relevant size ✓
Parallel integration	Simple ✓
Construction	Relatively fast and inexpensive (use of 3D printing) ✓

Other than the initially proposed design objectives, the final bioreactor design adds an interesting and, as already discussed, novel capability of having two parallel non contacting culture chambers for the same construct, one associated with each of the construct surfaces. This adds the possibility of the use of two different media compositions to each surface of the cell-scaffold construct culture which allows, in particular, the use of chondrogenic media in one side and media for bone differentiation on the other, allowing for possible recapitulation of the osteochondral tissue interaction *in vitro*. This has scientific interest as a model platform for osteochondral tissue but also in clinical application of osteochondral grafts culture for implantation.

The prototyping of the bioreactor was not fully completed, greatly due to the time of learning how to use the 3D printing and the problems that occurred with it but, most importantly, due to the fact that the ideation and design process dragged for a much longer time than expected in the beginning of this work.

The problems found in the 3D printing were associated to the problems the 3D printer had, with it having to be one time disassembled to solve a obstruction of the extruder but also due to the lack of knowledge and experience of the author with this sort of technique that produced numerous errors and failed attempts further delaying the process.

The stimulation control circuitry suffered from the same limitations of lack of initial knowledge and limited time by the extended period of ideation and design and was left for that reason unfinished. The proof of concept was possible but further development of the control solution was not possible in a timely fashion.

The prototyping in the end was uncompleted, but the most important parts were obtained. These parts were determined to be leak proof which was initially one of the major reservations towards the use of 3D printing for the production of a bioreactor with such intricate parts.

The major limitation of this work was the overall lack of verification of the effect of the designed mechanical stimulation apparatus. The simulation of the flow conditions within the culture chamber done with the Solidworks works flow simulation plug-in gave positive results of interstitial fluid velocities compatible with AC tissue engineering. These results, however, must be taken as solely indicative as the refinement of the mesh were left to the automatic mode of the program to obtain more accurate results. A more refined mesh would need to be used, demanding greater computing power, or alternatively a purpose built software should be used to obtain more refined results.

The lack of characterization of the mechanical stimulation with the biaxial compression/ contact shear loads characteristics being largely unknown was also a great limitation of this work. The calculation of the forces applied and the simulation of the deformation behavior of a tissue engineering construct under the designed loads would be of interest, moreover it would be of interest to refine the actuator shape to better the stimulation profile of the bioreactor. To do such simulations it was investigated how mechanics of continuous bodies and Finite elements modelling could be applied to modelling such a physical phenomenon. It was concluded that it could not be done with the time constraints of finishing the remaining work and the complexity of the biaxial movement and non-infinitesimal strain on the construct made simulation exceptionally complex.

Finally, to verify the effect of the current design on AC tissue engineering, a construct experiment should be designed and performed, validating or disproving the assumptions done in the design process that were based on the current available literature.

References

1. Anatomy & physiology. *OpenStax College* (2013).
2. DAVIES, D. V. Anatomy and physiology of diarthrodial joints. *Ann. Rheum. Dis.* (1945) doi:10.1136/ard.5.2.29.
3. Ricard-Blum, S. & Ruggiero, F. The collagen superfamily: From the extracellular matrix to the cell membrane. *Pathol. Biol.* (2005) doi:10.1016/j.patbio.2004.12.024.
4. Mow, V. C., Ateshian, G. A. & Spilker, R. L. Biomechanics of diarthrodial joints: A review of twenty years of progress. *Journal of Biomechanical Engineering* (1993) doi:10.1115/1.2895525.
5. Schättli, O. *et al.* A combination of shear and dynamic compression leads to mechanically induced chondrogenesis of human mesenchymal stem cells. *Eur. Cell. Mater.* (2011) doi:10.22203/eCM.v022a17.
6. Sophia Fox, A. J., Bedi, A. & Rodeo, S. A. The basic science of articular cartilage: Structure, composition, and function. *Sports Health* (2009) doi:10.1177/1941738109350438.
7. Stockwell, R. A. Chondrocytes. *Journal of clinical pathology. Supplement (Royal College of Pathologists)* (1978) doi:10.1385/1-59259-018-7:267.
8. Alford, J. W. & Cole, B. J. Cartilage restoration, part 1: Basic science, historical perspective, patient evaluation, and treatment options. *American Journal of Sports Medicine* (2005) doi:10.1177/0363546504273510.
9. Eyre, D. Articular cartilage and changes in Arthritis: Collagen of articular cartilage. *Arthritis Res* (2002) doi:10.1186/ar380.
10. Roughley, P. J. & Lee, E. R. Cartilage proteoglycans: Structure and potential functions. *Microsc. Res. Tech.* (1994) doi:10.1002/jemt.1070280505.
11. Huber, M., Trattinig, S. & Lintner, F. Anatomy, Biochemistry, and Physiology of Articular Cartilage : Investigative Radiology. *Invest. Radiol.* (2000).
12. Linn, F. C. & Sokoloff, L. Movement and composition of interstitial fluid of cartilage. *Arthritis Rheum.* (1965) doi:10.1002/art.1780080402.
13. McCutchen, C. W. The frictional properties of animal joints. *Wear* (1962) doi:10.1016/0043-1648(62)90176-X.
14. Elmore, S. M., Sokoloff, L., Norris, G. & Carmeci, P. Nature of 'imperfect' elasticity of articular cartilage. *J. Appl. Physiol.* (1963) doi:10.1152/jappl.1963.18.2.393.
15. Milz, S. & Putz, R. Quantitative morphology of the subchondral plate of the tibial plateau. *J. Anat.* (1994).
16. G., L. *et al.* Subchondral bone in osteoarthritis: Insight into risk factors and microstructural changes. *Arthritis Res. Ther.* (2013).
17. Coates, E. E. & Fisher, J. P. Phenotypic variations in chondrocyte subpopulations and their response to in vitro culture and external stimuli. *Annals of Biomedical Engineering* (2010) doi:10.1007/s10439-010-0096-1.
18. Malemud, C. J. Matrix metalloproteinases (MMPs) in health and disease: An overview. *Frontiers in Bioscience* (2006) doi:10.2741/1915.
19. Uusitalo, H., Hiltunen, A., Söderström, M., Aro, H. T. & Vuorio, E. Expression of cathepsins B, H, K, L, and S and matrix metalloproteinases 9 and 13 during chondrocyte hypertrophy and endochondral ossification in mouse fracture callus. *Calcif. Tissue Int.* (2000) doi:10.1007/s002230001152.
20. Goldring, M. B., Otero, M., Tsuchimochi, K., Ijiri, K. & Li, Y. Defining the roles of inflammatory and anabolic cytokines in cartilage metabolism. in *Annals of the Rheumatic Diseases* (2008). doi:10.1136/ard.2008.098764.
21. Cheah, K. S. E., Stoker, N. G., Griffin, J. R., Grosveld, F. G. & Solomon, E. Identification and characterization of the human type II collagen gene (COL2A1). *Proc. Natl. Acad. Sci. U. S. A.* (1985) doi:10.1073/pnas.82.9.2555.

22. Freije, J. M. P. *et al.* Molecular cloning and expression of collagenase-3, a novel human matrix metalloproteinase produced by breast carcinomas. *J. Biol. Chem.* (1994).
23. Canty, E. G. & Kadler, K. E. Procollagen trafficking, processing and fibrillogenesis. *Journal of Cell Science* (2005) doi:10.1242/jcs.01731.
24. Bi, W., Deng, J. M., Zhang, Z., Behringer, R. R. & De Crombrughe, B. Sox9 is required for cartilage formation. *Nat. Genet.* (1999) doi:10.1038/8792.
25. Zhang, Z., Yuan, L., Lee, P. D., Jones, E. & Jones, J. R. Modeling of time dependent localized flow shear stress and its impact on cellular growth within additive manufactured titanium implants. *J. Biomed. Mater. Res. - Part B Appl. Biomater.* (2014) doi:10.1002/jbm.b.33146.
26. Stokes, D. G. *et al.* Regulation of type-II collagen gene expression during human chondrocyte de-differentiation and recovery of chondrocyte-specific phenotype in culture involves Sry-type high-mobility-group box (SOX) transcription factors. *Biochem. J.* (2001) doi:10.1042/0264-6021:3600461.
27. Sekiya, I. *et al.* SOX9 enhances aggrecan gene promoter/enhancer activity and is up-regulated by retinoic acid in a cartilage-derived cell line, TC6. *J. Biol. Chem.* (2000) doi:10.1074/jbc.275.15.10738.
28. Wilson, M. & Koopman, P. Matching SOX: Partner proteins and co-factors of the SOX family of transcriptional regulators. *Current Opinion in Genetics and Development* (2002) doi:10.1016/S0959-437X(02)00323-4.
29. Bell, D. M. *et al.* SOX9 directly regulates the type-II collagen gene. *Nat. Genet.* (1997) doi:10.1038/ng0697-174.
30. Lefebvre, V., Li, P. & De Crombrughe, B. A new long form of Sox5 (L-Sox5), Sox6 and Sox9 are coexpressed in chondrogenesis and cooperatively activate the type II collagen gene. *EMBO J.* (1998) doi:10.1093/emboj/17.19.5718.
31. Kolettas, E., Muir, H. I., Barrett, J. C. & Hardingham, T. E. Chondrocyte phenotype and cell survival are regulated by culture conditions and by specific cytokines through the expression of Sox-9 transcription factor. *Rheumatology* (2001) doi:10.1093/rheumatology/40.10.1146.
32. Quintana, L., Zur Nieden, N. I. & Semino, C. E. Morphogenetic and regulatory mechanisms during developmental chondrogenesis: New paradigms for cartilage tissue engineering. *Tissue Eng. - Part B Rev.* (2009) doi:10.1089/ten.teb.2008.0329.
33. Wang, L., Shao, Y. Y. & Ballock, R. T. Thyroid hormone-mediated growth and differentiation of growth plate chondrocytes involves IGF-1 modulation of β -catenin signaling. *J. Bone Miner. Res.* (2010) doi:10.1002/jbmr.5.
34. Nixon, A. J. *et al.* Gene therapy in musculoskeletal repair. in *Annals of the New York Academy of Sciences* (2007). doi:10.1196/annals.1402.065.
35. Chimal-Monroy, J. *et al.* Analysis of the molecular cascade responsible for mesodermal limb chondrogenesis: Sox genes and BMP signaling. *Dev. Biol.* (2003) doi:10.1016/S0012-1606(03)00066-6.
36. Vortkamp, A. *et al.* Regulation of rate of cartilage differentiation by Indian Hedgehog and PTH-related protein. *Science* (1996) doi:10.1126/science.273.5275.613.
37. Goldring, M. B., Tsuchimochi, K. & Ijiri, K. The control of chondrogenesis. *Journal of Cellular Biochemistry* (2006) doi:10.1002/jcb.20652.
38. Pujol, J. P. *et al.* Interleukin-1 and transforming growth factor- β 1 as crucial factors in osteoarthritic cartilage metabolism. *Connective Tissue Research* (2008) doi:10.1080/03008200802148355.
39. Hui, W., Rowan, A. D. & Cawston, T. Modulation of the expression of matrix metalloproteinase and tissue inhibitors of metalloproteinases by TGF- β 1 and IGF-1 in primary human articular and bovine nasal chondrocytes stimulated with TNF- α . *Cytokine* (2001) doi:10.1006/cyto.2001.0950.
40. Murakami, S., Lefebvre, V. & De Crombrughe, B. Potent inhibition of the master chondrogenic factor Sox9 gene by interleukin-1 and tumor necrosis factor- α . *J. Biol. Chem.* (2000) doi:10.1074/jbc.275.5.3687.

41. Mengshol, J. A. IL-1 induces collagenase-3 (MMP-13) promoter activity in stably transfected chondrocytic cells: requirement for Runx-2 and activation by p38 MAPK and JNK pathways. *Nucleic Acids Res.* (2001) doi:10.1093/nar/29.21.4361.
42. Legendre, F., Dudhia, J., Pujol, J. P. & Bogdanowicz, P. JAK/STAT but not ERK1/ERK2 pathway mediates interleukin (IL)-6/soluble IL-6R down-regulation of type II collagen, aggrecan core, and link protein transcription in articular chondrocytes. Association with a down-regulation of Sox9 expression. *J. Biol. Chem.* (2003) doi:10.1074/jbc.M110773200.
43. Wang, N. Review of cellular mechanotransduction. *Journal of Physics D: Applied Physics* (2017) doi:10.1088/1361-6463/aa6e18.
44. Daniels, K. & Solorsh, M. Modulation of chondrogenesis by the cytoskeleton and extracellular matrix. *Journal of Cell Science* (1991).
45. Archer, C. W., Rooney, P. & Wolpert, L. Cell shape and cartilage differentiation of early chick limb bud cells in culture. *Cell Differ.* (1982) doi:10.1016/0045-6039(82)90072-0.
46. Glowacki, J., Trepman, E. & Folkman, J. Cell Shape and Phenotypic Expression in Chondrocytes. *Proc. Soc. Exp. Biol. Med.* (1983) doi:10.3181/00379727-172-41533.
47. Zanetti, N. C. & Solorsh, M. Induction of chondrogenesis in limb mesenchymal cultures by disruption of the actin cytoskeleton. *J. Cell Biol.* (1984) doi:10.1083/jcb.99.1.115.
48. Newman, P. & Watt, F. M. Influence of cytochalasin d-induced changes in cell shape on proteoglycan synthesis by cultured articular chondrocytes. *Exp. Cell Res.* (1988) doi:10.1016/0014-4827(88)90391-6.
49. Vinall, R. L., Lo, S. H. & Reddi, A. H. Regulation of articular chondrocyte phenotype by bone morphogenetic protein 7, interleukin 1, and cellular context is dependent on the cytoskeleton. *Exp. Cell Res.* (2002) doi:10.1006/excr.2001.5395.
50. Tew, S. R. & Hardingham, T. E. Regulation of SOX9 mRNA in human articular chondrocytes involving p38 MAPK activation and mRNA stabilization. *J. Biol. Chem.* (2006) doi:10.1074/jbc.M604322200.
51. Freeman, P. M., Natarajan, R. N., Kimura, J. H. & Andriacchi, T. P. Chondrocyte cells respond mechanically to compressive loads. *J. Orthop. Res.* (1994) doi:10.1002/jor.1100120303.
52. Parkkinen, J. J. *et al.* Influence of short-term hydrostatic pressure on organization of stress fibers in cultured chondrocytes. *J. Orthop. Res.* (1995) doi:10.1002/jor.1100130404.
53. Lee, D. A. *et al.* Chondrocyte deformation within compressed agarose constructs at the cellular and sub-cellular levels. *J. Biomech.* (2000) doi:10.1016/S0021-9290(99)00160-8.
54. Knight, M. M., Toyoda, T., Lee, D. A. & Bader, D. L. Mechanical compression and hydrostatic pressure induce reversible changes in actin cytoskeletal organisation in chondrocytes in agarose. *J. Biomech.* (2006) doi:10.1016/j.jbiomech.2005.04.006.
55. Ramage, L., Nuki, G. & Salter, D. M. Signalling cascades in mechanotransduction: Cell-matrix interactions and mechanical loading. *Scandinavian Journal of Medicine and Science in Sports* (2009) doi:10.1111/j.1600-0838.2009.00912.x.
56. Wang, N., Tytell, J. D. & Ingber, D. E. Mechanotransduction at a distance: Mechanically coupling the extracellular matrix with the nucleus. *Nature Reviews Molecular Cell Biology* (2009) doi:10.1038/nrm2594.
57. Urban, J. P. G., Hall, A. C. & Gehl, K. A. Regulation of matrix synthesis rates by the ionic and osmotic environment of articular chondrocytes. *J. Cell. Physiol.* (1993) doi:10.1002/jcp.1041540208.
58. Mobasheri, A. *et al.* Characterization of a stretch-activated potassium channel in chondrocytes. *J. Cell. Physiol.* (2010) doi:10.1002/jcp.22075.
59. Wu, Q. Q. & Chen, Q. Mechanoregulation of chondrocyte proliferation, maturation, and hypertrophy: Ion-channel dependent transduction of matrix deformation signals. *Exp. Cell Res.* (2000) doi:10.1006/excr.2000.4847.
60. Millward-Sadler, S. J. & Salter, D. M. Integrin-dependent signal cascades in chondrocyte mechanotransduction. *Ann. Biomed. Eng.* (2004) doi:10.1023/B:ABME.0000017538.72511.48.
61. Kock, L. M. *et al.* RGD-dependent integrins are mechanotransducers in dynamically

- compressed tissue-engineered cartilage constructs. *J. Biomech.* (2009) doi:10.1016/j.jbiomech.2009.05.039.
62. Ohashi, K., Fujiwara, S. & Mizuno, K. Roles of the cytoskeleton, cell adhesion and rho signalling in mechanosensing and mechanotransduction. *Journal of Biochemistry* (2017) doi:10.1093/jb/mvw082.
 63. Wright, M. O. *et al.* Hyperpolarisation of cultured human chondrocytes following cyclical pressure-induced strain: Evidence of a role for $\alpha 5\beta 1$ integrin as a chondrocyte mechanoreceptor. *J. Orthop. Res.* (1997) doi:10.1002/jor.1100150517.
 64. Haudenschild, D. R., D'Lima, D. D. & Lotz, M. K. Dynamic compression of chondrocytes induces a Rho kinase-dependent reorganization of the actin cytoskeleton. in *Biorheology* (2008). doi:10.3233/BIR-2008-0499.
 65. Haudenschild, D. R., Nguyen, B., Chen, J., D'Lima, D. D. & Lotz, M. K. Rho kinase-dependent CCL20 induced by dynamic compression of human chondrocytes. *Arthritis Rheum.* (2008) doi:10.1002/art.23797.
 66. Woods, A., Wang, G. & Beier, F. RhoA/ROCK signaling regulates Sox9 expression and actin organization during chondrogenesis. *J. Biol. Chem.* (2005) doi:10.1074/jbc.M409158200.
 67. Woods, A. & Beier, F. RhoA/ROCK signaling regulates chondrogenesis in a context-dependent manner. *J. Biol. Chem.* (2006) doi:10.1074/jbc.M509433200.
 68. Li, Z., Yao, S. J., Alini, M. & Stoddart, M. J. Chondrogenesis of human bone marrow mesenchymal stem cells in fibrin-polyurethane composites is modulated by frequency and amplitude of dynamic compression and shear stress. in *Tissue Engineering - Part A* (2010). doi:10.1089/ten.tea.2009.0262.
 69. Paul, J. P. Approaches to design. Force actions transmitted by joints in the human body. *Proc. R. Soc. London - Biol. Sci.* (1976) doi:10.1098/rspb.1976.0004.
 70. Hodge, W. A. *et al.* Contact pressures from an instrumented hip endoprosthesis. *J. Bone Jt. Surg. - Ser. A* (1989) doi:10.2106/00004623-198971090-00015.
 71. Katta, J., Jin, Z., Ingham, E. & Fisher, J. Biotribology of articular cartilage-A review of the recent advances. *Med. Eng. Phys.* (2008) doi:10.1016/j.medengphy.2008.09.004.
 72. Armstrong, C. G., Lai, W. M. & Mow, V. C. An analysis of the unconfined compression of articular cartilage. *J. Biomech. Eng.* (1984) doi:10.1115/1.3138475.
 73. Shepherd, D. E. T. & Seedhom, B. B. The 'instantaneous' compressive modulus of human articular cartilage in joints of the lower limb. *Rheumatology* (1999) doi:10.1093/rheumatology/38.2.124.
 74. Kutzner, I. *et al.* Loading of the knee joint during activities of daily living measured in vivo in five subjects. *J. Biomech.* (2010) doi:10.1016/j.jbiomech.2010.03.046.
 75. Sutter, E. G. *et al.* In Vivo Measurement of Localized Tibiofemoral Cartilage Strains in Response to Dynamic Activity. *Am. J. Sports Med.* (2015) doi:10.1177/0363546514559821.
 76. Chan, D. D. *et al.* In vivo articular cartilage deformation: Noninvasive quantification of intratissue strain during joint contact in the human knee. *Sci. Rep.* (2016) doi:10.1038/srep19220.
 77. Liu, B. *et al.* In Vivo Tibial Cartilage Strains in Regions of Cartilage-to-Cartilage Contact and Cartilage-to-Meniscus Contact in Response to Walking. *Am. J. Sports Med.* (2017) doi:10.1177/0363546517712506.
 78. Mündermann, A., Dyrby, C. O., D'Lima, D. D., Colwell, C. W. & Andriacchi, T. P. In vivo knee loading characteristics during activities of daily living as measured by an instrumented total knee replacement. *J. Orthop. Res.* (2008) doi:10.1002/jor.20655.
 79. Woo, S. L. & Buckwalter, J. A. AAOS/NIH/ORS workshop. Injury and repair of the musculoskeletal soft tissues. Savannah, Georgia, June 18-20, 1987. *J. Orthop. Res.* (1988) doi:10.1002/jor.1100060615.
 80. Lohmander, L. S., Dahlberg, L., Ryd, L. & Heinegård, D. Increased levels of proteoglycan fragments in knee joint fluid after injury. *Arthritis Rheum.* (1989) doi:10.1002/anr.1780321113.

81. Mankin, H. J. The response of articular cartilage to mechanical injury. *JBJS* **64**, 460–466 (1989).
82. Bhosale, A. M. & Richardson, J. B. Articular cartilage: Structure, injuries and review of management. *British Medical Bulletin* (2008) doi:10.1093/bmb/ldn025.
83. Furukawa, T., Eyre, D. R., Koide, S. & Glimcher, M. J. Biochemical studies on repair cartilage resurfacing experimental defects in the rabbit knee. *J. Bone Jt. Surg. - Ser. A* (1980) doi:10.2106/00004623-198062010-00012.
84. Nehrer, S., Spector, M. & Minas, T. Histologic analysis of tissue after failed cartilage repair procedures. *Clin. Orthop. Relat. Res.* (1999) doi:10.1097/00003086-199908000-00020.
85. Kampen, W. U. & Tillmann, B. Age-related changes in the articular cartilage of human sacroiliac joint. *Anat. Embryol. (Berl)*. (1998) doi:10.1007/s004290050200.
86. Årøen, A. *et al.* Articular Cartilage Lesions in 993 Consecutive Knee Arthroscopies. *Am. J. Sports Med.* (2004) doi:10.1177/0363546503259345.
87. Curl, W. W. *et al.* Cartilage injuries: A review of 31,516 knee arthroscopies. *Arthroscopy* (1997) doi:10.1016/S0749-8063(97)90124-9.
88. Brittberg, M. Cartilage repair. On cartilaginous tissue engineering with the emphasis on chondrocyte transplantation. *Department of Orthopaedics and Department of Clinical Chemistry* (1996).
89. Jafarzadeh, S. R. & Felson, D. T. Updated Estimates Suggest a Much Higher Prevalence of Arthritis in United States Adults Than Previous Ones. *Arthritis Rheumatol.* (2018) doi:10.1002/art.40355.
90. Junker, S. *et al.* Expression of adipokines in osteoarthritis osteophytes and their effect on osteoblasts. *Matrix Biol.* (2017) doi:10.1016/j.matbio.2016.11.005.
91. Wieland, H. A., Michaelis, M., Kirschbaum, B. J., & Rudolphi, K. A. Osteoarthritis—an untreatable disease? *Nat. Rev. Drug Discov.* **4**, 331 (2005).
92. Bijlsma, J. W. J., Berenbaum, F. & Lafeber, F. P. J. G. Osteoarthritis: An update with relevance for clinical practice. *The Lancet* (2011) doi:10.1016/S0140-6736(11)60243-2.
93. Anderson, D. D. *et al.* Post-traumatic osteoarthritis: Improved understanding and opportunities for early intervention. *J. Orthop. Res.* (2011) doi:10.1002/jor.21359.
94. Brown, T. D., Johnston, R. C., Saltzman, C. L., Marsh, J. L. & Buckwalter, J. A. Posttraumatic osteoarthritis: A first estimate of incidence, prevalence, and burden of disease. in *Journal of Orthopaedic Trauma* (2006). doi:10.1097/01.bot.0000246468.80635.ef.
95. Krishnan, Y. & Grodzinsky, A. J. Cartilage diseases. *Matrix Biology* (2018) doi:10.1016/j.matbio.2018.05.005.
96. Swärd, P., Frobell, R., Englund, M., Roos, H. & Struglics, A. Cartilage and bone markers and inflammatory cytokines are increased in synovial fluid in the acute phase of knee injury (hemarthrosis) - a cross-sectional analysis. *Osteoarthr. Cartil.* (2012) doi:10.1016/j.joca.2012.07.021.
97. Silawal, S., Triebel, J., Bertsch, T. & Schulze-Tanzil, G. Osteoarthritis and the complement cascade. *Clin. Med. Insights Arthritis Musculoskelet. Disord.* (2018) doi:10.1177/1179544117751430.
98. Bondeson, J., Wainwright, S. D., Lauder, S., Amos, N. & Hughes, C. E. The role of synovial macrophages and macrophage-produced cytokines in driving aggrecanases, matrix metalloproteinases, and other destructive and inflammatory responses in osteoarthritis. *Arthritis Res. Ther.* (2006) doi:10.1186/ar2099.
99. Gibofsky, A. Overview of epidemiology, pathophysiology, and diagnosis of rheumatoid arthritis. *Am. J. Manag. Care* (2012).
100. Zhu, Y., Pandya, B. J. & Choi, H. K. Prevalence of gout and hyperuricemia in the US general population: The National Health and Nutrition Examination Survey 2007-2008. *Arthritis Rheum.* (2011) doi:10.1002/art.30520.
101. El-Zawawy, H. & Mandell, B. F. Update on Crystal-Induced Arthritides. *Clinics in Geriatric Medicine* (2017) doi:10.1016/j.cger.2016.08.010.
102. Ravelli, A., Martini, A. Juvenile idiopathic arthritis. *Lancet* **369**, 767–778 (2007).

103. Dougados, M., & Baeten, D. Spondyloarthritis . *Lancet* **377**, 2127–2137 (2011).
104. Stancíková, M., Lukác, J., Istok, R., Cristalli, G. & Rovensky, J. Serum adenosine deaminase activity and its isoenzyme pattern in patients with systemic lupus erythematosus. *Clin. Exp. Rheumatol.* (1998).
105. Edmonds, E. W. & Polousky, J. A review of knowledge in osteochondritis dissecans: 123 years of minimal evolution from könig to the ROCK study group general. *Clinical Orthopaedics and Related Research* (2013) doi:10.1007/s11999-012-2290-y.
106. Lindén, B. the incidence of osteochondritis dissecans in the condyles of the femur. *Acta Orthop.* (1976) doi:10.3109/17453677608988756.
107. Trentham, D. E., Le, C. H. Relapsing polychondritis. *Ann. Intern. Med.* **129**, 114–122 (1998).
108. Terao, C. *et al.* Genotyping of relapsing polychondritis identified novel susceptibility HLA alleles and distinct genetic characteristics from other rheumatic diseases. *Rheumatol. (United Kingdom)* (2016) doi:10.1093/rheumatology/kew233.
109. A., S., K., G., K., S. & S., S. Relapsing polychondritis: A review. *Clin. Rheumatol.* (2013).
110. Rosenthal, A. K., Ryan, L. M. & Champion, E. W. Calcium pyrophosphate deposition disease. *New England Journal of Medicine* (2016) doi:10.1056/NEJMra1511117.
111. KOHN, N. N., HUGHES, R. E., McCARTY, D. J. & FAIRES, J. S. The significance of calcium phosphate crystals in the synovial fluid of arthritic patients: the 'pseudogout syndrome'. II. Identification of crystals. *Ann. Intern. Med.* (1962) doi:10.7326/0003-4819-56-5-738.
112. Felson, D. T., Anderson, J. J., Naimark, A., Kannel, W. & Meenan, R. F. The prevalence of chondrocalcinosis in the elderly and its association with knee osteoarthritis: The Framingham study. *J. Rheumatol.* (1989).
113. McCarty, D. J. Diagnostic mimicry in arthritis: patterns of joint involvement associated with calcium pyrophosphate dihydrate crystal deposits. *Bull. Rheum. Dis.* (1974).
114. Franchi, A. Epidemiology and classification of bone tumors. *Clinical Cases in Mineral and Bone Metabolism* (2012).
115. Riedel, R. F. *et al.* The clinical management of chondrosarcoma. *Current Treatment Options in Oncology* (2009) doi:10.1007/s11864-009-0088-2.
116. Gelderblom, H. *et al.* The Clinical Approach Towards Chondrosarcoma. *Oncologist* (2008) doi:10.1634/theoncologist.2007-0237erratum.
117. Gibson, J. N. A., White, M. D., Chapman, V. M. & Strachan, R. K. Arthroscopic lavage and debridement for osteoarthritis of the knee. *J. Bone Jt. Surg. - Ser. B* (1992) doi:10.1302/0301-620x.74b4.1624511.
118. Ficat, R. P., Ficat, C., Gedeon, P. & Toussaint, J. B. Spongialization: a new treatment for diseased patellae. *Clin. Orthop. Relat. Res.* (1979) doi:10.1097/00003086-197910000-00014.
119. Steadman, J. R., Rodkey, W. G., Singleton, S. B. & Briggs, K. K. Microfracture technique for full-thickness chondral defects: Technique and clinical results. *Oper. Tech. Orthop.* (1997) doi:10.1016/S1048-6666(97)80033-X.
120. Hangody, L. & Füles, P. Autologous osteochondral mosaicplasty for the treatment of full-thickness defects of weight-bearing joints: Ten years of experimental and clinical experience. in *Journal of Bone and Joint Surgery - Series A* (2003). doi:10.2106/00004623-200300002-00004.
121. Bentley, G. *et al.* A prospective, randomised comparison of autologous chondrocyte implantation versus mosaicplasty for osteochondral defects in the knee. *J. Bone Jt. Surg. - Ser. B* (2003) doi:10.1302/0301-620X.85B2.13543.
122. Menche, D. S., Pitman, M. I. & Peterson, L. Experimental model for chondrocyte transplantation in rabbits. in *Surgery and Arthroscopy of the Knee* (1986). doi:10.1007/978-3-642-71022-3_21.
123. Roberts, S. *et al.* Autologous chondrocyte implantation for cartilage repair: monitoring its success by magnetic resonance imaging and histology. *Arthritis Res. Ther.* (2003) doi:10.1186/ar613.
124. G., K. *et al.* A randomized trial comparing autologous chondrocyte implantation with

- microfracture: Findings at five years. *J. Bone Jt. Surg. - Ser. A* (2007).
125. Saris, D. B. F. *et al.* Characterized chondrocyte implantation results in better structural repair when treating symptomatic cartilage defects of the knee in a randomized controlled trial versus microfracture. *Am. J. Sports Med.* (2008) doi:10.1177/0363546507311095.
 126. Ng, K. W. *et al.* Passaged adult chondrocytes can form engineered cartilage with functional mechanical properties: A canine model. *Tissue Eng. - Part A* (2010) doi:10.1089/ten.tea.2009.0581.
 127. Adkisson, H. D. *et al.* The potential of human allogeneic juvenile chondrocytes for restoration of articular cartilage. *Am. J. Sports Med.* (2010) doi:10.1177/0363546510361950.
 128. Tran-Khanh, N., Hoemann, C. D., McKee, M. D., Henderson, J. E. & Buschmann, M. D. Aged bovine chondrocytes display a diminished capacity to produce a collagen-rich, mechanically functional cartilage extracellular matrix. *J. Orthop. Res.* (2005) doi:10.1016/j.orthres.2005.05.009.
 129. Pittenger, M. F. *et al.* Multilineage potential of adult human mesenchymal stem cells. *Science* (80-.). (1999) doi:10.1126/science.284.5411.143.
 130. Chamberlain, G., Fox, J., Ashton, B. & Middleton, J. Concise Review: Mesenchymal Stem Cells: Their Phenotype, Differentiation Capacity, Immunological Features, and Potential for Homing. *Stem Cells* (2007) doi:10.1634/stemcells.2007-0197.
 131. Alexander, P. G., Hofer, H. R., Clark, K. L. & Tuan, R. S. Mesenchymal Stem Cells in Musculoskeletal Tissue Engineering. in *Principles of Tissue Engineering: Fourth Edition* (2013). doi:10.1016/B978-0-12-398358-9.00054-9.
 132. Yoshimura, H. *et al.* Comparison of rat mesenchymal stem cells derived from bone marrow, synovium, periosteum, adipose tissue, and muscle. *Cell Tissue Res.* (2007) doi:10.1007/s00441-006-0308-z.
 133. Mendelson, A. *et al.* Chondrogenesis by chemotactic homing of synovium, bone marrow, and adipose stem cells in vitro. *FASEB J.* (2011) doi:10.1096/fj.10-176305.
 134. Vangsness, C. T. *et al.* Adult human mesenchymal stem cells delivered via intra-articular injection to the knee following partial medial meniscectomy A Randomized, Double-Blind, Controlled Study. *J. Bone Jt. Surg. - Ser. A* (2014) doi:10.2106/JBJS.M.00058.
 135. Tan, A. R. & Hung, C. T. Concise review: Mesenchymal stem cells for functional cartilage tissue engineering: Taking cues from chondrocyte-based constructs. *Stem Cells Translational Medicine* (2017) doi:10.1002/sctm.16-0271.
 136. Naghizadeh, F., Solouk, A. & Khoulenjani, S. B. Osteochondral scaffolds based on electrospinning method: General review on new and emerging approaches. *Int. J. Polym. Mater. Polym. Biomater.* (2018) doi:10.1080/00914037.2017.1393682.
 137. Seo, S. J., Mahapatra, C., Singh, R. K., Knowles, J. C. & Kim, H. W. Strategies for osteochondral repair: Focus on scaffolds. *Journal of Tissue Engineering* (2014) doi:10.1177/2041731414541850.
 138. Deponti, D. *et al.* Collagen scaffold for cartilage tissue engineering: The benefit of fibrin glue and the proper culture time in an infant cartilage model. *Tissue Eng. - Part A* (2014) doi:10.1089/ten.tea.2013.0171.
 139. Zhu, M., Feng, Q., Sun, Y., Li, G. & Bian, L. Effect of cartilaginous matrix components on the chondrogenesis and hypertrophy of mesenchymal stem cells in hyaluronic acid hydrogels. *J. Biomed. Mater. Res. - Part B Appl. Biomater.* (2017) doi:10.1002/jbm.b.33760.
 140. Varghese, S. *et al.* Chondroitin sulfate based niches for chondrogenic differentiation of mesenchymal stem cells. *Matrix Biol.* (2008) doi:10.1016/j.matbio.2007.07.002.
 141. Bryant, S. J. & Anseth, K. S. Hydrogel properties influence ECM production by chondrocytes photoencapsulated in poly(ethylene glycol) hydrogels. *J. Biomed. Mater. Res.* (2002) doi:10.1002/jbm.1217.
 142. Awad, H. A., Wickham, M. Q., Leddy, H. A., Gimble, J. M. & Guilak, F. Chondrogenic differentiation of adipose-derived adult stem cells in agarose, alginate, and gelatin scaffolds. *Biomaterials* (2004) doi:10.1016/j.biomaterials.2003.10.045.

143. Chou, C. H. *et al.* TGF- β 1 immobilized tri-co-polymer for articular cartilage tissue engineering. *J. Biomed. Mater. Res. - Part B Appl. Biomater.* (2006) doi:10.1002/jbm.b.30432.
144. Hwang, N. S., Varghese, S., Zhang, Z. & Elisseeff, J. Chondrogenic differentiation of human embryonic stem cell-derived cells in arginine-glycine-aspartate-modified hydrogels. *Tissue Eng.* (2006) doi:10.1089/ten.2006.12.2695.
145. Nguyen, L. H., Kudva, A. K., Guckert, N. L., Linse, K. D. & Roy, K. Unique biomaterial compositions direct bone marrow stem cells into specific chondrocytic phenotypes corresponding to the various zones of articular cartilage. *Biomaterials* (2011) doi:10.1016/j.biomaterials.2010.10.009.
146. Jeon, J. E., Vaquette, C., Klein, T. J. & Hutmacher, D. W. Perspectives in multiphasic osteochondral tissue engineering. *Anat. Rec.* (2014) doi:10.1002/ar.22795.
147. Byers, B. A., Mauck, R. L., Chiang, I. E. & Tuan, R. S. Transient exposure to transforming growth factor beta 3 under serum-free conditions enhances the biomechanical and biochemical maturation of tissue-engineered cartilage. *Tissue Eng. - Part A.* (2008) doi:10.1089/ten.tea.2007.0222.
148. Mauck, R. L., Nicoll, S. B., Seyhan, S. L., Ateshian, G. A. & Hung, C. T. Synergistic action of growth factors and dynamic loading for articular cartilage tissue engineering. *Tissue Eng.* (2003) doi:10.1089/107632703768247304.
149. Liming Bian *et al.* Effects of dexamethasone on the functional properties of cartilage explants during long-term culture. *Am. J. Sports Med.* (2010) doi:10.1177/0363546509354197.
150. Tsuchiya, K., Chen, G., Ushida, T., Matsuno, T. & Tateishi, T. The effect of coculture of chondrocytes with mesenchymal stem cells on their cartilaginous phenotype in vitro. *Mater. Sci. Eng. C* (2004) doi:10.1016/j.msec.2003.12.014.
151. Kubosch, E. J., Heidt, E., Bernstein, A., Böttiger, K. & Schmal, H. The trans-well coculture of human synovial mesenchymal stem cells with chondrocytes leads to self-organization, chondrogenic differentiation, and secretion of TGF β . *Stem Cell Res. Ther.* (2016) doi:10.1186/s13287-016-0322-3.
152. Wu, L. *et al.* Trophic effects of mesenchymal stem cells increase chondrocyte proliferation and matrix formation. *Tissue Eng. - Part A* (2011) doi:10.1089/ten.tea.2010.0517.
153. Meyer, E. G., Buckley, C. T., Thorpe, S. D. & Kelly, D. J. Low oxygen tension is a more potent promoter of chondrogenic differentiation than dynamic compression. *J. Biomech.* (2010) doi:10.1016/j.jbiomech.2010.05.020.
154. Sheehy, E. J., Buckley, C. T. & Kelly, D. J. Oxygen tension regulates the osteogenic, chondrogenic and endochondral phenotype of bone marrow derived mesenchymal stem cells. *Biochem. Biophys. Res. Commun.* (2012) doi:10.1016/j.bbrc.2011.11.105.
155. Tognana, E. *et al.* Adjacent tissues (cartilage, bone) affect the functional integration of engineered calf cartilage in vitro. *Osteoarthr. Cartil.* (2005) doi:10.1016/j.joca.2004.10.015.
156. Salinas, E. Y., Hu, J. C. & Athanasiou, K. A Guide for Using Mechanical Stimulation to Enhance Tissue-Engineered Articular Cartilage Properties. *Tissue Eng. - Part B Rev.* (2018) doi:10.1089/ten.teb.2018.0006.
157. Albro, M. B. *et al.* Dynamic loading of deformable porous media can induce active solute transport. *J. Biomech.* (2008) doi:10.1016/j.jbiomech.2008.08.023.
158. Buckwalter, J. A. & Mankin, H. J. Articular cartilage: tissue design and chondrocyte-matrix interactions. *Instructional course lectures* (1998).
159. Panadero, J. A., Lanceros-Mendez, S. & Ribelles, J. L. G. Differentiation of mesenchymal stem cells for cartilage tissue engineering: Individual and synergetic effects of three-dimensional environment and mechanical loading. *Acta Biomaterialia* (2016) doi:10.1016/j.actbio.2016.01.037.
160. Mouw, J. K., Connelly, J. T., Wilson, C. G., Michael, K. E. & Levenston, M. E. Dynamic Compression Regulates the Expression and Synthesis of Chondrocyte-Specific Matrix Molecules in Bone Marrow Stromal Cells. *Stem Cells* (2006) doi:10.1634/stemcells.2006-0435.
161. Elder, B. D. & Athanasiou, K. A. Hydrostatic pressure in articular cartilage tissue engineering:

- From chondrocytes to tissue regeneration. *Tissue Engineering - Part B: Reviews* (2009) doi:10.1089/ten.teb.2008.0435.
162. Waters, R. L., Lunsford, B. R., Perry, J. & Byrd, R. Energy-speed relationship of walking: Standard tables. *J. Orthop. Res.* (1988) doi:10.1002/jor.1100060208.
 163. Urban, J. P. G. The chondrocyte: A cell under pressure. *Rheumatology* (1994) doi:10.1093/rheumatology/33.10.901.
 164. Mizuno, S., Watanabe, S. & Takagi, T. Hydrostatic fluid pressure promotes cellularity and proliferation of human dermal fibroblasts in a three-dimensional collagen gel/sponge. *Biochem. Eng. J.* (2004) doi:10.1016/j.bej.2003.09.019.
 165. Mizuno, S., Tateishi, T., Ushida, T. & Glowacki, J. Hydrostatic fluid pressure enhances matrix synthesis and accumulation by bovine chondrocytes in three-dimensional culture. *J. Cell. Physiol.* (2002) doi:10.1002/jcp.10180.
 166. Carver, S. E. & Heath, C. A. Semi-continuous perfusion system for delivering intermittent physiological pressure to regenerating cartilage. *Tissue Eng.* (1999) doi:10.1089/ten.1999.5.1.
 167. Duraine, G. D. & Athanasiou, K. A. ERK activation is required for hydrostatic pressure-induced tensile changes in engineered articular cartilage. *J. Tissue Eng. Regen. Med.* (2015) doi:10.1002/term.1678.
 168. Toyoda, T. *et al.* Hydrostatic Pressure Modulates Proteoglycan Metabolism in Chondrocytes Seeded in Agarose. *Arthritis Rheum.* (2003) doi:10.1002/art.11250.
 169. Correia, C. *et al.* Dynamic culturing of cartilage tissue: The significance of hydrostatic pressure. *Tissue Eng. - Part A* (2012) doi:10.1089/ten.tea.2012.0083.
 170. Candiani, G., Raimondi, M. T., Aurora, R., Laganà, K. & Dubini, G. Chondrocyte response to high regimens of cyclic hydrostatic pressure in 3-dimensional engineered constructs. *Int. J. Artif. Organs* (2008) doi:10.1177/039139880803100604.
 171. Ikenoue, T. *et al.* Mechanoregulation of human articular chondrocyte aggrecan and type II collagen expression by intermittent hydrostatic pressure in vitro. *J. Orthop. Res.* (2003) doi:10.1016/S0736-0266(02)00091-8.
 172. Parkkinen, J. J. *et al.* Effects of cyclic hydrostatic pressure on proteoglycan synthesis in cultured chondrocytes and articular cartilage explants. *Arch. Biochem. Biophys.* (1993) doi:10.1006/abbi.1993.1062.
 173. Wagner, D. R. *et al.* Hydrostatic pressure enhances chondrogenic differentiation of human bone marrow stromal cells in osteochondrogenic medium. *Ann. Biomed. Eng.* (2008) doi:10.1007/s10439-008-9448-5.
 174. Angele, P. *et al.* Cyclic hydrostatic pressure enhances the chondrogenic phenotype of human mesenchymal progenitor cells differentiated in vitro. *J. Orthop. Res.* (2003) doi:10.1016/S0736-0266(02)00230-9.
 175. Miyanishi, K. *et al.* Effects of hydrostatic pressure and transforming growth factor- β 3 on adult human mesenchymal stem cell chondrogenesis in vitro. *Tissue Eng.* (2006) doi:10.1089/ten.2006.12.1419.
 176. Mauck, R. L. *et al.* Functional tissue engineering of articular cartilage through dynamic loading of chondrocyte-seeded agarose gels. *J. Biomech. Eng.* (2000) doi:10.1115/1.429656.
 177. Gemmiti, C. V. & Guldberg, R. E. Shear stress magnitude and duration modulates matrix composition and tensile mechanical properties in engineered cartilaginous tissue. *Biotechnol. Bioeng.* (2009) doi:10.1002/bit.22440.
 178. sharifi, N. & Gharravi, A. M. Shear bioreactors stimulating chondrocyte regeneration, a systematic review. *Inflamm. Regen.* (2019) doi:10.1186/s41232-019-0105-1.
 179. Mellor, L. F., Baker, T. L., Brown, R. J., Catlin, L. W. & Oxford, J. T. Optimal 3D culture of primary articular chondrocytes for use in the rotating wall vessel bioreactor. *Aviat. Sp. Environ. Med.* (2014) doi:10.3357/ASEM.3905.2014.
 180. Li, S. *et al.* Application of an acoustofluidic perfusion bioreactor for cartilage tissue engineering. *Lab Chip* (2014) doi:10.1039/c4lc00956h.
 181. Jin, M., Emkey, G. R., Siparsky, P., Trippel, S. B. & Grodzinsky, A. J. Combined effects of

- dynamic tissue shear deformation and insulin-like growth factor I on chondrocyte biosynthesis in cartilage explants. *Arch. Biochem. Biophys.* (2003) doi:10.1016/S0003-9861(03)00195-4.
182. Di Federico, E., Bader, D. L. & Shelton, J. C. Design and validation of an in vitro loading system for the combined application of cyclic compression and shear to 3D chondrocytes-seeded agarose constructs. *Med. Eng. Phys.* (2014) doi:10.1016/j.medengphy.2013.11.007.
 183. Waldman, S. D., Spiteri, C. G., Grynepas, M. D., Pilliar, R. M. & Kandel, R. A. Long-term intermittent shear deformation improves the quality of cartilaginous tissue formed in vitro. *J. Orthop. Res.* (2003) doi:10.1016/S0736-0266(03)00009-3.
 184. Vainieri, M. L., Wahl, D., Alini, M., van Osch, G. J. V. M. & Grad, S. Mechanically stimulated osteochondral organ culture for evaluation of biomaterials in cartilage repair studies. *Acta Biomater.* (2018) doi:10.1016/j.actbio.2018.09.058.
 185. Gooch, K. J. *et al.* Effects of mixing intensity on tissue-engineered cartilage. *Biotechnol. Bioeng.* (2001) doi:10.1002/1097-0290(20000220)72:4<402::AID-BIT1002>3.0.CO;2-Q.
 186. Vunjak-Novakovic, G. *et al.* Dynamic cell seeding of polymer scaffolds for cartilage tissue engineering. *Biotechnol. Prog.* (1998) doi:10.1021/bp970120j.
 187. Mizuno, S., Allemann, F. & Glowacki, J. Effects of medium perfusion on matrix production by bovine chondrocytes in three-dimensional collagen sponges. *J. Biomed. Mater. Res.* (2001) doi:10.1002/1097-4636(20010905)56:3<368::AID-JBM1105>3.0.CO;2-V.
 188. M.T., R. *et al.* The effect of hydrodynamic shear on 3D engineered chondrocyte systems subject to direct perfusion. *Biorheology* (2006).
 189. Carmona-Moran, C. A. & Wick, T. M. Transient Growth Factor Stimulation Improves Chondrogenesis in Static Culture and Under Dynamic Conditions in a Novel Shear and Perfusion Bioreactor. *Cell. Mol. Bioeng.* (2015) doi:10.1007/s12195-015-0387-6.
 190. Anderson, D. E. & Johnstone, B. Dynamic mechanical compression of chondrocytes for tissue engineering: A critical review. *Frontiers in Bioengineering and Biotechnology* (2017) doi:10.3389/fbioe.2017.00076.
 191. Nebelung, S. *et al.* Simultaneous anabolic and catabolic responses of human chondrocytes seeded in collagen hydrogels to long-term continuous dynamic compression. *Ann. Anat.* (2012) doi:10.1016/j.aanat.2011.12.008.
 192. Lacroix, D. & Prendergast, P. J. A mechano-regulation model for tissue differentiation during fracture healing: Analysis of gap size and loading. *J. Biomech.* (2002) doi:10.1016/S0021-9290(02)00086-6.
 193. Huwe, L. W., Sullan, G. K., Hu, J. C. & Athanasiou, K. A. Using Costal Chondrocytes to Engineer Articular Cartilage with Applications of Passive Axial Compression and Bioactive Stimuli. *Tissue Eng. - Part A* (2018) doi:10.1089/ten.tea.2017.0136.
 194. Elder, B. D. & Athanasiou, K. A. Effects of confinement on the mechanical properties of self-assembled articular cartilage constructs in the direction orthogonal to the confinement surface. *J. Orthop. Res.* (2008) doi:10.1002/jor.20480.
 195. WISEMAN, M., HENSON, F., LEE, D. A. & BADER, D. L. Dynamic compressive strain inhibits nitric oxide synthesis by equine chondrocytes isolated from different areas of the cartilage surface. *Equine Vet. J.* (2010) doi:10.2746/042516403775600532.
 196. Lee, D. A. & Bader, D. L. Compressive strains at physiological frequencies influence the metabolism of chondrocytes seeded in agarose. *J. Orthop. Res.* (1997) doi:10.1002/jor.1100150205.
 197. Lee, C. R., Grodzinsky, A. J. & Spector, M. Biosynthetic response of passaged chondrocytes in a type II collagen scaffold to mechanical compression. *J. Biomed. Mater. Res. - Part A* (2003) doi:10.1002/jbm.a.10443.
 198. Hoenic, E. *et al.* High amplitude direct compressive strain enhances mechanical properties of scaffold-free tissue-engineered cartilage. *Tissue Eng. - Part A* (2011) doi:10.1089/ten.tea.2010.0395.
 199. Stoddart, M. J., Ettinger, L. & Häuselmann, H. J. Enhanced matrix synthesis in de novo,

- scaffold free cartilage-like tissue subjected to compression and shear. *Biotechnol. Bioeng.* (2006) doi:10.1002/bit.21052.
200. Grogan, S. P. *et al.* Effects of perfusion and dynamic loading on human neocartilage formation in alginate hydrogels. *Tissue Eng. - Part A* (2012) doi:10.1089/ten.tea.2011.0506.
 201. Zignego, D. L., Hilmer, J. K. & June, R. K. Mechanotransduction in primary human osteoarthritic chondrocytes is mediated by metabolism of energy, lipids, and amino acids. *J. Biomech.* (2015) doi:10.1016/j.jbiomech.2015.10.038.
 202. Kisiday, J. D., Frisbie, D. D., McIlwraith, C. W. & Grodzinsky, A. J. Dynamic compression stimulates proteoglycan synthesis by mesenchymal stem cells in the absence of chondrogenic cytokines. *Tissue Eng. - Part A* (2009) doi:10.1089/ten.tea.2008.0357.
 203. Kisiday, J. D., Jin, M., DiMicco, M. A., Kurz, B. & Grodzinsky, A. J. Effects of dynamic compressive loading on chondrocyte biosynthesis in self-assembling peptide scaffolds. *J. Biomech.* (2004) doi:10.1016/j.jbiomech.2003.10.005.
 204. Wimmer, M. A. *et al.* Tribology approach to the engineering and study of articular cartilage. *Tissue Eng.* (2004) doi:10.1089/ten.2004.10.1436.
 205. Martin, I., Wendt, D. & Heberer, M. The role of bioreactors in tissue engineering. *Trends in Biotechnology* (2004) doi:10.1016/j.tibtech.2003.12.001.
 206. Sutherland, R. M. *et al.* Oxygenation and Differentiation in Multicellular Spheroids of Human Colon Carcinoma. *Cancer Res.* (1986).
 207. Martin, I., Obradovic, B., Freed, L. E. & Vunjak-Novakovic, G. Method for Quantitative Analysis of Glycosaminoglycan Distribution in Cultured Natural and Engineered Cartilage. *Ann. Biomed. Eng.* (1999) doi:10.1114/1.205.
 208. Brunelli, M., Perrault, C. & Lacroix, D. A Review of Bioreactors and Mechanical Stimuli. in (2019). doi:10.1007/978-981-10-8075-3_1.
 209. Ferrari, C. *et al.* Investigation of growth conditions for the expansion of porcine mesenchymal stem cells on microcarriers in stirred cultures. *Appl. Biochem. Biotechnol.* (2014) doi:10.1007/s12010-013-0586-3.
 210. Mabvuure, N., Hindocha, S. & S. Khan, W. The Role of Bioreactors in Cartilage Tissue Engineering. *Curr. Stem Cell Res. Ther.* (2012) doi:10.2174/157488812800793018.
 211. Bancroft, G. N., Sikavitsas, V. I. & Mikos, A. G. Design of a flow perfusion bioreactor system for bone tissue-engineering applications. *Tissue Eng.* (2003) doi:10.1089/107632703322066723.
 212. Cartmell, S. H., Porter, B. D., García, A. J. & Guldberg, R. E. Effects of Medium Perfusion Rate on Cell-Seeded Three-Dimensional Bone Constructs in Vitro. in *Tissue Engineering* (2003). doi:10.1089/10763270360728107.
 213. Shahin, K. & Doran, P. M. Strategies for enhancing the accumulation and retention of extracellular matrix in tissue-engineered cartilage cultured in bioreactors. *PLoS One* (2011) doi:10.1371/journal.pone.0023119.
 214. Santoro, R. *et al.* Bioreactor based engineering of large-scale human cartilage grafts for joint resurfacing. *Biomaterials* (2010) doi:10.1016/j.biomaterials.2010.08.009.
 215. Thibault, R. A., Mikos, A. G. & Kasper, F. K. Protein and mineral composition of osteogenic extracellular matrix constructs generated with a flow perfusion bioreactor. *Biomacromolecules* (2011) doi:10.1021/bm200975a.
 216. Alves Da Silva, M. L. *et al.* Cartilage tissue engineering using electrospun PCL nanofiber meshes and MSCs. *Biomacromolecules* (2010) doi:10.1021/bm100476r.
 217. Weyand, B. *et al.* A Differential Pressure Laminar Flow Reactor Supports Osteogenic Differentiation and Extracellular Matrix Formation from Adipose Mesenchymal Stem Cells in a Macroporous Ceramic Scaffold. *Biores. Open Access* (2012) doi:10.1089/biores.2012.9901.
 218. Kim, J. & Ma, T. Regulation of autocrine fibroblast growth factor-2 signaling by perfusion flow in 3D human mesenchymal stem cell constructs. *Biotechnol. Prog.* (2012) doi:10.1002/btpr.1604.
 219. Griffon, D. J., Abulencia, J. P., Ragetly, G. R., Fredericks, L. P. & Chaieb, S. A comparative study of seeding techniques and three-dimensional matrices for mesenchymal cell attachment. *J.*

- Tissue Eng. Regen. Med.* (2011) doi:10.1002/term.302.
220. Zvicer, J. & Obradovic, B. Bioreactors with hydrostatic pressures imitating physiological environments in intervertebral discs. *Journal of Tissue Engineering and Regenerative Medicine* (2018) doi:10.1002/term.2533.
 221. Waldman, S. D., Couto, D. C., Grynepas, M. D., Pilliar, R. M. & Kandel, R. A. A single application of cyclic loading can accelerate matrix deposition and enhance the properties of tissue-engineered cartilage. *Osteoarthr. Cartil.* (2006) doi:10.1016/j.joca.2005.10.007.
 222. Correia, V. *et al.* Design and validation of a biomechanical bioreactor for cartilage tissue culture. *Biomech. Model. Mechanobiol.* (2016) doi:10.1007/s10237-015-0698-5.
 223. Shahin, K. & Doran, P. M. Tissue engineering of cartilage using a mechanobioreactor exerting simultaneous mechanical shear and compression to simulate the rolling action of articular joints. *Biotechnol. Bioeng.* (2012) doi:10.1002/bit.24372.
 224. Gharravi, A. M. *et al.* Design and fabrication of anatomical bioreactor systems containing alginate scaffolds for cartilage tissue engineering. *Avicenna J. Med. Biotechnol.* (2012).
 225. Bilgen, B., Chu, D., Stefani, R. & Aaron, R. K. Design of a biaxial mechanical loading bioreactor for tissue engineering. *J. Vis. Exp.* (2013) doi:10.3791/50387.
 226. Jeong, H.-J. *et al.* Bioreactor mimicking knee-joint movement for the regeneration of tissue-engineered cartilage. *J. Mech. Sci. Technol.* (2019) doi:10.1007/s12206-019-0336-8.
 227. Trevino, R. L. *et al.* Establishing a live cartilage-on-cartilage interface for tribological testing. *Biotribology* (2017) doi:10.1016/j.biotri.2016.11.002.
 228. Simões, A. & Reis, T. *Dinâmica de Fluidos para Engenharia Química.* (2016).
 229. Sobachkin, A. & Dumnov, G. *Numerical Basis of CAD-Embedded CFD. NAFEMS World Congress 2013* (2013).
 230. SOLIDWORKS Flow Simulation. *Dassault Systemes* <https://www.solidworks.com/product/solidworks-flow-simulation> (2019).
 231. Sørensen, L. S. An introduction to Computational Fluid Dynamics: The Finite Volume Method. in *DTU Orbit, Annual report year: 1999* (1999).
 232. Hartcher-O'Brien, J., Evers, J. & Tempelman, E. Surface roughness of 3D printed materials: Comparing physical measurements and human perception. *Mater. Today Commun.* (2019) doi:10.1016/j.mtcomm.2019.01.008.
 233. Wong, K. V. & Hernandez, A. A Review of Additive Manufacturing. *ISRN Mech. Eng.* (2012) doi:10.5402/2012/208760.
 234. Su, C. K., Yen, S. C., Li, T. W. & Sun, Y. C. Enzyme-Immobilized 3D-Printed Reactors for Online Monitoring of Rat Brain Extracellular Glucose and Lactate. *Anal. Chem.* (2016) doi:10.1021/acs.analchem.6b00272.
 235. Neches, R. Y., Flynn, K. J., Zaman, L., Tung, E. & Pudlo, N. On the intrinsic sterility of 3D printing. *PeerJ* (2016) doi:10.7717/peerj.2661.
 236. Von Der Mark, K., Gauss, V., Von Der Mark, H. & Müller, P. Relationship between cell shape and type of collagen synthesised as chondrocytes lose their cartilage phenotype in culture [26]. *Nature* (1977) doi:10.1038/267531a0.
 237. Stops, A. J. F., Heraty, K. B., Browne, M., O'Brien, F. J. & McHugh, P. E. A prediction of cell differentiation and proliferation within a collagen-glycosaminoglycan scaffold subjected to mechanical strain and perfusive fluid flow. *J. Biomech.* (2010) doi:10.1016/j.jbiomech.2009.10.037.
 238. Prendergast, P. J., Huiskes, R. & Søballe, K. Biophysical stimuli on cells during tissue differentiation at implant interfaces. *J. Biomech.* (1997) doi:10.1016/S0021-9290(96)00140-6.
 239. Lafont, J. E., Talma, S., Hopfgarten, C. & Murphy, C. L. Hypoxia promotes the differentiated human articular chondrocyte phenotype through SOX9-dependent and -independent pathways. *J. Biol. Chem.* (2008) doi:10.1074/jbc.M707729200.
 240. Portron, S. *et al.* Inverse regulation of early and late chondrogenic differentiation by oxygen tension provides cues for stem cell-based cartilage tissue engineering. *Cell. Physiol. Biochem.* (2015) doi:10.1159/000369742.

241. Merceron, C. *et al.* Differential effects of hypoxia on osteochondrogenic potential of human adipose-derived stem cells. *Am. J. Physiol. - Cell Physiol.* (2010) doi:10.1152/ajpcell.00398.2009.
242. Daly, A. C., Sathy, B. N. & Kelly, D. J. Engineering large cartilage tissues using dynamic bioreactor culture at defined oxygen conditions. *J. Tissue Eng.* (2018) doi:10.1177/2041731417753718.
243. Wenger, R., Kurtcuoglu, V., Scholz, C., Marti, H. & Hoogewijs, D. Frequently asked questions in hypoxia research. *Hypoxia* (2015) doi:10.2147/hp.s92198.
244. Ito, A. *et al.* Culture temperature affects human chondrocyte messenger RNA expression in monolayer and pellet culture systems. *PLoS One* (2015) doi:10.1371/journal.pone.0128082.
245. Vinatier, C. & Guicheux, J. Cartilage tissue engineering: From biomaterials and stem cells to osteoarthritis treatments. *Annals of Physical and Rehabilitation Medicine* (2016) doi:10.1016/j.rehab.2016.03.002.
246. Vinatier, C., Guicheux, J., Daculsi, G., Layrolle, P. & Weiss, P. Cartilage and bone tissue engineering using hydrogels. *Bio-Medical Materials and Engineering* (2006).
247. Camp, C. L., Stuart, M. J. & Krych, A. J. Current Concepts of Articular Cartilage Restoration Techniques in the Knee. *Sports Health* (2014) doi:10.1177/1941738113508917.
248. Ng, J. *et al.* Extracellular matrix components and culture regimen selectively regulate cartilage formation by self-assembling human mesenchymal stem cells in vitro and in vivo. *Stem Cell Res. Ther.* (2016) doi:10.1186/s13287-016-0447-4.
249. COMMISSION, E. Annex 1 Manufacture of Sterile Medicinal Products (corrected version). *EU Guidelines to Good Manufacturing Practice Medicinal Products for Human and Veterinary Use* 1–16 http://academy.gmp-compliance.org/guidemgr/files/ANNEX_01%5B2008%5D.PDF (2008).
250. Raveling, A. R., Theodossiou, S. K. & Schiele, N. R. A 3D printed mechanical bioreactor for investigating mechanobiology and soft tissue mechanics. *MethodsX* (2018) doi:10.1016/j.mex.2018.08.001.
251. Silva, J. C. *et al.* Extruded Bioreactor Perfusion Culture Supports the Chondrogenic Differentiation of Human Mesenchymal Stem/Stromal Cells in 3D Porous Poly (ϵ -Caprolactone) Scaffolds. *Biotechnol. J.* (2019) doi:10.1002/biot.201900078.
252. Daneshgar, A. *et al.* Teburu—Open source 3D printable bioreactor for tissue slices as dynamic three-dimensional cell culture models. *Artif. Organs* (2019) doi:10.1111/aor.13518.
253. Chen, J. *et al.* Improvement of In Vitro Three-Dimensional Cartilage Regeneration by a Novel Hydrostatic Pressure Bioreactor. *Stem Cells Transl. Med.* (2017) doi:10.5966/sctm.2016-0118.
254. Spitters, T. *A Dual Flow Bioreactor for Cartilage tissue Engineering. Thesis* (2014).
255. Cinbiz, M. N., Tiğli, R. S., Beşkardeş, I. G., Gümüşderelioglu, M. & Çolak, Ü. Computational fluid dynamics modeling of momentum transport in rotating wall perfused bioreactor for cartilage tissue engineering. *J. Biotechnol.* (2010) doi:10.1016/j.jbiotec.2010.09.950.
256. Song, X. *et al.* A novel human-like collagen hydrogel scaffold with porous structure and sponge-like properties. *Polymers (Basel)*. (2017) doi:10.3390/polym9120638.
257. Bakker, B. de. How to control a stepper motor with A4988 driver and Arduino. *Makerguides.com* <https://www.makerguides.com/a4988-stepper-motor-driver-arduino-tutorial/>.
258. Kon, E., Roffi, A., Filardo, G., Tesei, G. & Marcacci, M. Scaffold-based cartilage treatments: With or without cells? A systematic review of preclinical and clinical evidence. *Arthroscopy - Journal of Arthroscopic and Related Surgery* (2015) doi:10.1016/j.arthro.2014.11.017.